THE EFFECT OF SURFACTANTS AND POYOLS ON PROTEIN FIBRILLATION MECHANISM AND KINETICS

Thesis submitted by

E. Kiran Kumar

10LTPH06

in partial fulfilment of the requirements for the degree of Doctor of Philosophy

Under supervision of

Dr. N. Prakash Prabhu

Assistant Professor

DEPARTMENT OF BIOTECHNOLOGY AND BIOINFORMATICS

SCHOOL OF LIFE SCIENCE,

UNIVERSITY OF HYDERABAD,

HYDERABAD 500046, INDIA

DEPARTMENT OF BIOTECHNOLOGY AND BIOINFORMATICS
SCHOOL OF LIFE SCIENCE, UNIVERSITY OF HYDERABAD, HYDERABAD 500046, INDIA

CERTIFICATE

This is to certify that thesis entitled "**The Effect of Surfactants and Polyols on Protein Fibrillation Mechanism and Kinetics"** submitted to the University of Hyderabad by **Mr. E. Kiran Kumar** for the degree of Doctor of Philosophy, is based on the studies carried out by him under my supervision. This work has not been submitted before for the award of degree or diploma from any University or Institution.

Dr. N. Prakash Prabhu
Supervisor

Head
Department of Biotechnology and Bioinformatics

Dean
School of Life Science

CERTIFICATE

This is to certify that the thesis entitled **""** Submitted by **E.Kiran Kumar** bearing registration number **10LTPH06** in partial fulfilment of the requirements for award of Doctor of Philosophy in the school of **Life Science** is a bonafide work carried out by him under my supervision and guidance.

This thesis is free from plagiarism and has not been submitted previously in part or in full to this or any other university or institute for award of any degree or diploma.

Part of this thesis has been:

A. Published in the following publications:

1. Differential Effects of Ionic and Non-ionic Surfactants on Lysozyme Fibrillation. E.K.Kumar, N.P. Prabhu, Phys.Chem.Chem.Phys. 2016 (14), 24076.	**Chapter 3 of Thesis**
2. Sodium Dodecyl Sulphate (SDS) Induced Changes In Propensity & Kinetics of α-Lactalbumin. E.K.Kumar, S.Qamar, N.P. Prabhu, Int.J.Biol.Macr, 2015 (81), 754-758.	**Chapter 4 of Thesis**

B. Published in the following conference:

1._____, (National/International)

2._____, (National/International)

Further, the student has passed the following courses towards fulfilment of coursework requirement for PhD degree was award.

	Course code	Name	Credits	Pass/Fail
1	BT801	Analytical technique	4	Pass
2	BT802	Res. ethics, Stats. & Data analysis	3	Pass
3	BT803	Lab work and seminar	5	Pass

Dr. N. Prakash Prabhu

Supervisor

Head of Department of Biotechnology and Bioinformatics

Dean of School of Life Science

In loving memory of my Dad…

who enabled, encouraged and entrusted me

Acknowledgements

I would like to acknowledge my supervisor and mentor Dr.N.Prakash Prabhu for his constant support and guidance throughout the tenure of my research work. I am really thankful for his encouragement and confidence he showed in me. I would like to heartfully acknowledge his openness to the ideas that allowed me to venture into the field of Biophysics. I see him as my motivational icon and would like to improve upon and learn.

I would also like to thank my doctoral research committee members for their constant review and comments on my research work. The help from Department of Biotechnology & Bioinformatics and support extended by present and former Heads' of the Department is greatly acknowledged. I express a deep sense of gratitude to the present and former and Deans' of School of Life Sciences for their continued assistance during my research tenure. All the faculties of Life Sciences from whom I got the motivation for research is highly indebted.

The funding support of UGC, CSIR, DBT, DST, DBT-CREBB, DST-FIST, UGC-SAP, UPE is greatly acknowledged. I am also thankful for the staff of School of Life Sciences and Department of Biotechnology, Shekhar, Rahul, Rajashekhar for their co-operation in official work.

I have taken efforts in completing this research work. However, it would have not been possible without the kind support and help of many individuals and organizations.

I thank my lab members Chaitu, Neshath, Tejaswi, Bramhini, Suraj, Deepak, Shamsul, Shravani, Abhilash, Sharath, Haider, Subhasree, Archi, Yogesh, Deepesh for their kind co-operation and stimulating discussions that enabled shaping my research.

I would like to thank friends who gave me constant support and encouragement during my stay and tenure of research in HCU, Dr.Satish bhai, Dr.Praveen bhai, Mouli bhai, Yashwanth, Srinu hazare, Dr.Suresh enfield, Dr.Suresh Digumarthi gaaru, Shreeky, Satveer, Rahul, Bunny for their intellectual discussions and exchange of ideas that span wide spectrum of concepts.

I would like to sincerely thank my teachers Dr.Mary, Dr.Vijay, Dr.Uma, Dr.S.Padma, Dr.Sai Padma, Usha madam for their guidance, encouragement and helping me in navigating through the research field.

I owe my gratitude to Sasi, Yasin and Ramakrishna anna for their guidance and in making me better understand the concepts in biophysics that allowed me to take a leap in research.

I am thankful for the help extended by friends, Sunilkanth, Srinivas Karimnagar, Swaroop mama, Dr.Sunil, Dr.Srinu, Kumar bro, Loki, Vikranth, Nitash, Sireesh, Shekhar babu, PaWon, Sayan, Santosh, Pranay for their scientific and motivational discussions.

I heartily thank the staff of CIL, Department of Physics, CNF, School of chemistry, SEST for their help in allowing me use their facilities. I would like to take a chance to mention a few who helped in making my research work smoothly by their timely help, Ahmed Sir, Pavan, Yellaiah, Yadav, Srikanth Sir, Sunitha, Reshma, Pankaj.

I am grateful for friends who helped me through this journey- Prasanna, Sita, Durga, Lachi, Narsing, Vikas, Ravi motu, Sai HMT, Sai, Anil iscariot, Rathod, Uma, Anand, Shiva Chiru, Raj, Sai ram, Srikanth, Sanjeeth, Murali, Khan, Sameer, Dilip, Katta Anil, Rahul IQ, Ramesh, Suman, Venki, Sanjeev, Suraj, Swapna, Madhu poornima.

I would like to take a chance to thank my little champs Dhiru, Honey, Lucky, Apple, Pandu, Mani, Rahul, Billu, Sweety, Anjali, Nikhil, Divya, Ramya for their role in successful completion of my thesis.

I cannot end without the acknowledgement of the love and support of my Family members, especially my Mother without whom I cannot imagine this thesis.

Abbrevations

AEF	Amyloid Enhancing Factor
AFM	Atomic Force Microscopy
α-LA	Alpha Lactalbumin
ANS	8-Anilino-1-Naphthalene Sulphonic acid
AVT	Available Volume Theory
β-LG	Beta Lactoglobulin
BSA	Bovine Serum Albumin
CAC	Critical Aggregation Concentration
C_{crt}	Concentration of Critical Nucleus
CR	Congo Red
Csup	Concentration of Super-Critical Nucleus
Cm	Concentration Mid-point
CMC	Critical Micelle Concentration
CTAB	Cetyl Trimethyl Ammonim Bromide
Cp	Centipoise
DTAB	Dodecyl Trimethyl Ammonium Bromide
EG	Ethylene Glycol
F_{α}	Fraction of Protein Converted Into Fibril
[F]	Matured Fibrils
Fext	Rate of Fibril Extension
$[F_n]$	Number Concentration of Fibrils
GdmCl	Guanindinium Chloride
ΔG	Free Energy Change
ΔΔG	Difference In Free Energy Change
Γ	Scaling Factor
HbS	Sickle Haemoglobin
HEWL	Hen Egg White Lysozyme
k_{el}	Apparent Fibril Elongation Rate
kcal/mol	Kilocalories Per Mol
kfb+	Rate of Fibril Fragmentation
kfb-	Rate of Monomer Addition on Seed
K_{nu}	Magnitude of Fibril Growth

k_a	Relative amplitude of nucleation over growth
k_b	Rate of nucleus formation
k_{nu+}	Equ. constant between monomers & nucleus
knu-	Rate of nucleus dissociation
k_{agg}	Rate of initial aggregation
Ḱ	Rate of filament multiplication
LTAB	Lauryl Trimethyl Ammonim Bromide
n_c	Order of primary nucleation
n_2	Order of secondary nucleation
N_{nu}	Nucleus size
N_{fb}	Fibril size
n	Order of reaction
[P]	Monomeric protein
PEG	Polyethylene Glycol
pI	Isoelectric point
$[P_{ini}]$	Initial protein concentration
$[P_{agg}]$	Polymeric aggregation
$[P_{tot}]$	Total protein concentration
Rnase	Ribonuclease
[S]	Number concentration of seeds
$S_{\alpha-}$	Mass fraction of Seed added
SCML	S-Carboxymethyl-α-Lactalbumin
SDS	Sodium Dodecyl Sulphate
Snase	Staphylococcal nuclease
SPT	Scaled Particle Theory
TEG	Triethylene Glycol
TEM	Transmission Electron Microscopy
Tm	Thermal denaturation Midpoint
ThT	Thioflavin-T
TNS	P-Toulidino-Naphthalene Sulphonic Acid
tlag	Lag Time
Trp	Tryptophan
Tx	Triton X 100

Table of Contents

Chapter 1. Introduction

Chapter 2. Concentration Dependent Switch in the Kinetic Pathway of Lysozyme

Chapter 3. Surfactant Induced Changes on Lysozyme Fibrillation- Differential Effects of Ionic and Non-ionic Surfactants

Chapter 1

Introduction

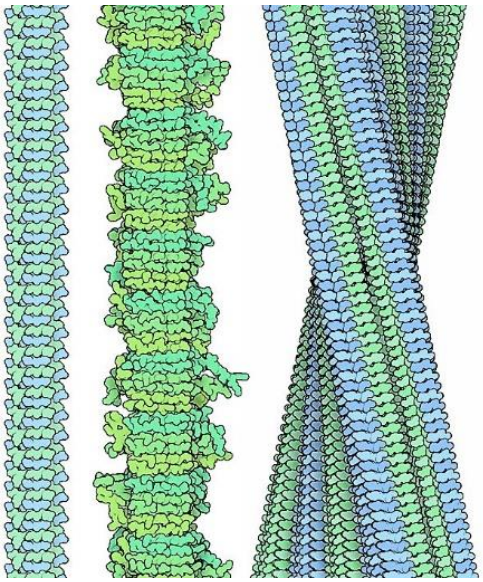

1.1 Introduction

Protein needs to fold into a specific three-dimensional structure, known as native conformation, for its biological function. Cellular responses such as heat shock response and unfolded protein response (UPR), are activated in the event of misfolding which might result in proper refolding of the protein or protein degradation.[1] When proteins fail either to fold properly or to remain correctly folded in their optimally packed and functional states, it results in accumulation of misfolded/unfolded proteins due to failure or dysregulation of these processes which in turn results in protein misfolding diseases, generally referred as protein conformational diseases.[2,3] According to the landscape model, misfolded intermediates are protein configurations that are kinetically trapped non-native structures dominated by low free-energy.[3] Folding from such conformations must proceed by slow reconfiguration travelling uphill in the energy surface and thus becomes more unfolded in energetic sense before proceeding to the native state. Aggregation doesn't proceed *via* global unfolding, but rather involves a locally unfolded state accessed through thermal fluctuations and should be only separated by low free-energy barriers from the native state.

These biologically non-functional forms of the proteins may accumulate to form deposits of insoluble aggregates. Virchow was the first in 1851 to show that the aggregates on cerebral corpora amylacea upon stained with iodine showed blue which further turned into violet by the addition of sulphuric acid. He then suggested that the abnormal deposits could be cellulose in origin and named it 'amyloid'.[4] The nomenclature is still retained, in spite of the fact that in 1859 Friedrich and Kekule showed these mass deposits to be indeed protein aggregates.[4] This process of protein aggregation which can damage the functions of cells and tissues, and leading to disease conditions are named as amyloidosis. Amyloidoses are heterogeneous disease conditions that it may involve one or more organs.[5,6] In the case of local amyloidoses, the fibril deposits are observed in the organ/tissue where the precursor protein is synthesized as it is commonly found in Alzheimer's, spongiform encephalopathies, Parkinson's, and Huntington's disease conditions. In systemic amyloidosis, the deposition of fibrils occurs at different sites from where the precursor protein is expressed as in the cases of human light chain amyloidosis, familial amyloidotic polyneuropathy, and lysozyme amyloidosis and they are extracellular fibril deposits.[5,6] So far, more than thirty disease conditions are identified related to amyloidosis.[2,5,7,8] Aging, mutations or conformational changes in precursor proteins, defective proteolysis, an increase in local concentration of precursor proteins, and association of amyloid enhancing factor (AEF) are considered to be common disease causing conditions for amyloidosis, though all may not operate together.[5]

1.2. Fibril formation – a generic property of proteins

Studies suggest that the proteins which are non-amyloidogenic under *in vivo* conditions can form fibrils, if appropriate solution conditions are provided.[9,10] This even includes α-helical proteins such as myoglobin,[11] cytochrome *c*,[12-13] and some plant proteins.[14,15] Hence, it is widely accepted that fibril formation could be a generic property of almost all the proteins irrespective of their sequence and native structure. Anfinsen's classic experiments has shown that the amino acid sequence of a protein chain contains all the necessary information to attain the functional fold.[16] The question that is intriguing for past four decades in the field of structural biology is "how the one dimensional sequence of a protein determines the biologically active conformation?". Since the number of possible conformations of a polypeptide chain is astronomically large and as main chains have identical composition but differ in the side chain composition, how does a given sequence find its specific native structure in a finite time. "As the doubling time of bacteria is nearly 30 minutes it is clear that evolution has found an effective solution to this combinatorial problem". [17] It is also proposed that when the native structure of a protein is destabilized, the partially unfolded conformation can facilitate specific intermolecular interactions to form fibrils.[18,19] Distinguishing feature of folding is the extreme heterogeneity of the reaction and complex interplay between entropic and enthalpic contributions to the free energy of the system during folding. Urea and guanidine chloride (GdmCl) are commonly employed denaturants to obtain unfolded state of a protein. Denatured protein usually resembles 'random coil' in which local interactions dominate conformational behaviour and is extremely heterogenous both globally and at individual residues.[20,21] Number of accessible conformers may approach the number of possible conformations discussed as in Levinthal's paradox.[22]

The new view of protein folding provides a simple way of understanding why the paradox is not a real problem.[17,21] Denatured and folded state are separated by a sizeable enthalpic difference of up to 30-100 *kcal/mol* [17] and to achieve folding it provides a sufficient bias of conformational space to avoid the need to search through an impossibly large number of configurations. Fast *two-state* folding can occur, if collapse involves only a small subset of highly stabilizing native contacts in the core region or nucleus.[23,24] If there are more uniform or hydrophobic attractions between the residues, there is a rapid collapse to a disorganized globule with the slow step in folding involving reorganizational events within a compact ensemble of denatured states. Irrespective of the native secondary structure and the globular state of a protein, populating an intermediate with ordered secondary structure and non-native tertiary interactions with the propensity to form cross β-sheets through self-assembly process

can convert any protein into amyloidogenic.[9,10] This common mechanism of fibrillogenesis further suggests that the organisms might have adapted protein fibril formation through evolution. In fact, in many organisms including humans, amyloid fibrils are found to be involved in their cellular physiology which is referred as 'functional amyloids'.[2, 25,26]

1.3. Functional Amyloids

Amyloid structures are also naturally found in many functional roles,[2,27-28] though they have been primarily associated with pathological behaviour ever since their discovery.[29,30] Bacterial coatings,[31] catalytic scaffolds,[2] agents mediating epigenetic-information storage and transfer, Orb2 (neuronal RNA-binding protein participating in memory consolidation in *Drosophila*) has amyloid-like structure in its functional form.[32] Adhesives[33] and structures for the storage of peptide hormones[34] represent prominent examples of such functional amyloid materials. Amyloids often are energetically more favourable compared with the soluble native state[29] and represents a more general ordered state for proteins. Not just single cell organisms possess amyloid scaffold but a key physiological role has emerged in the biosynthesis of melanin in humans.[2,35] A further natural application of functional amyloids has been revealed recently in the secretory granules in pituitary glands in the form of high density packing of peptide hormones.[34]

Moreover, the scaling of interactions in amyloid fibrils can be compared with materials and provides a platform for designing novel nanobiomaterials.[35,36] The nature of the fundamental intermolecular interactions that bind their constituents into larger scale hierarchical systems reflect the mechanical properties of materials.[37] Bio-nanotechnology field has been in limelight by recent advances that helped the broadening of the applications and scope of hybrid nanomaterials in biological field. Unique architectures and exceptional physical properties of carbon nanomaterials (such as fullerenes, nanotubes and graphene)[38] and amyloid fibrils have attracted great attention and are eminent examples of functional nanostructure materials of undisputed impact in nanotechnology. Combination of these two classes of nanomaterials into functional hybrids is far from trivial. For an example, inhibition or promotion of amyloid fibrillation by presence of carbon nanomaterials that in turn depends on their structural architectures and starting amyloid proteins or peptides considered.[39] Hybridizing desirable properties of these nanomaterials open up new avenues for use in electronics, actuators, sensing, biomedicine[40,41,42-43] and structural materials.

1.4. Structural features of amyloid fibrils

The amyloid fibrils formed by proteins show common structural features despite having differences in amino acid sequences, varying native secondary structure contents, and

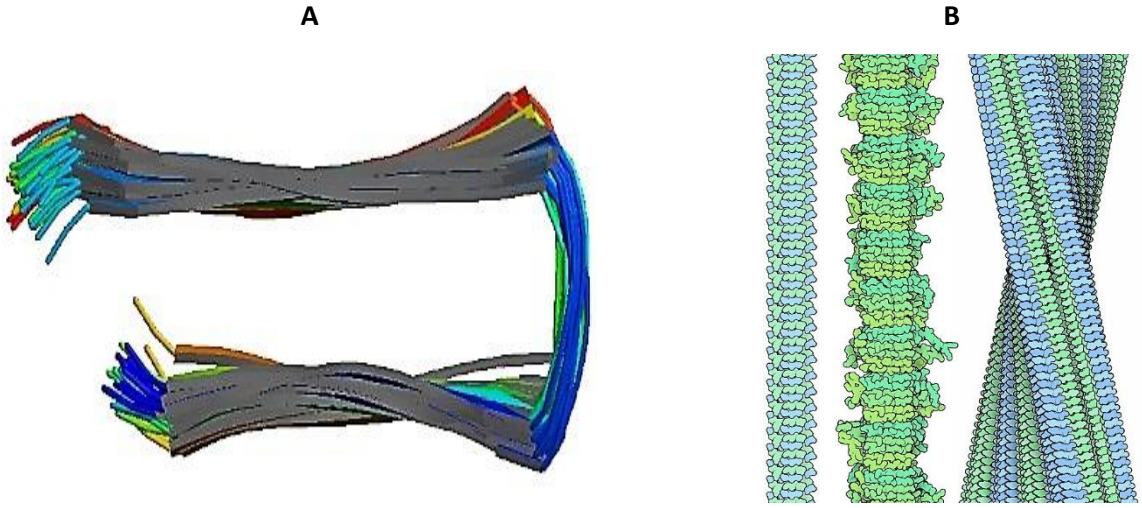

Figure 1.1 (A) Solution-NMR obtained 3D structure of amyloid-beta fibril (1-42) (PDB id: 2BEG). (B) *Left-* The crystal structure of human prion protein peptide with 6 amino acids GYMLGS (PDB id: 3NHC). *Center* The structure of yeast prion HET-s (PDB id: 2KJ3) and *Right:* a peptide from transthyretin (PDB id: 3ZPK)[44].

biological functions. Homotypic polymerization of monomers of size ranging from 3 to 30 kDa results in fibrils that are typically long, unbranched filamentous structure with 5–15 nm in diameter and several micrometers in length.[45,46]

X-ray fiber diffraction patterns of amyloids obtained from different proteins show meridional reflections of ~4.8 Å and equatorial reflections of ~10 Å suggesting a regularly repeating, ordered structural form with the general characteristic of cross-β structures. Due to this common diffraction pattern, the amyloid disease conditions are sometimes referred as β-fibrilloses.[45] The fibrils are composed of multiple thin fibers called protofilaments intertwined with each other. A single protofilament may contain two to six β-sheets separated by a distance of ~10 Å. The protofilament consists of multiple β-sheets running parallel to the fiber axis, with individual β-strands perpendicular to the fiber axis. The β-sheets are found to be in parallel or antiparallel orientation, however, in most of the cases parallel orientation is preferred.[2,47]

1.5. Fibrillation Mechanism and Kinetics

Two major goals in modelling any protein aggregation include: 1) validation of a plausible mechanism by reducing a given proposal to a kinetic scheme whose predictions such as time course of a reaction, concentration dependence, etc., can be compared with experiments

and 2) determination of molecular ingredients, once available scheme has been established i.e., what are the rate constants and what factors determine their observed values.[48,49] The key question in any molecular self-assembly process such as in the formation of filamentous structures as amyloid fibrils is to establish relation between the bulk experimental assays and the individual microscopic steps that contribute to the overall reaction.[50] In all the assembly processes, there is a competition between the formation of intermolecular bonds and the greater translational and rotational entropy of monomers in solution.[51,49] An aggregate is termed post-nuclear, if for a given concentration of monomers, their addition increases its stability rather than decreasing. In kinetic terms, once the nucleus size is surpassed, rate of monomer addition

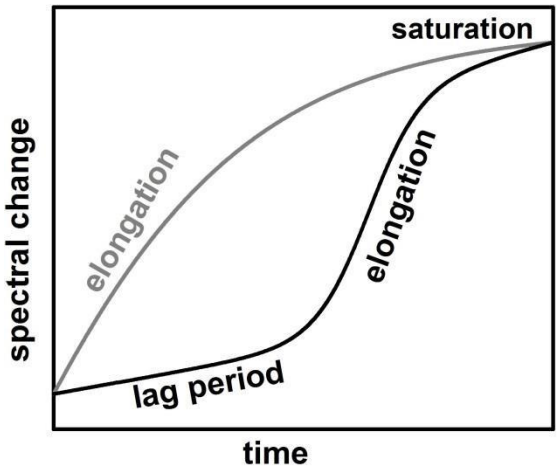

Figure 1.2 Representative kinetic profiles of protein fibril formation by nucleation-dependent (black) and nucleation-independent (gray) pathways.

to the aggregate exceeds the rate of monomer loss, but not before.[51] Major advances in understanding the mechanism of protein aggregation as in the case of many chemical reactions has been achieved by studying rate laws that govern the overall assembly process.[52] Rate laws, the workhorses of chemical kinetics are in general challenging in a closed form expression for complex assembly pathways since the system consists of number of molecular species that can interconvert through a multitude of processes.[52,53]

The kinetics of amyloid fibril formation is analysed using different mathematical equations representing simple exponential to complex secondary processes to interpret the changes measured from different biophysical techniques. Broadly, the fibrillation steps may be characterized into lag phase, elongation phase and saturation phase (Fig. 1.2). However, each macroscopic phase can consist of many microscopic events to contribute which are continuous and mutually influencing each other. Further, experiments to understand specific event could also be performed. For instance, to monitor the elongation phase alone fibril seeds were added

into protein monomers and the fibril elongation on the seed surface was followed.[54,55] In another instance, polymeric surfaces were used to follow the fibril assembly in order to understand specific physical interactions affecting the fibril aggregation mechanisms.[56,57] Some of the major models proposed to study aggregation is discussed below in the order of their complexity of the rate equation rather than the chronological development of different kinetic models.

1.5.1. Simple exponential kinetics

During fibril formation, some of the proteins show a simple exponential (de)increase of spectroscopic signals. In such cases, fibril formation is assumed to be a nucleus-independent event as the monomeric-native forms could be the highest energy species in those proteins. Once partially unfolded, fibril-facilitating conformation is attained, the process becomes downhill polymerization. In such cases, first-order rate equations can be used to calculate the rate of fibril formation.[13,58,59] This assumption has also been used to investigate the effect of mutations and small ions on the rate of fibrillation. Also, studies with the specific objective to probe the fibril elongation rate alone have used a simple exponential function to analyse the kinetic profiles. For instance, in the case of seeding-induced fibril formation reactions (Fig. 1.3) where initial nucleation phase is not observed, this analysis

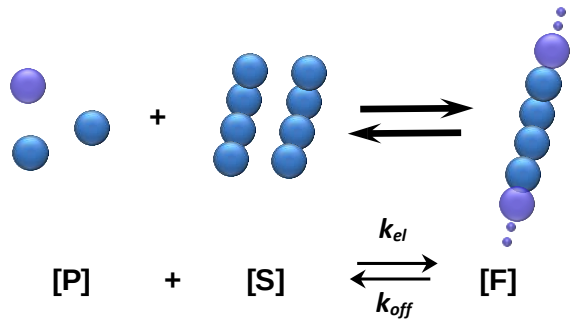

Figure 1.3 Seed-assisted fibril formation process: Addition of monomeric (P) proteins to pre-formed fibril seeds (S) leads to the formation of matured fibrils (F).

provides simpler solution.[60] Generally, the fibril extension kinetics of seeded-fibrillation reaction is described by, $F_{ext} = (k_{el}\,[P] - k_{off})[S]$ (1.1)

where, $[S]$ is the number concentration of the seed, [P] is monomeric protein concentration and k_{el} and k_{off} are the apparent rate constants of fibril elongation and dissociation, respectively. In

this relation, it may be assumed that $k_{off} << k_{el}$ [P] in most of the conditions which further simplifies the equation. At the same time, during the conditions of fibril dissociation, the single exponential function may not be enough to explain the biphasic kinetic profiles. Therefore, exponential-linear functions or double-exponential functions are used to derive the kinetic parameters[60] such as,

$$F_{off} = A_0 + A_1 \, exp^{-k'_{off}(t-t_o)} + A_2 \, exp^{-k''_{off}(t-t_o)} \quad (1.2)$$

where, A_0, A_1 and A_2 are coefficients and k'_{off} and k''_{off} represent the rate constants of biphasic kinetics. However, these analyses assume that the fibril elongation reaction is a homogeneous process, while secondary nucleation and related processes might also contribute to the change in kinetic mechanism.

1.5.2. Three-stage kinetic models

As proposed by Oosawa & Kasai,[61] the transformation of a globular protein to fibrillar aggregation could be viewed as monomers forming linear aggregates which above certain critical concentration form helical aggregates (Fig. 1.4). In later studies, the initial aggregates were essentially suggested to be primary nucleus during fibril formation. Based on the thermodynamic assumptions of aggregation-nucleation, nucleus is a stable identifiable intermediate on the reaction pathway and in equilibrium with its monomers. The nucleation rate is said to be controlled by both the equilibrium constant of nucleus formation and the rate constant of nucleus elongation. Thus, the extent of protein monomers converted to aggregates is given by,

$$[P_{agg}] = \frac{1}{2} \, k_{el}^2 \, K_{nu} \, [P]^{N_{nu}+2} t^2 \quad (1.3)$$

where [P] is initial concentration of monomeric protein, N_{nu} is the number of monomers forming the critical nucleus, K_{nu} is the equilibrium constant between monomers and the nucleus, and k_{el} is second-order fibril elongation rate. It is assumed here that k_{el} is identical for both seeded and non-seeded fibril forming reactions. It is also interesting to note that polyglutamine aggregation kinetics which could be analysed using equation 1.4 showed that the critical nucleus contains only one monomer (N_{nu}=1). Hence, it is reasonable to assume that the nucleus formation could be "unfavourable protein folding reaction" rather than aggregation.[62] Further fibril elongation occurs by the interaction between the nucleus and other unfolded polypeptide chains.

Another form of three-stage kinetic model was proposed by Lee *et al.*[63] for the proteins which are in such cases, oligomer dissociation is considered to be the fibril initiation process

which is followed by nucleation and fibril assembly. In this model, dissociation of oligomers may be replaced with protein misfolding

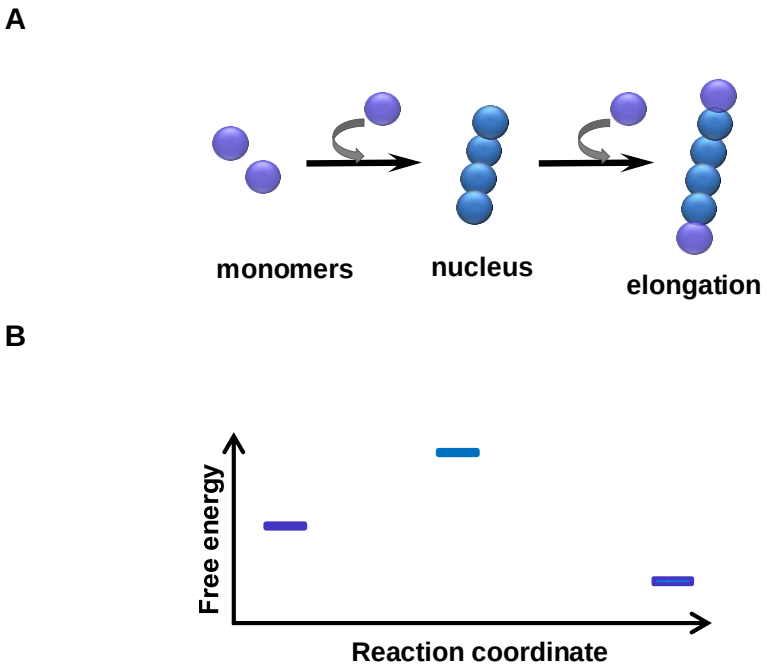

Figure 1.4 Three-stage fibril formation model: (A) At above the critical concentration, monomeric protein forms nucleus. The addition of further monomers with the nucleus leads to fibril elongation at an exponential rate. (B) Relative free energies of different species in the fibrillation reaction.

event for other proteins which could further lead to fibril formation. For instance, fibrillation of insulin is initiated by dissociation of hexameric protein (P^*_6) into monomers followed by nucleation (P_{agg}) and elongation to form matured fibrils (F) as given in Scheme 1.[63] The rate of fibril mass balance could be calculated as,

$$dF/dt = (N_{fb}^2 k_{nu+} - N_{fb}\, k_{fb+})F^2 + (k_{fb+}\,[P_{ini}] - 2\,N_{fb}\,k_{nu+} - k_{fb-})F + k_{nu+}\,[P_{ini}]^2 \qquad (1.4)$$

where, N_{fb} is mean fibril size, $[P_{ini}]$ is initial concentration of monomer, k_{nu+}, k_{fb+}, and k_{fb-} are apparent rate constants for nucleation, fibrillation, and fibril dissociation, respectively. The two real roots of the quadratic equation, r_1, and r_2, correspond to steady-state fibril concentrations. The solution for equation (1.4) is given as,

$$[F] = r_1 + \frac{(r_2 - r_1)}{1 + exp^{-(t-t_o)/k_{el}}} \qquad (1.5)$$

where, k_{el} is the apparent fibril elongation rate and t_o-$2k_{el}$ corresponds to lag time which can be calculated from the following relations:

$$1/\,k_{el} = (N_{fb}\,k_{fb+} - N_{fb}^{\,2} k_{nu+})\,(r_2 - r_1) \qquad \text{and} \qquad (1.6)$$

$$t_o = k_{el}\,ln\,(-r_2/r_1) \qquad (1.7)$$

It is assumed here that k_{nu+}, k_{fb+}, and k_{fb-} are independent of the size of the nucleus. This equation is similar to the empirical relation proposed by Fink *et al.*[55] to calculate lag time and elongation time of fibrillation process by assuming three-stage kinetics of nucleation, elongation, and saturation.

$$y = y_i + \left(\frac{y_f}{1+\exp -(t-t_{1/2})/k_{el}}\right) \tag{1.8}$$

where, y is experimentally observed optical signal, y_i and y_f are the initial and final values of the signal during kinetics, $t_{1/2}$ is the time to reach half of the maximum signal, and k_{el} is elongation. The lag time or nucleation time (t_{lag}) can be evaluated as ($t_{1/2}$ - $2k_{el}$). This equation has been used in many experiments to calculate the kinetic parameters.[64,65]

1.5.3. Secondary-nucleation models

Understanding the microscopic events during the polymerization of proteins has been of interest since the gelation of haemoglobin S (HbS) was characterized. HbS gelation is a major event in sickle cell disease.[48] Based on the concentration dependence of the kinetics, the stochastic behaviour in small volumes and the auto-catalytic property of polymerization, HbS aggregation was modelled using double-nucleation or secondary-nucleation mechanism.

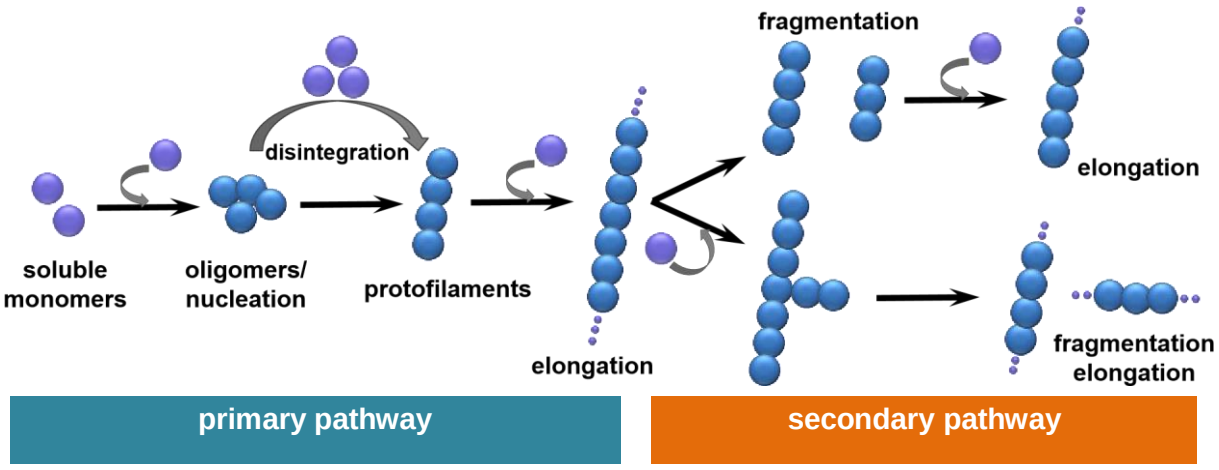

Figure 1.5 Schematic representation of different microscopic events during protein fibrillation reaction. Adapted from refs [51, 65].

This model proposes that the polymerization is initiated by formation of primary homogeneous nucleus. It is followed by the addition of oligomers on the surface of existing nucleus called heterogeneous nucleation (or secondary nucleation)[49] (Fig. 1.5). Though the loss of translational and rotational entropies due to aggregation thermodynamically unfavours the

polymerization, the intermolecular interactions favour the process. At a certain aggregate size, the addition of monomers become favourable compared to the loss of monomers from the aggregate which is referred as 'critical nucleus'. The size of such a nucleus is generally considered to be varying with respect to the protein and the environmental conditions. Further addition of monomers on the surface of the nucleus and subsequent growth of the fibrils are considered as irreversible steps. The kinetic models for HbS have also shown that the mechanism, thus the kinetic parameters, could be better explained by assuming heterogeneous size distribution of the nucleus. However, this model has limitations such as it does not include the effect of ordering and the spatial orientation of the monomers.[48,49]

Secondary-nucleation model has been further extended to analyze the kinetic profiles of the other proteins as well since this could explain the events involved in the sudden exponential increase in the rate of fibril growth after a lag period. The kinetic equations have been developed to address the mechanisms where fibril formation is a nucleation-dependent process and the formation of primary nuclei is slower than the elongation rate. Further, the secondary nucleation processes which assist the formation of additional nuclei from protofilaments are also involved in the fibril growth. The importance of fibril fragmentation as a part of the secondary process comes from the experimental results showing the sensitivity of fibril growth rate against mechanical shear.

The kinetic equation incorporating all these microscopic events could be expressed in terms of either number concentration F_n or mass concentration $[F]$ of fibril growth rate[66,52] as following:

$$F_n = C_1 e^{-\kappa t} + C_2 e^{-\kappa t} - \frac{N_{nu}\, k_{nu+}\, [P_{tot}]^{(N_{nu}-1)}}{2k_+} \tag{1.9}$$

$$[F] = \frac{2k_{fb+}\,[P_{tot}]\,C_1}{\kappa} e^{\kappa t} - \frac{2\,k_{fb+}\,[P_{tot}]\,C_2}{\kappa} e^{-\kappa t} - \frac{k_{nu+}\,[P_{tot}]^{N_{nu}}}{k_{fb-}} \tag{1.10}$$

where, C_1 and C_2 are constants, N_{nu} is the size of the nucleus, $[P_{tot}]$ is total protein concentration, and k_{nu+}, k_{fb+}, and k_{fb-} are the rates of nuclei formation, fibril elongation, and fibril fragmentation, respectively. $\kappa \left(= \sqrt{2k_{el}k_{-}P_{tot}}\right)$ represents the rate of multiplication of filament.

The rate of filament multiplication κ is a crucial parameter and is influenced by both fibril elongation rate k_{el} and the fragmentation rate k_{fb-}. The above equations assume that the rate of nucleus fragmentation is independent of filament length. It was also noted that sigmoidal growth kinetics were observed as a result of secondary nucleation even in the absence of rate limiting primary nucleation events. This is in contrast to the classical homogeneous-nucleation

depended polymerization where the initial aggregation determines the lag phase of fibrillation kinetics. This is further confirmed by the analysis of kinetic parameters which showed that the maximal rate ($t_{max} = \kappa^{-1}\ log\ [1/C_+]$ where C_+ is integration constant during solving the kinetic equation) depends only on the rate of filament multiplication (κ) and not on the other parameters such as primary nucleation rate. However, at the concentrations where protein monomers are sufficiently lower than the seed concentration; κ could be essentially related with lag phase by,

$$t_{lag} = [log\ (1/C_+) - \exp+1]\ \kappa^{-1} \qquad (1.11)$$

This could be understood in a way that in the absence of seeded-fibrillation, primary nucleation is the essential step. However, when secondary-nucleation is active, the lag phase is determined by the early growth rates of fibrils. Under these conditions as well, a correlation between the lag phase and maximum fibril growth rate could be observed due to the fact that both of them depend on a single parameter, i.e., the rate of filament multiplication (κ).

Reaction order is another crucial factor in the rate equations. The order of aggregation (n) during fibril formation can be obtained from the scaling behaviour of macroscopic kinetic parameters (lag time, elongation rate, or half-time).[50]

$$t_{1/2} \propto [P]^{\gamma} \qquad (1.12)$$

where γ is the scaling factor. The slope of a log-log plot of half-time against protein concentration gives the value of γ. If the kinetics is dominated by primary nucleation pathway, γ is approximately equal to $-n_c/2$. On the other hand, if the kinetics is dominated by secondary pathway, $\gamma \approx -(1+n_2)/2$ (where, n_c and n_2 represent the order of primary and secondary nucleation processes, respectively). In a secondary nucleation dominated pathway, if $n_2 = 0$ (i.e., $\gamma \approx -½$), it will suggest that the fibrillation is a monomer-independent secondary pathway. If $n_2 > 0$, it will suggest that the fibrillation is monomer-dependent. In the monomer-independent process, the rate depends only on the existing fibrils and the rate limiting step would be fibril fragmentation whereas in the monomer-dependent process the rate limiting step includes the secondary nucleation of monomers on the existing fibrils' surface.[66] The distinction between the dominance of primary and secondary nucleation pathways may be identified by analysing fibrillation at the early stages, where the monomeric protein concentration is nearly constant and aggregate formation is less. During this period, the relation between reaction rate and aggregate formation could provide information on the nucleation process. If the reaction follows a simple primary-nucleation process, the early changes in the rate might be quadratic in time, $\sim t^2$. If some intermediate species are involved, it may attain a

slightly higher order polynomial. However, the involvement of complex primary nucleation reactions and the dominating secondary-nucleation reactions would lead to very higher order or exponential functions. In those scenarios, the contribution of secondary-nucleation could be studied only through separate experimental procedures such as seeded experiments. At the same time, analysing the later part of the kinetics could predict the fibril growth mechanisms.

The combined mechanism of secondary nucleation along with the nucleation polymerization could also occur during fibrillation.[67] Following initial aggregates, protofibrils, and the matured fibril formation by Aβ-peptide using AFM has shown that the protofibrils may adapt different fibril elongation pathways such as lateral addition and fragmentation, simultaneously. The concentration-dependent changes in the kinetic profiles and the analysis of AFM images collected at different time points during the fibrillation process also support this mechanism.[68]

Based on the above knowledge and framework, objectives have been designed to get an understanding about the relation between the solvent-cosolvent environment and their effect on fibrillation mechanism**.** Also, the relation between the effect of different kinds of small molecules on kinetics and the associated rate constants can provide a larger picture about the proteins' capacity to respond to the surrounding environment which can be correlated with some of the conditions prevailing *in vivo*. Small molecules such as surfactants[69], sugars,[70,] polyols,[71,72,] ionic liquids,[73] salts,[74] alcohols,[75] even variation of solution pH effect the protein structure *via* various mechanism's[76,77,78] and can significantly alter the various phases of fibrillation[10,13 79-80] . The structure that will normally be adopted in the fibrils will be the lowest in free energy and/or the most kinetically accessible. What is clear, therefore, is that the interactions of the various side chains with each other and with solvent are crucial in determining the variations in the fibrillar architecture even though the main-chain interactions determine the overall framework within which these variations can occur. Though the final fibril structure may have common features irrespective of the initial protein sequence and structure, the mechanism of fibril formation may be different depending on varying intrinsic and extrinsic factors. Probing all the microscopic events during this process is difficult. However, the analysis of kinetic profiles of fibril formation obtained at different concentrations and environmental conditions could provide more detailed insight into these processes. This could further pave the way to rightly intervene during the fibrillation process and would also help to design molecules for inhibition of fibril formation.

Chapter 2

Concentration Dependent Switch in the Kinetic Pathway of Lysozyme Fibrillation

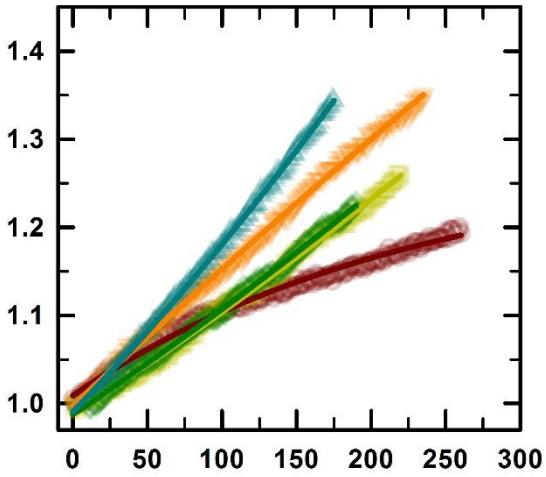

Abstract

Formation of amyloid fibrils has been found to be a general tendency of many proteins. To decipher their role in amyloid diseases, investigating the mechanism and structural features of the intermediates and the final fibrillar state has become crucial. Lysozyme readily formed fibrils at neutral pH and showed two different kinetic pathways that depend on the urea concentration employed. In 2M urea, lysozyme followed nucleation-dependent fibril formation pathway which was not altered by varying protein concentration from 2 mg/ml to 8 mg/ml. However, in 4M urea, the protein exhibited concentration dependent change in the mechanism. At lower protein concentrations, lysozyme formed fibrils without any detectable nuclei (nucleation-independent pathway). When the concentration of the protein was increased above 3 mg/ml, the protein followed nucleation-dependent pathway as observed in the case of 2M urea condition. The different kinetic parameters such as lag time, elongation rate, and fibrillation half-time showed linear dependency against the initial monomeric protein concentration suggesting that under the nucleation-dependent pathway conditions, the protein followed primary-nucleation mechanism without any significant secondary nucleation events. The results also suggested that the difference in the initial protein conformation might alter the mechanism of fibrillation; however, at higher protein concentrations lysozyme shifts to nucleation-dependent pathway which could be kinetically preferable.

2.1 Introduction

Amyloid fibril formation by proteins has been implicated in more than 25 disease conditions.[2,81] Despite of the differences in their amino acid sequences and native three-dimensional structure, the final fibril filaments formed by all of the proteins possesses a common cross β-structure.[46,82] This common tendency of many proteins to form fibrils *in vitro*, in optimized solution conditions,[19] raises many intriguing questions on the guiding principles of fibril formation such as protein stability, structural intermediates, and kinetic mechanism. The fibrillation could be generally initiated from mildly denaturing conditions of the proteins without any additional biological factors which advocates for 'protein-only' hypothesis.[24,83] The necessity of initial partially unfolded state for fibril formation is further supported by readily fibrillating tendency of intrinsically disordered proteins such as α-synuclein[84] and κ-casein.[85] Even stable globular proteins have been converted into fibrillar forms by denaturing their native conformations.[13,86] This proposes that the amyloid fibril state could be another

energy minimum state in the folding landscape of proteins which might be guided through misfolded conformations of the proteins during folding.[87–89]

The studies carried out on the fibrillation of different proteins suggest that the proteins initially form a nucleus which is a slow rate-limiting step. The nuclei upon further interactions form fibrils at an exponential rate.[58,90] Under certain conditions, formation of nuclei may be a non-rate determining step as found in the case of acylphosphatase.[91] Formation of homogenous aggregates or nuclei followed by elongation into fibrils is referred as primary nucleation pathway. Apart from this, other secondary processes like nucleus fragmentation and secondary-nucleation also contributes for overall fibril growth. These major steps further consist of many microscopic events as well.[15,18–20] In order to understand the different fibrillation pathways, many experiments have been carried out to characterize the intermediates during the process. Many intermediate states such as amorphous aggregates, oligomers, protofibrils, and annular aggregates have been identified during fibril reaction.[21,22] Amorphous aggregates generally consist of random coil structure and in certain cases they are found to be irreversible structural conformations or off-pathway products during amyloid formation.[84] Oligomers are simple association of denatured monomeric species and are generally spherical in shape. This is a polymorphic, metastable state and considered to be early key intermediates in the fibril reaction before nucleus formation.[21] Though no specific secondary structural element could be attributed to their conformation, they possess some common properties such as interaction with oligomer-specific antibodies.[23] Protofibrils are kinetically late intermediates which consist of similar β-structures and tinctorial property with thioflavin T (ThT) and congo red (CR) as matured fibrils.[24] However, they are shorter in length, thinner and do not have periodic symmetry as fibrils.[25] The determination of identified intermediates as on- or off-pathway during fibril formation reaction and the relation between kinetic and equilibrium intermediates are still elusive.[14,21] Structural characterization of the intermediates and the kinetics followed by different methods have suggested different kinetic mechanisms on protein fibrillation ranging from simple-exponential models to complex secondary nucleation processes. [16,26] The models are used to calculate the rate constants of different steps and the effect of various parameters such as concentration, pH, temperature and ionic strength on the fibrillation pathway.[15,18,20,27,19] In these studies, concentration dependent changes in the kinetic parameters have been commonly used to define the kinetic mechanism of the protein at particular solution conditions. However, to the best of our knowledge, concentration dependent change in the kinetic mechanism has not been identified in any of the studied conditions. Herein, we report

the effect of protein concentration on the selection of fibrillation pathway between nucleation-dependent and nucleation-independent kinetic mechanisms by lysozyme. The results suggest that the protein undergoes nucleation-independent pathway only at lower concentrations in the presence of 4M urea at neutral pH whereas at higher concentrations it switches-over to nucleation-dependent pathway which could be a kinetically-controlled reaction.

2.2. Materials and Methods

2.2.1. Materials: Hen egg white lysozyme (HEWL), thioflavin-T (ThT), and 8-anilinonaphthalene-1-sulfonic acid (ANS) were obtained from Sigma-Aldrich. Urea, Phosphate salts for buffer were from SRL, India.

2.2.2. Sample Preparation: Varying concentrations of the protein from 2 mg/ml to 8 mg/ml was dissolved in either 2M urea or 4M urea solutions maintained at pH 7 using 20 mM of phosphate buffer. The protein was heated at 60 °C for 10-12 hours to form fibrils. The fibril formation was verified using 40 μM of ThT directly added into the protein solution and monitoring the spectral changes of the dye, by measuring its fluorescence emission between 460 and 540 nm upon excitation at 440 nm, before and after heating.

2.2.3. Microscopic Images: For imaging under transmission electron microscope (TEM), fibrils were dried under ambient conditions on 200 mesh carbon coated copper grids obtained from Ted Pella, then stained with 2% uranyl acetate. Lysozyme fibrils were imaged using Tecnai transmission electron microscope at an accelerating voltage of 200 kV. For atomic force microscopic (AFM) images, the protein samples were kept on a freshly cleaved mica surface for 15–30 min, washed with deionized water, and allowed to dry. Images were collected using an SPA400 (Seiko) microscope under tapping mode at the scan rate of 1–2 Hz and a resonance frequency of 110–150 kHz.

2.2.4. Spectroscopic Analysis: For kinetic experiments, 40 μM ThT was added in to the protein samples with different initial concentrations in 2M or 4M urea at pH 7. The samples were heated at 60 °C in the spectrofluorometer attached with Peltier. The ThT fluorescence changes were followed at 485 nm at regular time intervals. The kinetic traces were fitted to an empirical equation,[28]

$$Y = (y_i - m_i x) + \left[(y_f - m_f x)/1 + exp^{k_{el}(x-x_o)}\right] \quad (2.1)$$

where, Y is fluorescence changes, (y_i - $m_i x$) and (y_f - $m_f x$) represents the initial and final baselines, respectively. x_o is the time needed to reach half of the total fluorescence change and t (=1/k_{el}) is elongation time constant. Lag time can be evaluated using the relation, $t_{lag} = x_o - 2t$. Similarly, the initial nucleation was followed using the fluorescence change of ANS dye at 470 nm after exciting at 380 nm. The obtained kinetic traces were fitted to simple exponential function to calculate the rate of initial aggregation. All of the experiments were carried out in Horiba-fluoromax3 spectrofluorometer.

Circular dichroism (CD) spectra of lysozyme in different conditions were measured in far-UV region using Jasco-1500 spectropolarimeter. The spectra of protein were obtained at room temperature before initiating the fibril reaction, during lag period, and at the end of fibril formation. It may be noted that the ellipticity changes could not be directly correlated to the extent of fibril formation since the fibrils are partially insoluble, particularly at higher protein concentrations.

2.3. Results

2.3.1. Lysozyme fibril formation: Lysozymes are glycosidases involving in the lyses of bacterial cell walls. Two of its natural mutants Ile56Thr and Asp67His are known to cause hereditary non-neuropathic systemic amyloidosis in human.[29] Structural studies show that these variants and the native form of the protein have similar structures. Also, the morphology of the fibrils formed by these variants is similar to the fibrils formed by the native protein at different conditions.[30] However, the mutants have reduced activity at physiological conditions and reduced stability against temperature.[31] Therefore, structural and fibril studies of human lysozyme and it mutants are considered as a good model to probe the fibril mechanism. The human lysozyme has nearly 60% homology with the hen egg white lysozyme (HEWL), thus considered as an effective alternate model to study the fibrillation mechanism of proteins *in vitro*.

Hen egg white lysozyme is a 129-amino acid length globular protein and mainly consists of alpha-helices. Different fibril forming conditions have been identified for lysozyme by altering solution pH, temperature, and co-solvents.[32–34] Though studies were carried out either under acidic or alkaline pH conditions, following the changes at near neutral pH would

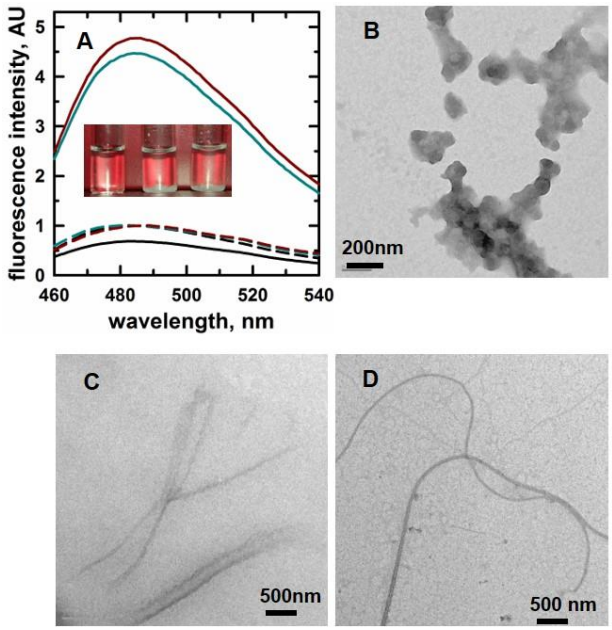

Figure 2.1 Effect of urea on HEWL fibrillation. (A) ThT spectra of HEWL in the presence of 0M (black), 2M (red), 4M (cyan) urea before (dashed lines) and after heating (solid lines) at 60 ℃ for 10-12 hrs. Inset shows the photographic image of final protein sample in 0M, 2M, and 4M urea from left to right direction. TEM images in the absence (B) and presence of 2M urea (C) and 4M urea (D).

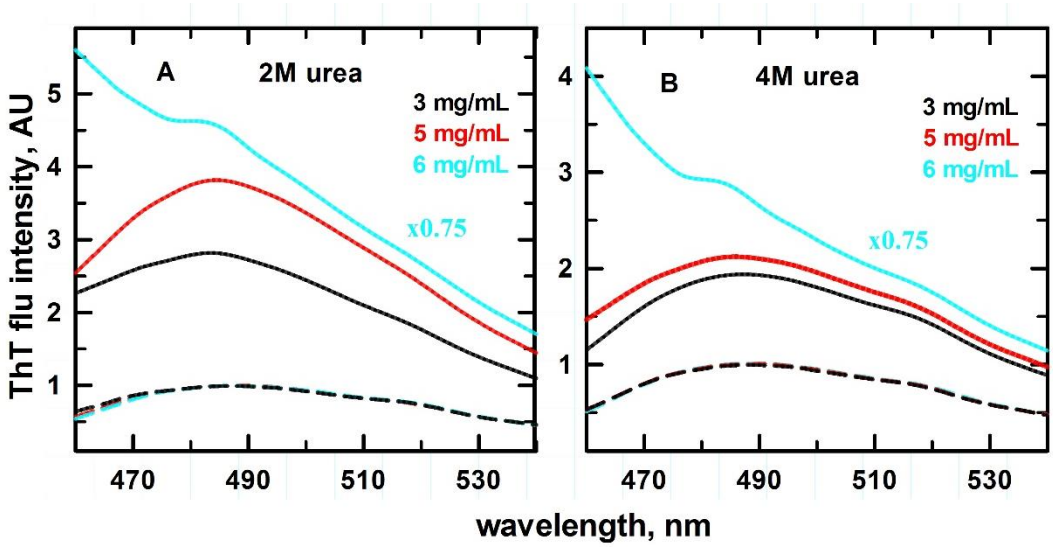

Figure 2.2 Effect of protein concentration on HEWL fibrillation at 60 ℃ for 10-12 hrs. (A) Representative ThT spectra of lysozyme ranging from 2mg/mL to 6mg/mL in 2M urea. (B) Representative ThT spectra of lysozyme ranging from 2mg/mL to 6mg/mL in 4M urea.

be more insightful to correlate their role in both normal and aberrant biological processes.[106] To the best of our knowledge, only two solution conditions were identified for lysozyme fibrillation at neutral pH.[32,33]

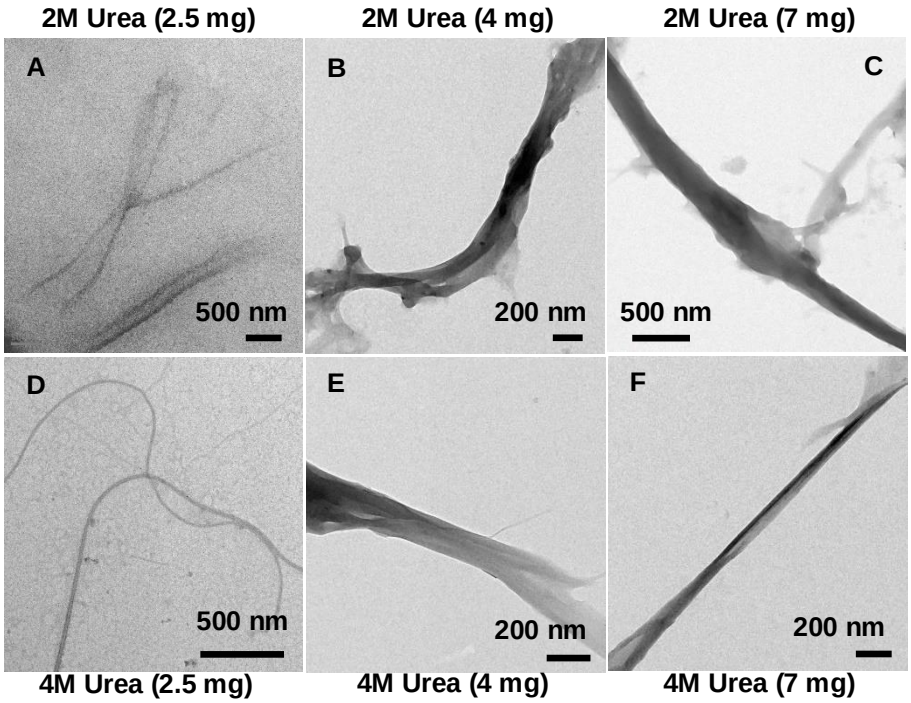

Figure 2.3 TEM images of the HEWL fibril samples in different concentrations (parentheses) in 2M urea (A-C) and in presence of 4M urea (D-F).

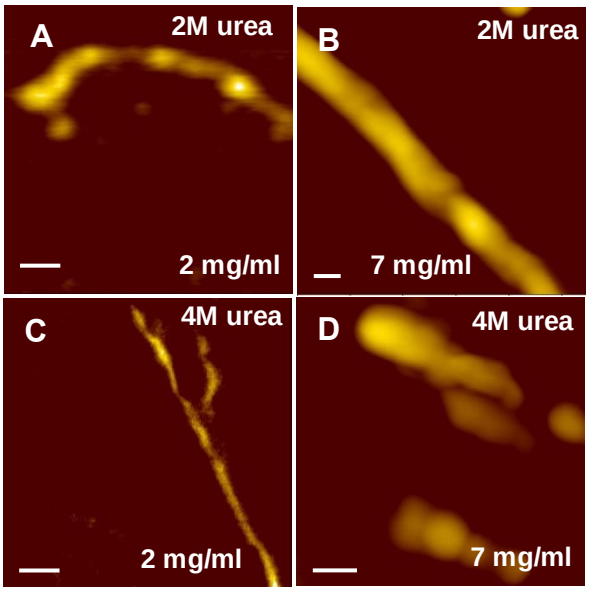

Figure 2.4 Representative AFM images of HEWL fibrils formed upon heating at 60°C for 10-12 hrs in 2M (A and B) and 4M (C and D) urea at neutral pH. The protein concentrations were 2 mg/ml in A&C and 7 mg/ml in B&D. The bar scales represent the dimension of 100 nm.

Following the method of *Wang et al.*[106] HEWL in the presence and absence of urea at neutral pH was heated at 60 ^{o}C for fibril formation. The protein turned turbid after heating for 10–12

h in 2 M and 4 M urea, but no turbidity was observed in the absence of urea. All the samples were assayed with ThT fluorescence. The samples with urea showed an increase in ThT emission intensity, which is characteristic of fibril formation, whereas without urea the intensity slightly decreased. The samples were imaged under TEM for further characterization. The TEM images clearly showed that in the presence of urea lysozyme forms fibrils (Fig 2.1 C & D), but in the absence of urea the protein forms small aggregates (Fig 2.1B), which are not characteristic of amyloid fibrils. Further, the effect of initial protein concentration on the fibrillation process and the associated kinetic mechanism was monitored. Fibrillation of lysozyme from different initial concentrations ranging from 2 mg/ml to 8mg/ml in 2M and 4M urea solutions upon heating at 60 °C for 10-12 h was monitored using ThT. The increase in ThT fluorescence after heating (Fig 2.2) suggested that the protein formed fibrils at all the concentrations. For further verification, the fibrils were imaged using TEM (Fig 2.3) and AFM (Fig 2.4). Though there were slight differences in the morphology of the fibrils, the images clearly showed that lysozyme formed fibrils at all the experimental concentrations.

2.3.2. Kinetics of fibrillation: Lysozyme fibril formation was monitored at regular time intervals using increase in ThT fluorescence as a probe. ThT specifically binds to the fibrils, but not with the early aggregates.[24] In 2M urea conditions, lysozyme showed a three-stage kinetic profile (Fig 2.5A). Initially, there was no significant change in ThT fluorescence

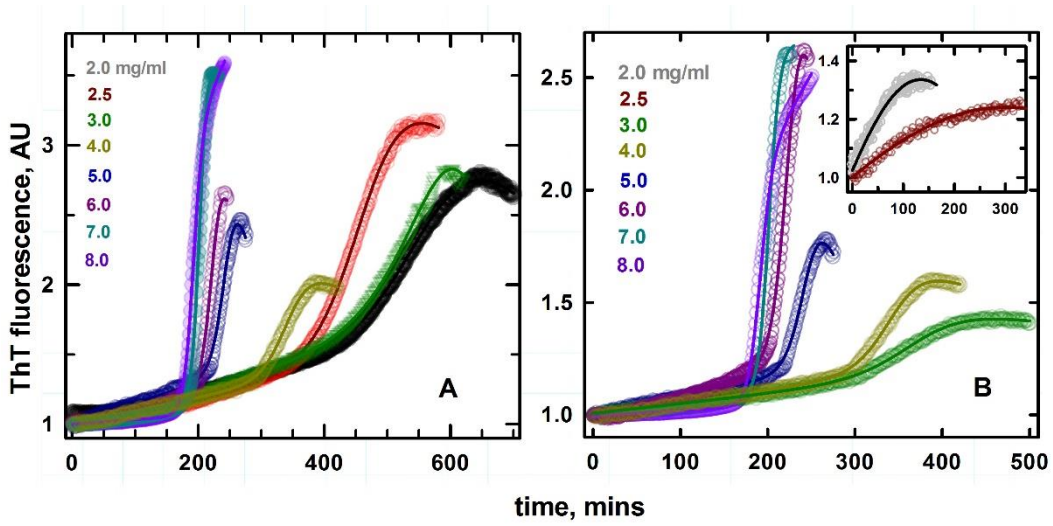

Figure 2.5 Lysozyme fibrillation monitored using increase in ThT fluorescence at 485 nm. Fibril formation in 2M urea (A) and in 4M (B) from different initial lysozyme concentrations are represented by circles in different colors as shown in the labels, respectively. The solid lines represent the fit to equation (2.1). The inset shows the fibril reactions at the lower concentrations of lysozyme in 4M urea which follow nucleation-independent mechanism and the solid line represents the fit to simple-exponential function. The kinetic parameters obtained from curve fit are shown in Table 2.1.

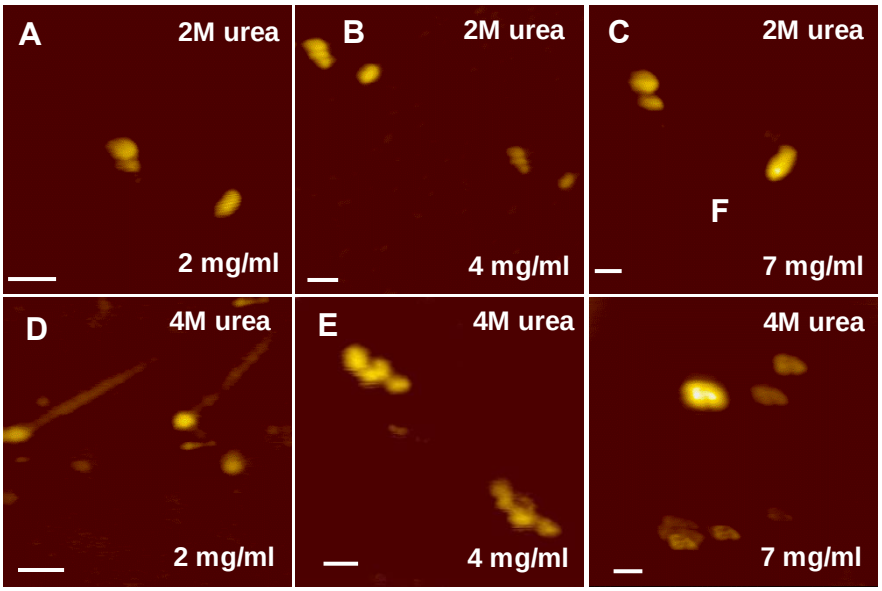

Figure 2.6 AFM images of lysozyme captured after 60 mins upon heating at 60℃ in 2M (A, B and C) and 4M (D, E and F) urea. The protein concentrations were 2 mg/ml in A&D, 4 mg/ml in B&E, and 7 mg/ml in C&F. The bar scales represent the dimension of 200 nm.

suggesting the absence of any early fibril or protofibril formation which is commonly refereed as lag phase. After the lag phase, there was an exponential increase in ThT fluorescence called elongation phase which arises from the formation of fibrils. Following the elongation phase, there was no increase in the fluorescence of the dye suggesting the saturation of formation of matured fibrils by the protein.

In order to verify whether the lag phase consisted of initial nuclei formed by aggregation of unfolded lysozyme monomers, the protein samples were collected after an hour of initiation of the fibrillation reaction and were analysed under AFM. The AFM images (Fig 2.6A-C) evidently showed that the initial phase contained aggregation of the proteins, not matured fibrils. The kinetic traces were fitted to the equation (2.1) to evaluate the major parameters: fibrillation half-time (x_o), lag time (t_{lag}) and elongation rate (k). The obtained values are presented in Table 2.1.

However, in 4M urea, lysozyme showed concentration-dependent change in the kinetic profiles (Fig 2.5B). At lower concentrations of lysozyme (below 3 mg/ml), the fibrillation process did not show any lag phase and ThT fluorescence increased exponentially from the beginning of the experiment. As the concentration of the protein was increased above 3 mg/ml, ThT fluorescence showed three-stage kinetic profile as seen in the case of 2M urea conditions. The early exponential increase in ThT fluorescence suggested that lysozyme might directly

Table 2.1 Lag time and elongation rate of lysozyme fibril formation in 2M

HEWL (mg/mL)	Half time (min)	Lag time (min)	Elongation rate (min^{-1})	k_{agg} ($\times 10^{-2}$ min^{-1})
2.0	572.1	466.9	0.019	…
2.5	465.1	391.0	0.027	…
3.0	619.8	524.4	0.021	…
4.0	344.1	304.4	0.054	0.11
5.0	245.0	224.5	0.0977	0.19
6.0	223.9	206.5	0.1154	0.49
7.0	202.3	189.7	0.1583	0.53
8.0	189.8	176.0	0.1446	0.47

Table 2.1 Lag time and elongation rate of lysozyme fibril formation in 4M urea

HEWL (mg/mL)	Half time (min)	Lag time (min)	Elongation rate (min^{-1})	k_{agg} ($\times 10^{-2}$ min^{-1})
2.0	170.0	…	0.0025	..
2.5	150.0	…	0.002	...
3.0	371.7	307.1	0.031	...
4.0	343.9	304.3	0.050	0.40
5.0	345.0	224.5	0.0975	0.049
6.0	225.2	207.5	0.1129	0.10
7.0	201.5	189.1	0.1621	0.093
8.0	190.5	176.1	0.1394	0.15

form protofibrils followed by matured fibrils without any detectable nucleation processes. This

was further verified by imaging the protein samples collected after an hour of initiation of the fibrillation reaction. The AFM images suggested that protofibrils were detectable at lower lysozyme concentration at early stages of fibrillation (Fig 2.6-D) whereas aggregated-nuclei were found at higher concentrations of lysozyme (Fig 2.6-E and F). The kinetic traces were fitted using simple-exponential and empirical logistic equation (eqn. 2.1), respectively and the obtained parameters are presented in Table 2.2.

In order to understand the structural changes at the different stages of fibril pathway, secondary structural changes of lysozyme were monitored in far-UV region using CD (Fig. 2.7). The ellipticity values gradually increased as the protein concentration was increased from 2 mg/ml to 8 mg/ml both in the presence of 2M and 4M urea. The ellipticity of lysozyme samples were measured during the lag period of the fibrillation at the time points obtained from Table 1. In 2M urea, during the lag period helical structure of lysozyme was significantly lost at all the protein concentrations. Nevertheless, in 4M urea, at lower protein concentration (2 mg/ml) loss of helical structure was observed at the initial period and at higher protein concentrations significant change in the spectral profile corresponding to the induction of more β-sheets was noticed during lag time. Further analysis of the protein structure at the end of reaction times in different conditions invariably showed the formation of high β-sheet contents corresponding to fibril formation. However, these ellipticity values

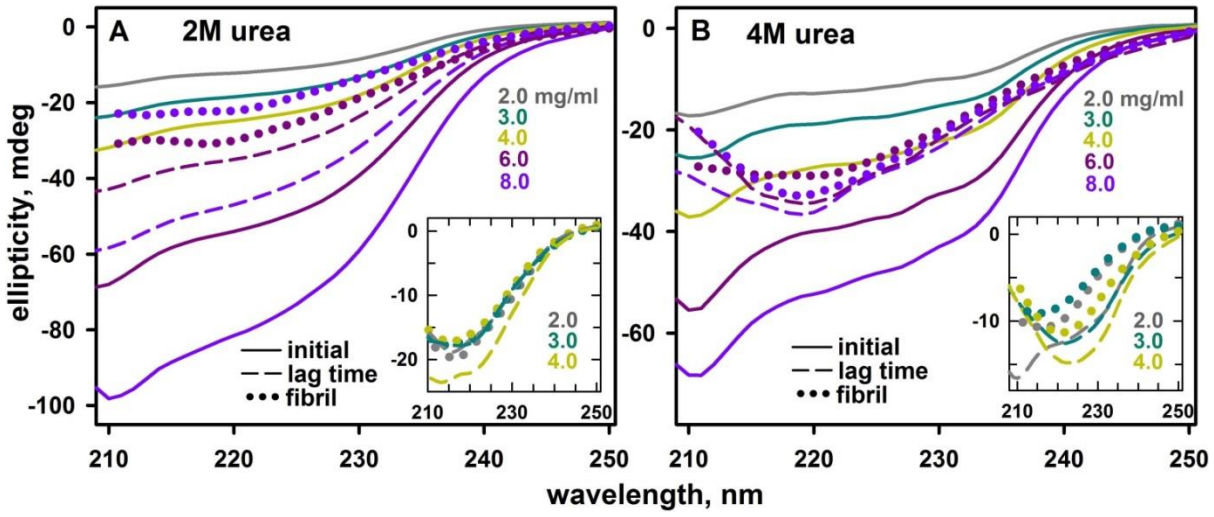

Figure. 2.7 Secondary structural changes of lysozyme in 2M urea (A) and 4M urea (B) followed by ellipticity changes at far-UV region. Representative protein concentrations presented are 2 (gray), 3 (cyan), 4 (green), 6 (pink), and 8 mg/ml (purple). The solid lines are the spectra obtained before initiating fibril reaction, dashed lines are the spectra obtained during lag period (ref. Tables 2.1 and 2.2) and dotted lines are the final fibrils. The spectra of 2, 3, and 4 mg/ml protein concentrations measured at lag time and at the end of fibrillation are presented in insets.

could not be directly correlated to the fibril yield at different condition as the final fibrils were found not to be completely soluble in most of the conditions.

2.3.3. Scaling factor and fibrillation pathway: Scaling factor or scaling exponent (γ) is defined by the relation, $x_o \approx m_i^{\gamma}$ where, m_i is the initial monomeric concentration of

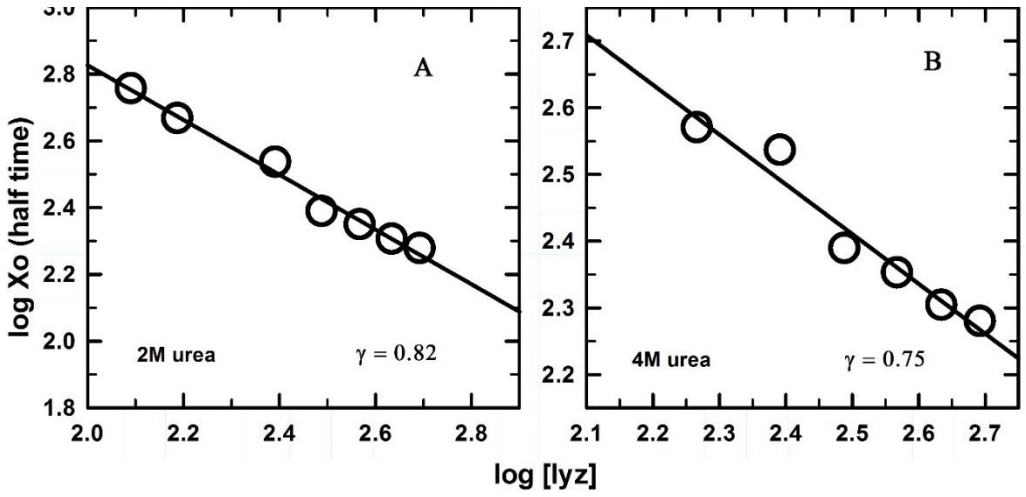

Figure 2.8 A double logarithmic plot of fibrillation half-time against initial protein concentration in 2M urea (A) and 4M urea (B) conditions. The solid lines represent a linear fit and the slopes of the lines correspond to scaling factor (γ).

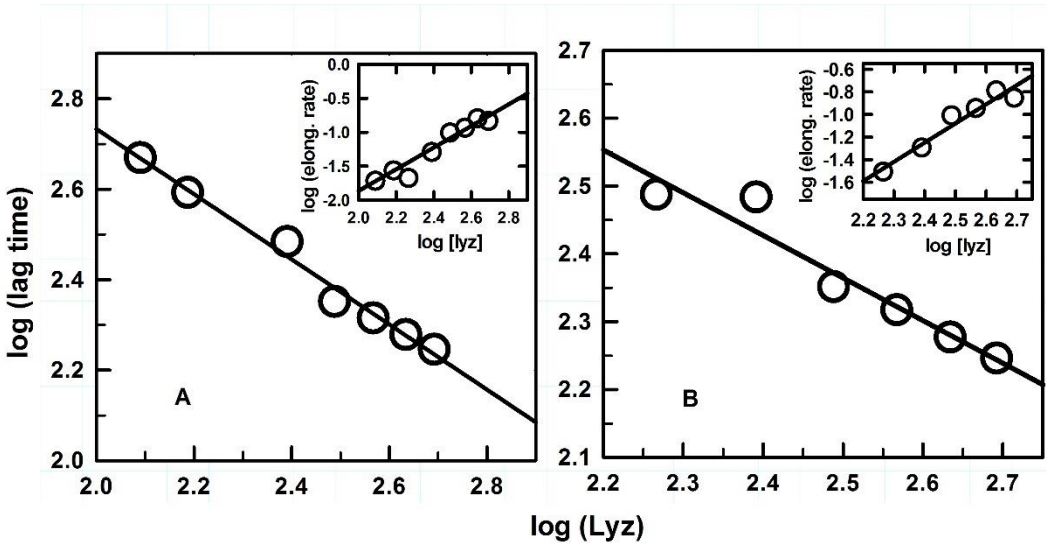

Figure 2.9 Change in lag time against the increasing protein concentration in 2M urea (A) and in 4M urea (B) conditions. The solid lines represent a linear fit and the slopes correspond to λ-value. The insets show the linear relation between elongation rates and initial protein concentration at the respective conditions.

protein.[18,19] The scaling factor can be determined using a double logarithmic plot of half-time versus initial concentration.

The change in x_o against lysozyme concentration in 2M urea showed a linear decrease in x_o with increasing protein concentration (Fig 2.8A) with a scaling factor of 0.82. For the fibrillation reactions in 4M urea, the x_o values obtained from the conditions showing sigmoidal kinetic curves (i.e., [lysozyme] ≥3 mg/ml) were only considered to evaluate the scaling factor of nucleation-dependent kinetic reactions which was calculated to be 0.75 (Fig 2.8B). Further, the values of lag time were plotted against the initial protein concentration (Fig 2.9). This showed a linear relation with the slope (λ) of 0.72 and 0.63 in 2M and 4M urea conditions, respectively which were comparable with that of the insets). The value of scaling factors closer to one and the linearity of the lag time and elongation rate against initial monomeric concentration of the protein suggested that the fibrillation process might be dominated by primary nucleation pathway and the influence of secondary nucleation events could be insignificant[19] at least acted as nucleus for further elongation into fibrils where the secondary processes such as fibril fragmentation and secondary nucleation events were very minimal.

2.3.4. Initial aggregation rate: Considering primary-nucleation mechanism dominated fibrillation pathway of lysozyme both in 2M and in 4M urea conditions, it could be reasonably assumed that the initial lag time would be dominated majorly by the aggregation

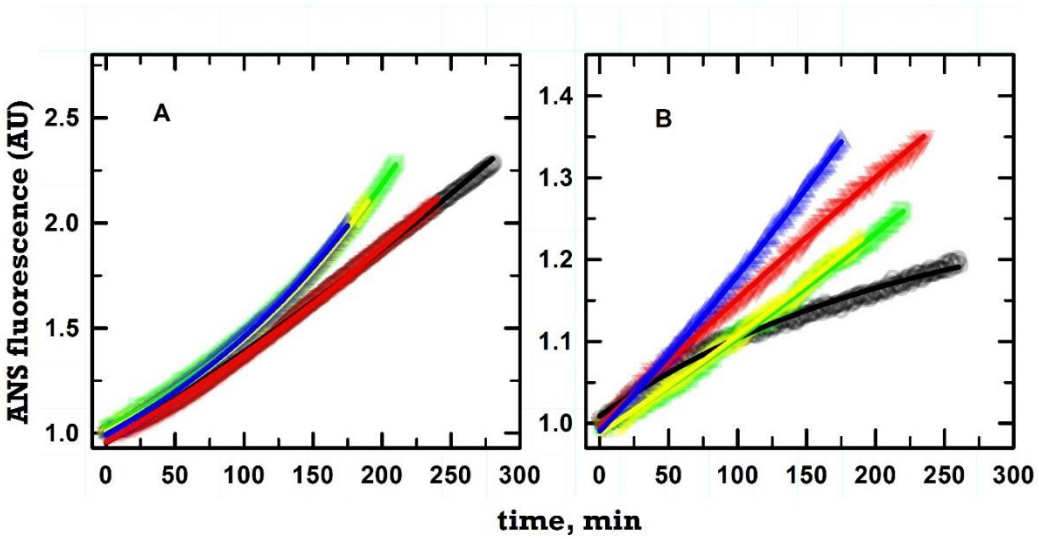

Figure 2.10 Fluorescence emission of ANS dye monitored at 470 nm for the lag period of fibril formation initiated from varying protein concentrations ranging from 4 mg/ml (black), 5 mg/ml (red), 6 mg/ml (green), 7 mg/ml (yellow) and 8 mg/ml (blue) in 2M urea (A) and in 4M urea (B) solutions. The solid lines represent curve fit with simple-exponential function and the calculated initial rates are shown in Table 2.1 & 2.2

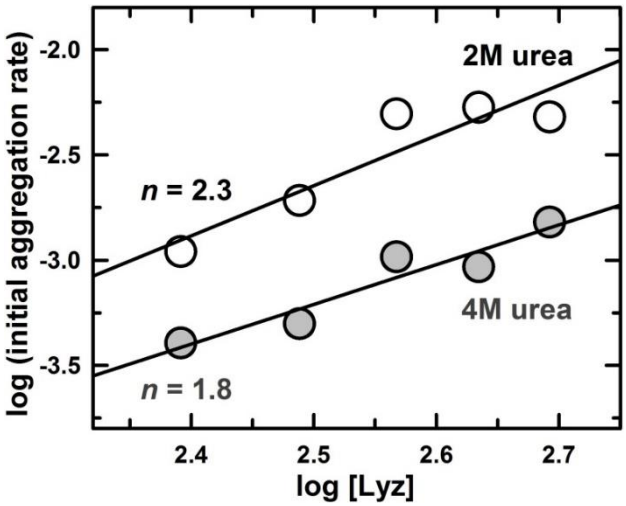

Figure 2.11 The apparent rate of initial aggregation (k_{agg}) evaluated using ANS fluorescence change is plotted against the protein concentration in 2M urea (open circles) and in 4M urea (filled circles). The solid lines represent linear fit and the slopes of the lines correspond to the order of aggregation (*n*).

reaction. Though this aggregation process may consist of many microscopic reactions, the apparent rate of initial aggregation (k_{agg}) could provide more insights into the early stages of the fibrillation reaction.

Since the dye ThT specifically interacts with fibrils alone, it cannot be used to monitor the early aggregation reaction. At the same time, other fluorophoric dyes such as ANS could be used to identify the unfolded and aggregated forms of the proteins as their fluorescence emission increases when they bind to hydrophobic protein surfaces.[35] However, ANS binds to fibrils as well which also increases their fluorescence emission.[36] At the same time, it could be assumed that the lag time calculated for the protein at different concentrations (Table 2.1 & 2.2) using ThT fluorescence changes and the equation (2.1) could be used to scale the time for complete aggregation or nucleation to occur and above this point fibril elongation would be the dominating process. With this assumption in place, ANS fluorescence was followed only up to the aggregation time point (equivalent to lag time) and the kinetic curves obtained were fitted into simple exponential equation to calculate the apparent initial rate of aggregation (k_{agg}) in 2M and 4M urea conditions (Fig 2.10). The aggregation rates were found to be linearly increasing with the initial concentration of the monomeric protein in both the conditions (Fig 2.11). The order of reaction (*n*) was calculated using the relation $log\ m_i \approx n\ log\ (k_{agg})$. The *n* values were found to be 2.3 and 1.8, respectively, suggesting that the fibrillation followed simple primary- nucleation reaction pathway.[20] The high order polynomial (*n*-value) or exponential increase of k_{agg} would have suggested that the nucleation reaction involved complicated intermediated steps such as cascade nucleation. Further, the relation between *n*

and γ, i.e., $\gamma \approx n/2$ further affirmed the fact that the fibrillation is primary-nucleation dominated reaction.[19,37]

2.4. Discussion

2.4.1 Effect of protein concentration on the kinetic pathway:

In 2M urea, lysozyme followed primary nucleation pathway with nucleus formation as a rate-limiting step at all the concentrations. However, in 4M urea, lysozyme showed concentration-dependent change in the kinetic mechanism. At lower concentrations, the protein formed fibrils without any spectroscopically detectable nucleus formation suggesting that at these concentrations the protein followed nucleation-independent pathway which might be accessible through lower energy barrier compared to the nucleation-dependent pathway.

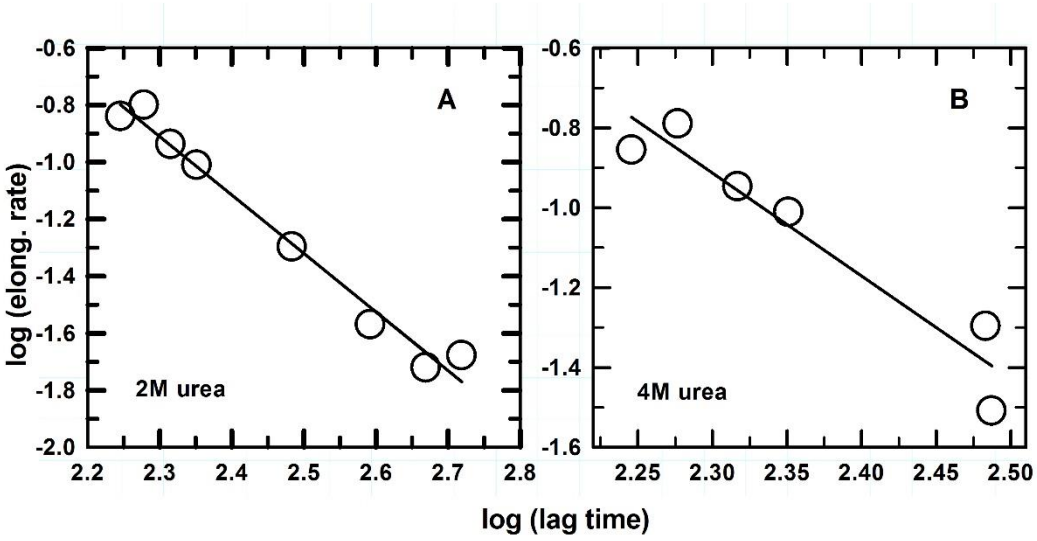

Figure 2.12 Change in the elongation rate against the increasing protein concentration in 2M urea (A) and in 4M urea conditions. The solid lines represent a linear fit.

However, as the concentration of lysozyme was increased the pathway with slightly higher-energy barrier could become accessible (Fig. 2.13). Comparative analysis of the kinetic parameters for nucleation-dependent concentration conditions in the presence of 2M and 4M urea showed that as the nucleation became rate-limiting step, only small changes were observed in the parameters such as γ and λ. Further, the orders of initial aggregation at both the conditions were found to be ~2. The relation between lag time and elongation rate (Fig. 2.12) was also found to be similar in both the cases with comparable slopes. These factors suggest

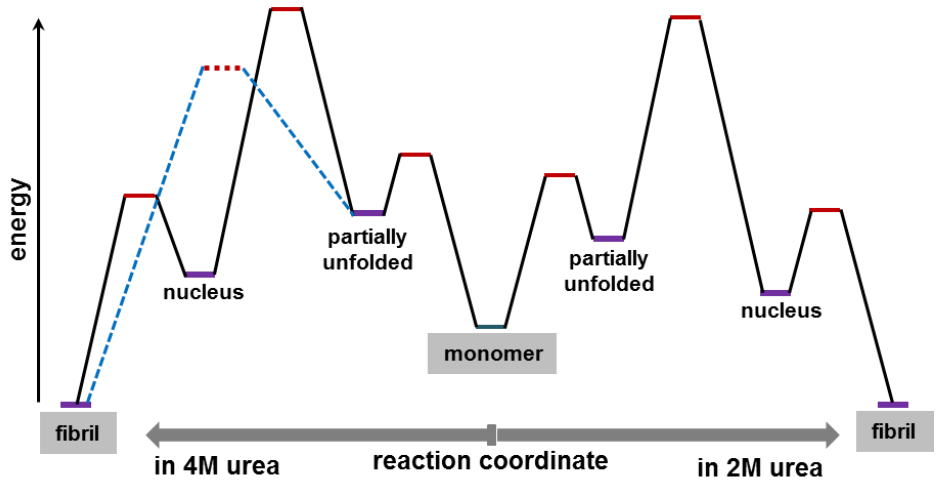

Figure 2.13 Energy diagram explaining the probable fibrillation pathways in 2M urea (on the right) and 4M urea (on the left) conditions. The nucleation-dependent and nucleation-independent pathways are represented by solid and dotted lines, respectively. Initial monomer and final fibril stages are highlighted for visual clarity. Though smooth lines are drawn to represent the pathway, the energy surfaces are generally rough with many intermediate stages.

that at the concentrations where lysozyme follows nucleation-polymerization mechanism, the energy barriers and pathway might be similar in both 2M and 4M urea. Overall, these results propose that nucleus formation followed by fibril elongation would be the more preferable pathway, though it may be kinetically slower. Differences in the initial conformation of the protein might influence the fibrillation mechanism, as observed in the other cases as well.[27,32,34] However, the increase in protein concentration drives the monomers to prefer nucleation-dependent pathway.

2.5. Summary

The fibril formation by lysozyme from different initial protein concentrations has been studied in the presence of 2M and 4M urea at neutral pH. In 2M urea, lysozyme follows nucleation-polymerization mechanism at all the concentrations. In 4M urea, at lower concentrations of the protein, fibrillation reaction follows nucleation-independent pathway whereas at higher concentrations the protein switches over to nucleation-polymerization pathway and this shift might be kinetically-controlled. Different fibrillation-related parameters such as γ, λ, and n obtained at nucleation-dependent conditions show similar values illustrating that both in 2M and in 4M urea lysozyme follows similar kinetic pathway at sufficiently higher protein concentrations, i.e. above 3mg/ml. The probable energy diagram for different reaction pathways has been described.

Chapter 3

Surfactant Induced Changes on Lysozyme Fibrillation: Differential Effects of Ionic and Non-ionic Surfactants

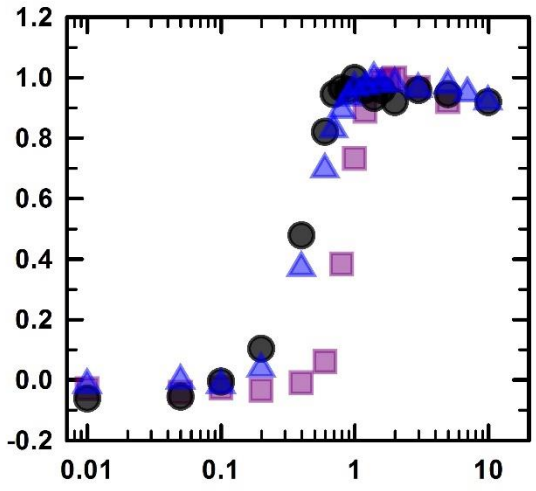

Abstract

Fibril formation tendency is encoded in many polypeptide chains, though not all are associated with diseases. Surface charge on the protein and the added co-solvents is one of the key determinants of the path a protein takes during fibrillation and the associated kinetics. In order, to understand the vital role of this phenomenon, the effects of anionic, cationic and non-ionic surfactants on lysozyme fibrillation were studied. Our earlier studies on lysozyme (chapter 1) showed that it forms fibrils in 2M and 4M urea solutions following nucleation-dependent and nucleation-independent pathways, respectively, at neutral pH. Under these conditions, the effects of sodium dodecyl sulfate (SDS), cetyltrimethyl-ammonium bromide (CTAB), and triton X-100 (Tx) were investigated for their ability to alter the rate constants and or switch the mechanism. The results indicate that there are differential effects of ionic and non-ionic surfactants on fibrillation. Lysozyme could not form fibrils in the presence of SDS and CTAB above their critical micelle concentrations (CMC). However, non-ionic Tx does not inhibit fibril formation at all concentrations. Note that the time for complete fibril formation is increased by Tx. The initial nucleation phase was increased by all the surfactants; however, the extent of increase is less at near the CMC of the ionic surfactants and at above the CMC of Tx. The rates of fibril elongation became faster in 2M urea conditions in the presence of same surfactant class or in comparison to other surfactant type in 4M urea conditions. The results suggest that the nucleation phase of lysozyme fibrillation is primarily controlled by charge interactions and micellation of the surfactants, but multiple factors might influence the fibril elongation. Furthermore, the surfactants do not alter the fibrillation pathway from nucleation-dependent to nucleation-independent or *vice versa* in the studied conditions.

3.1. Introduction

Surfactants are surface active agents that reduce the interfacial tension between two phases by acting at interfaces. Protein-surfactant interactions is not yet clearly understood that depends on the protein under consideration and the nature of surfactant (charge on the head group and length of tail). Denaturation in the presence of surfactants requires almost 1000 times less concentration compared to chemical denaturants and does so by increasing the affinity towards denatured state.[69,111,77] Monomeric and micellar forms of surfactants interact differently with proteins and their micellation is significantly affected in presence of proteins.[69] It has been shown that the aggregation propensity of proteins is also altered by surfactants though a general mechanism cannot be attributed to how different forms of surfactants alter the protein assembly

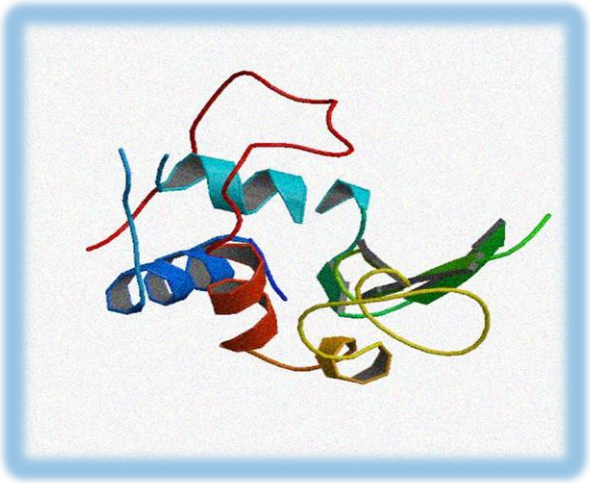

Figure 3.1 Cartoon diagram of hen egg white lysozyme obtained from the crystal structure (PDB id: 2HUB)

pathways.[112,113,114,115,116,117]

Lysozyme-surfactant complexes have been studied for long time to understand the harboured charge and hydrophobic interactions. HEWL's 18 cationic and 10 anionic sites give it a surface charge of +8 at neutral pH and has pI of 11. This positive charge neutralization by oppositely charged surfactant such as sodium dodecyl sulphate (SDS) has been studied to understand the role of charge on solubility and stability of lysozyme. Lower concentrations of SDS precipitates lysozyme that gets solubilized at higher concentrations[118]. Neutron scattering[119] and binding isotherms[120] experiments showed that initial charge neutralization and the subsequent hydrophobic interactions are the factors behind the solubility changes. These characteristics further prompted the studies on the aggregation of lysozyme in SDS, most of which were either under acidic or alkaline conditions. Probing the changes at near neutral pH would provide better understanding of protein-surfactant interaction since charge interactions are crucial and can alter fibril formation. Only two solution conditions have been identified at near neutral pH for lysozyme fibril formation.[105,106] These studies employed the most commonly used denaturants urea and Gdmcl that populate partially unfolded states of lysozyme at neutral pH that further rearrange to form amyloid fibrils in the temperature range 45 ^{o}C to 55 ^{o}C. However, Gdm an ionic denaturant can interfere with the charge interactions between protein and surfactant. Also, the studies reported earlier were mostly limited to lower concentration range of surfactants and mostly anionic surfactants. Our study reported in previous chapter (chapter 2) showed that HEWL forms fibrils at neutral pH in the presence of

moderate concentrations of urea. In 2M urea the protein adapts a nucleation-dependent pathway whereas in 4M urea fibrils are formed *via* nucleation-independent pathway. Under these solution conditions, work done in the present objective considers how anionic, cationic and neutral surfactants in a wider concentration range affect the kinetics and mechanism of fibrillation. The results showed that ionic surfactants inhibit fibrillation in the concentration range above CMC whereas non-ionic surfactants do not inhibit at any concentration range. Further surfactants affect nucleation and elongation phases distinctly and points towards the role of charge interactions between protein and surfactant.

3.2. Materials and Methods

3.2.1. Materials: Chemicals and the necessary reagents were procured as mentioned in section 2.2.1.

3.2.2. Sample preparation: Different concentrations of surfactants ranging from 0.1 to 25 mM SDS, 0.01mM to 20.0 mM CTAB, 0.001 mM to 10.0 mM of Tx were prepared in phosphate buffer at pH 7. Desired protein concentration of 170 μM or 15 μM was achieved by adding lysozyme directly to the aliquots for fibril or unfolding studies respectively. Fibrils were formed by incubating the protein in presence of urea at 60 ℃ for 10-12hrs. Kinetics were followed in presence of 40 μM ThT by heating the samples inside the spectrophotometer using an air-cooled Peltier. Earlier studies showed that micelles of the dye bind more efficiently to fibrils and so the concentration was kept well above its CMC of 4 μM[121] .

The exposure of hydrophobic residues in HEWL were followed by external fluorophoric probe TNS (*p*-toulidino-naphthalene sulphonic acid). Samples with varying concentrations of SDS, CTAB, and Tx were prepared in the presence and absence of urea with 40 μM of TNS in 10mM of phosphate buffer at pH 7. The fluorescence of TNS was measured after exciting the samples at 320 nm and recording the emission between 380 nm and 500 nm. Then, HEWL was added to the samples in such a way that total volume change is ≤ 1% only. Emission was recorded again after equilibrating the samples for an hour.

3.2.3. Spectroscopic measurements: ThT emission spectra were recorded as described in section 2.2.1. For the kinetics measurements, method described earlier in section 2.2.3 was followed. The protein's fluorescence changes were measured by exciting the samples at 280 nm and the spectra were recorded from 300 nm to 400 nm. All the spectra were obtained using

a Horiba Jobin Yvon -fluoromax-3 spectrofluorometer. Ellipticity changes at the far-UV region were measured in a Jasco-810 spectropolarimeter. The ellipticity changes could not be followed for lysozyme in Tx due to its interference in the measurements, probably because of its weak absorption at 280 nm.[122] Thermal denaturation studies were carried out by following the ellipticity changes at 220 nm at temperature intervals of every one degree from 20 to 90 ^{o}C.

3.2.4. Microscopic Imaging*:* TEM and AFM were performed following the same protocol as mentioned in section 2.1.2 to obtain the images of fibrils.

3.3. Results

3.3.1. Effect of surfactants on HEWL fibrillation: HEWL forms fibrils in moderate concentrations of urea either through nucleation-dependent mechanism (2M urea) or through nucleation-independent mechanism (4M urea). These solution conditions standardized were taken as a control upon which the effects of the surfactants, SDS (anionic), CTAB (cationic), and Tx (non-ionic) on the fibrillation were analysed to determine the interplay between protein surface charge and surfactant type. The surfactants exist as monomers at lower concentrations, and form micelles at higher concentrations (above CMC). The concentration at which a surfactant forms micelles is generally affected by the buffer conditions and the co-solvents

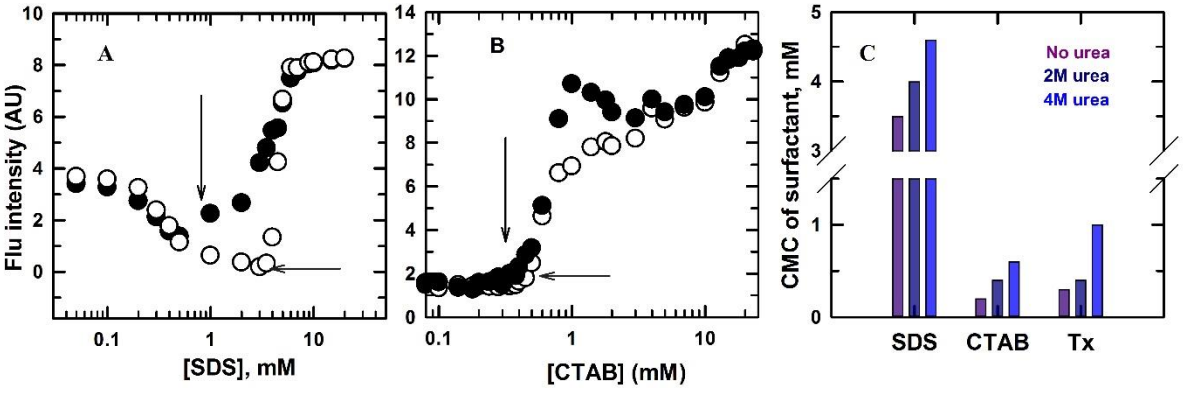

Figure.3.2 (A) Fluorescence emission of safranine measured at 570 nm, after excitation at 420 nm in varying concentrations of SDS in the presence (filled circles) and the absence (open circles) of HEWL. (B) Fluorescence emission of TNS measured at 445 nm, after excitation at 320 nm in varying concentrations of CTAB in 2M urea in the presence (filled circles) and the absence (open circles) of HEWL. The arrows represent the CMC of the surfactants in the presence (filled) and the absence (open) of the protein. (C) Graphical representation of the changes in CMC of surfactants.

Table 3.1 Critical micelle concentration (mM) of surfactants in the presence and absence of urea

Surfactant	SDS	CTAB	Tx
No urea	3.5	0.2	0.3
2M urea	4.0	0.4	0.4
4M urea	4.6	0.6	1.0

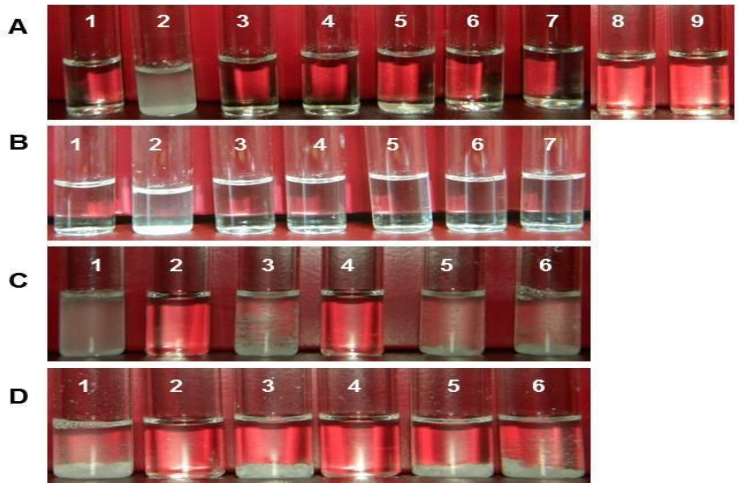

Figure 3.3. HEWL in different surfactant solutions. Solution conditions are given below in the table 3.2

Table 3.2 showing the solution conditions for the images in Fig. 3.3

Row	1	2	3	4	5	6	7	8	9
A	No urea No SDS	No urea 0.5mM SDS	No urea 10mM SDS	No urea 0.1mM CTAB	No urea 5mM CTAB	No urea 0.1mM Tx	No urea 5mM Tx	2M urea 5.0mM SDS	2M urea 5.0mM SDS
B	No urea No SDS	No urea 0.5mM SDS	No urea 10mM SDS	No urea 0.1mM CTAB	No urea 5mM CTAB	No urea 0.1mM Tx	No urea 5mM Tx	---	---
C	2M urea 0.5mM SDS	2M urea 10mM SDS	2M urea 0.1mM SDS	2M urea 5mM CTAB	2M urea 0.1mM Tx	2M urea 5mM Tx	---	---	---
D	4M urea 0.5mM SDS	4M urea 10mM SDS	4M urea 0mM SDS	4M urea 5mM CTAB	4M urea 0.1mM Tx	4M urea 5mM Tx	---	---	---

added; in particular, the CMC of surfactants increases with the addition of urea.[123,124] Therefore, the CMC of the selected surfactants in the presence of 2M and 4M urea were calculated using fluorescence probes, such as safranin and TNS for the buffer conditions used in our experiments. The fluorescence intensity of these probes increases steeply when the surfactants form micelles. This property was used to measure the CMC of the surfactants in the presence and in the absence of lysozyme (Fig 3.1). There is early micellation in the presence of protein and more prominent in the case of SDS (Fig 3.2A) that bears opposite charge compared to the changes observed in the presence of CTAB (Fig 3.2B) (has same head group as proteins surface charge) or Tx. This suggests that polypeptide chain acts as nucleation site for the aggregation of monomers to micelles. The results show that all three surfactants form micelles at higher concentrations in the presence of urea (Table 3.1 and Fig 3.2C). Furthermore, at lower concentrations of SDS, lysozyme formed a precipitate, which dissolved into solution at higher concentrations of SDS, as found in earlier studies.[118] We then examined whether this transition occurs in the presence of urea and in the case of other surfactants, CTAB and Tx, aswell. The protein solutions prepared in CTAB and Tx did not show any turbidity. Moreover, the protein showed complete dissolution at lower concentration of SDS in the presence of 2M and 4M urea (Fig. 3.3A).

In order to evaluate the effect of the surfactants on lysozyme fibrillation, different concentrations of the surfactants, ranging from their monomeric to micelle concentrations, were added to the protein solution in the presence of 2M or 4M urea and heated at 60 ^{o}C for 10-12 hrs. The ThT fluorescence intensity was measured before and after incubating the samples at the higher temperature and the increase in ThT fluorescence was considered to indicate the formation of fibrils. ThT is known to show higher fluorescence in the presence of SDS micelles, but not in CTAB or Tx.[121] To avoid the surfactant's effect, the fluorescence intensities were normalised, with the fluorescence of the respective samples measured before heating. In the presence of 2M urea, ThT showed an increase in fluorescence intensity for the lysozyme samples containing lower concentrations of SDS and CTAB. However, in the presence of higher concentrations, that is above the CMC of SDS and CTAB in 2M urea, the fluorescence intensity was similar to the samples measured at room temperature (Fig. 3.4A & B). Lysozyme, in the presence of all the concentrations of Tx, showed an increase in ThT fluorescence upon incubation at the higher temperature. There were also considerable changes in the visual appearance of the samples. In the presence of lower concentrations of SDS and CTAB, the samples showed turbidity, but in the presence of micellar concentrations of these

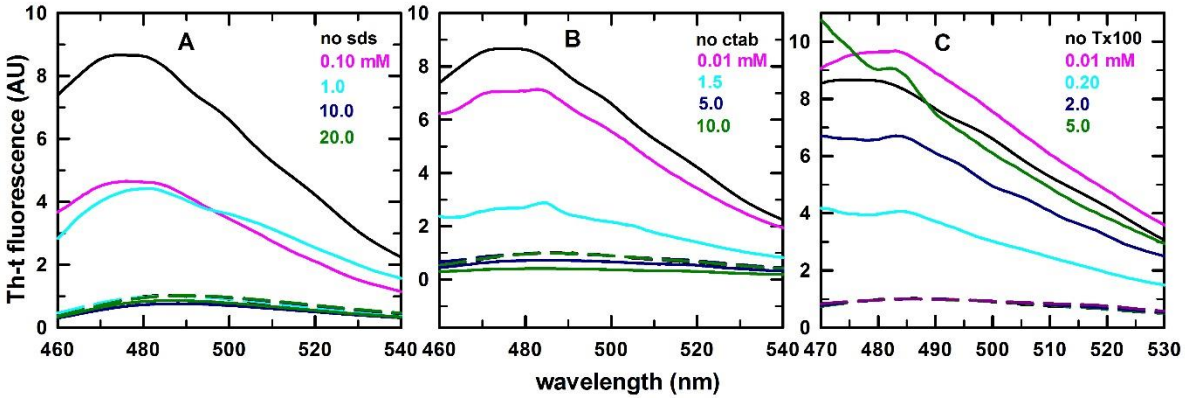

Figure 3.4. Effect of surfactants on HEWL fibrillation in 2M urea. Dashed and solid lines represent ThT spectra measured before and after heating at 60 ºC. (A) ThT fluorescence in presence of 0 (black), 0.1 (pink), 1.0 (cyan), 10 (blue), 20 (green) SDS. (B) 0 (black), 0.01 (pink), 1.5 (cyan), 5 (blue), 10 (green) CTAB. (C) 0 (black), 0.01 (pink), 0.2 (cyan), 2.0 (blue), 5.0 (green) Tx.

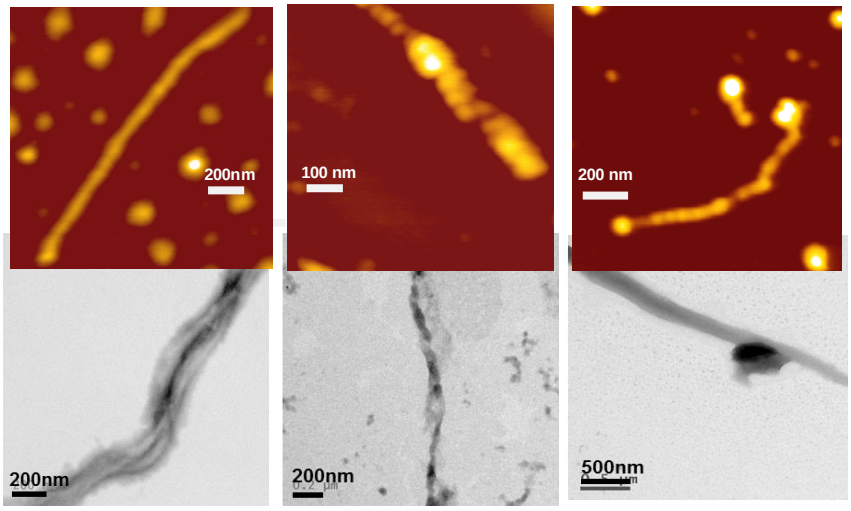

Figure 3.5. (A-C) Representative AFM images and (D-F) the TEM images of the protein fibrils formed in presence of 0.1 mM SDS, 0.3 mM CTAB, and 5.0 mM Tx.

surfactants, the samples were clear and transparent. In Tx, irrespective of the surfactant concentration, lysozyme showed a turbid insoluble component (Fig. 3.3C). The insoluble components with a turbid appearance might be due to fibril formation of the protein under these conditions. For further characterization, the samples were imaged under AFM and TEM. The TEM images showed that the samples contained long and twisted fibrils, similar morphologies were obtained from AFM also (Fig.3.5A-B). The same experiments were repeated for lysozyme in the presence of 4M urea. The results were found to be similar to the 2M urea samples. The ThT fluorescence of lysozyme samples in the lower concentrations of SDS and

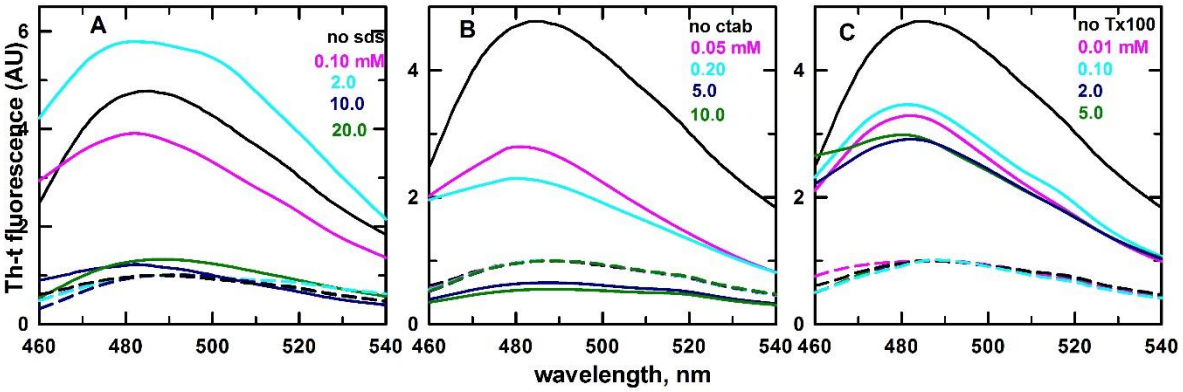

Figure 3.6. Effect of surfactants on HEWL fibrillation in 4M urea. Dashed and solid lines represent ThT spectra measured before and after heating at 60 ºC. (A) ThT fluorescence in presence of 0 (black), 0.1 (pink), 2.0 (cyan), 10 (blue), 20 (green) SDS. (B) 0 (black), 0.05 (pink), 0.2 (cyan), 5 (blue), 10 (green) CTAB. (C) 0 (black), 0.01 (pink), 0.1 (cyan), 2.0 (blue), 5.0 (green) Tx.

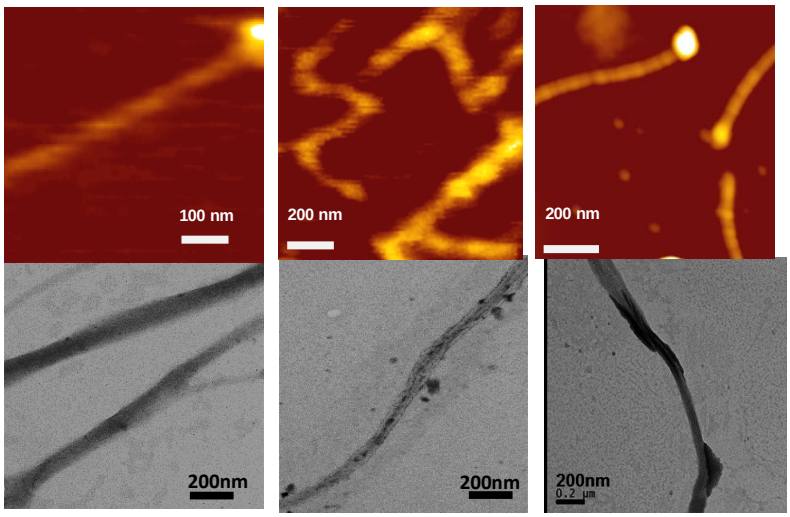

Figure 3.7 (A-C) Representative AFM images and (D-F) the TEM images formed in presence of 0.2 mM SDS, 0.5 mM CTAB, and 5.0 mM Tx.

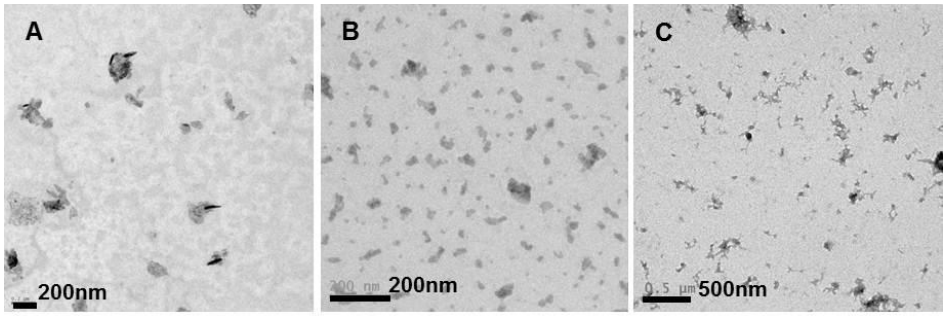

Figure 3.8 TEM images of HEWL heated at 60 ℃ for 10-12 hours in (A) 5mM Tx 100 without urea, (B) 5mM CTAB and 2M urea, and (C) 20mM SDS and 4M urea.

CTAB and in all the concentrations of Tx showed an increase in intensity, but above the micellar concentrations of SDS and CTAB, Th- T did not show any increase in the fluorescence intensity (Fig. 3.6A–C). Moreover, the samples with higher fluorescence intensity were turbid (Fig. 3.3-D). The AFM and TEM images of these samples also showed long and twisted fibrils, but with slightly different morphologies (Fig. 3.7A-C and Fig. 3.7D-F). The experiments carried out in the absence of urea did not show any significant change in the sample appearance (Fig. 3.3-B) or ThT fluorescence. The TEM images of the representative samples at different conditions that did not show any characteristics of fibrils are presented as shown in fig 3.8.

3.3.2. Kinetics of Fibril formation: The fibril formation was followed using the change in ThT fluorescence. Lysozyme in the absence of urea did not show any significant change in ThT fluorescence over time, whereas in the presence of 2M and 4M urea showed different kinetics profiles (Fig. 3.10 & 3.11). The kinetics traces were analyzed using eqn (2.1)[125] and the resultant parameters are presented in Table 3.3. In 2M urea, lysozyme showed an initial nucleation or lag phase, followed by a fibrillation or elongation phase. In the absence of any surfactant molecules, lysozyme showed ~2 h of initial lag phase in 2M urea. The initial lag phase was extended for lysozyme in the presence of all three of the surfactants under the fibril forming conditions, except in SDS near the CMC. For SDS and CTAB, even with concentrations below the CMC, two distinct regions were observed. The lag phase was longer at the lower concentrations compared to the lag time at the concentrations near the CMC. In Tx, the lag phase of lysozyme was extended at concentrations below the CMC, compared to the lag time at the micellar concentrations. However, the rate of fibril elongation did not change significantly in the presence of any of the surfactants, although slower rates were observed in higher concentrations of SDS (~2 mM). Above the CMC of SDS and CTAB, no increase in the fluorescence of ThT was observed, which is consistent with the results discussed in the previous section.

In 4 M urea, lysozyme fibrillation did not show any lag phase (Fig.3.11A–C). The ThT fluorescence exponentially increased from the onset of the kinetics, suggesting the presence of only a fibrillation phase. In the lower concentrations of SDS and in the higher concentrations of CTAB and Tx, lysozyme fibrillations lowered down. In other concentrations of the surfactants, the fibrillation rate was not significantly affected (Table 3.3 and Fig. 3.11C). Similar to the results observed in the 2 M urea conditions, the micellar concentrations of SDS and CTAB did not increase the ThT fluorescence, reiterating the absence of fibril formation at

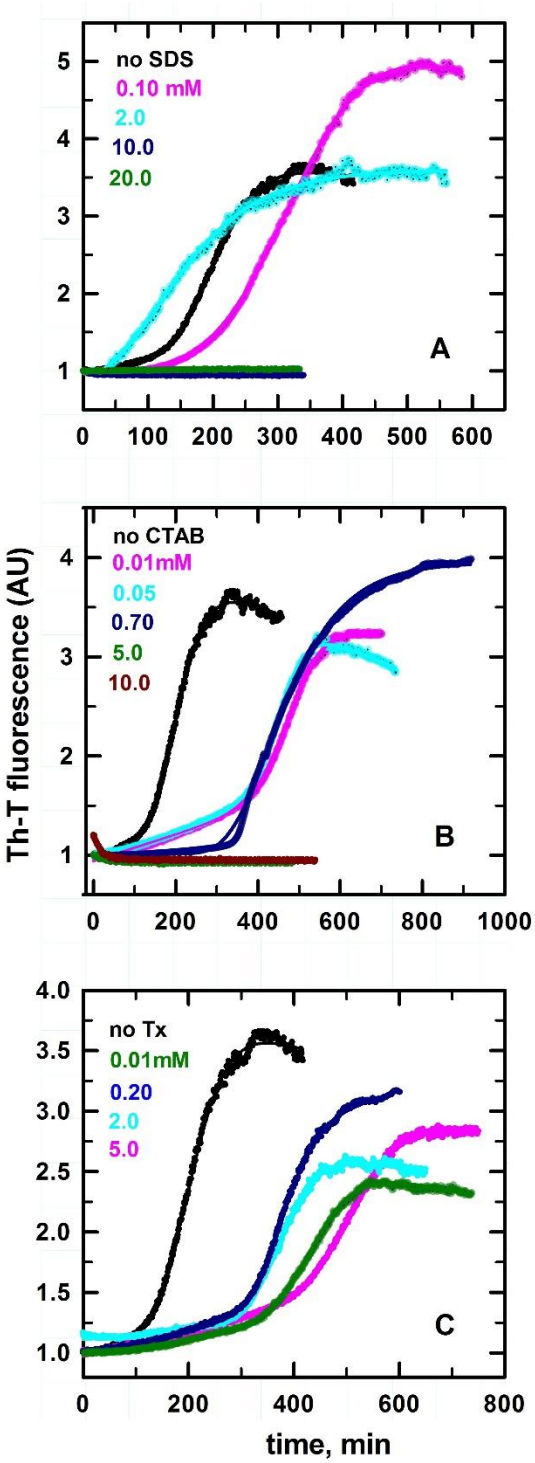

Figure 3.10. (A-C) Representative kinetic curves of HEWL fibrillation in 2M urea followed by changes in ThT fluorescence. The color corresponding to the kinetic curves represent the concentration of surfactants used for following their kinetics. There is no increase in the fluorescence intensity of samples with higher concentrations of SDS and CTAB in plots A & B

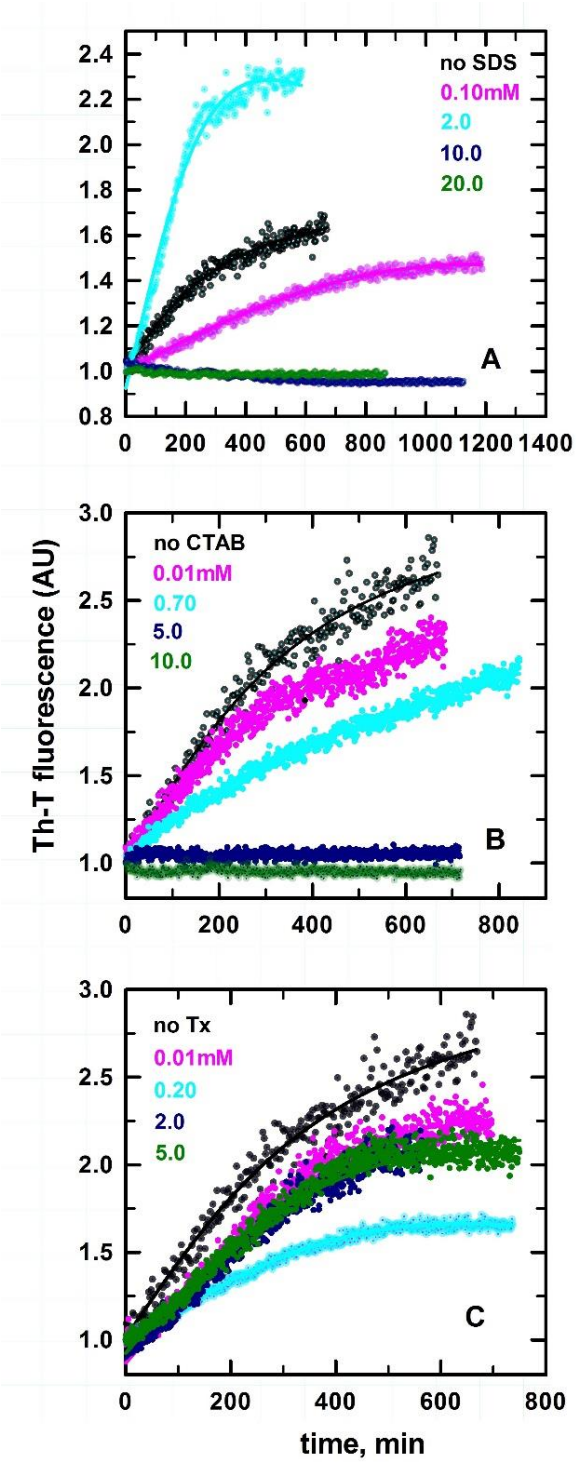

Figure 3.11. (A-C) Representative kinetic curves of HEWL fibrillation in 4M urea followed by changes in ThT fluorescence. The color corresponding to the kinetic curves represent the concentration of surfactants used for following their kinetics. There is no increase in the fluorescence intensity of samples with higher concentration of SDS and CTAB in plots A and B

Table 3.3. Lag time and elongation rate of lysozyme fibrillation

Surfactant	Concentration (mM)	2 M urea		4 M urea‡
		Lag time (min)	Rate (min^{-1})	Rate (min^{-1})
-	0	125.4	0.027	0.0053
SDS	0.1	188.2	0.019	0.0011
	0.2	136.2	0.037	0.0018
	2.0	67.4	0.005	0.0074
CTAB	0.01	398.5	0.025	0.0065
	0.05	386.2	0.029	0.0076
	0.2	278.9	0.034	0.0076
	0.7	315.4	0.020	0.0031
Tx	0.001	367.0	0.021	0.0059
	0.01	421.3	0.021	0.0050
	0.1	422.2	0.020	0.0049
	0.2	308.9	0.028	0.0025
	0.5	282.3	0.036	0.0029
	2.0	307.6	0.028	0.0022
	5.0	313.8	0.031	0.0023

‡ - no lag phase is observed

these concentrations. The amplitude of ThT fluorescence was similar in the case of the CTAB and Tx samples, but varied in SDS concentrations. This could be due to the varying interaction of SDS with ThT, which alters the fluorescence emission of ThT.[121] However, the amplitude change between the samples with 2 M and 4 M urea might be due to the differences in the morphology of the fibrils formed under these conditions.

Furthermore, to characterize the protein in the lag phase and elongation phase, TEM images were obtained during the fibrillation process i.e., after 80 minutes of the initialization of the kinetics. The images showed that the protein formed aggregates at the initial stages of the kinetics in 2 M urea, which could represent the nucleation for further fibrillation. However, in the 4 M urea condition, the formation of thin fibrils at the early stage suggested a nucleation

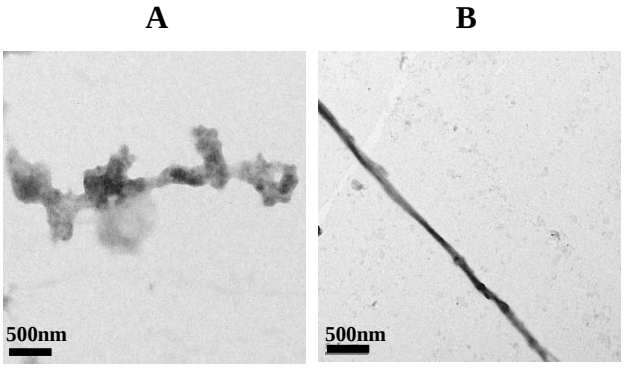

Figure 3.9 TEM images of HEWL heated at 60 °C for 80 mins, i.e., at the early stage of fibrillation in (A) 2 M urea and (B) 4M urea.

independent pathway (Fig.3.9B). These results further affirm the facts observed in equilibrium experiments, the differences in the kinetics pathway adapted and the role of morphology of the fibrils formed under different conditions employed, in the presence and absence of urea as well as in the presence and absence of surfactants.

3.3.3. Surfactant-induced denaturation: To investigate the conformational changes of lysozyme in the presence of surfactants, changes in the intrinsic fluorescence of the protein were measured. HEWL has six tryptophan residues, among which four of them are in the α-domain and the other two are in the loop region connecting the α- and β-domains. Upon excitation at 280 nm, and in the presence of surfactants, lysozyme invariably showed an

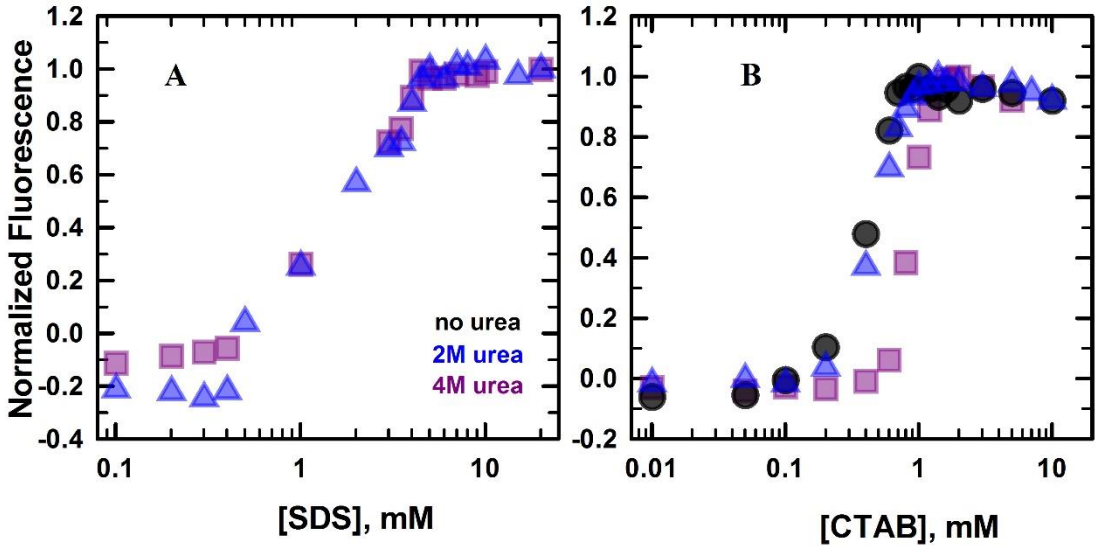

Figure 3.12. Changes in the fluorescence emission of HEWL followed at 350 nm in (A) increasing concentrations of SDS in 2M urea (blue triangles) and 4M urea (dark pink squares), and in (B) iincreasing concentrations of CTAB in 0M (black circles), 2M (blue triangles) and 4M urea (pink squares).

emission maximum at 350 nm. The fluorescence emission intensity changes are presented in Fig. 3.12. However, due to the insolubility of lysozyme in SDS at lower concentrations in the absence of urea, the fluorescence changes could not be measured for those samples. When lysozyme was titrated against SDS in the presence and in the absence of 2M and 4M urea, it showed a two-state cooperative transition (Fig. 3.12A). Up to 0.4 mM of SDS, the fluorescence intensity was not altered; while further increases in the SDS concentration increased the intensity cooperatively up to ~5 mM. Increasing the surfactant concentration above 5 mM (in 4 M urea) or 6 mM (in 2 M urea) or 6.5 mM (without urea) did notalter the fluorescence emission. However, in the case of CTAB, the pre-transition region was also affected by the presence of urea (Fig. 3.12B). The lysozyme fluorescence emission was not changed up to 0.1 mM of CTAB, but it increased after the addition of CTAB up to 0.7 mM. Further additions of CTAB did not change the fluorescence in the absence of urea. The fluorescence intensity of the protein started to increase from 0.2 mM and 0.4 mM of CTAB concentrations in 2M and 4M urea, respectively. There were no fluorescence changes observed above 0.95 mM and 1.4 mM of CTAB in 2M and 4M urea, respectively. Fluorescence changes in the presence of Tx could not be measured because of its strong absorption at 275 nm and 283 nm.[122]

3.3.4. TNS Fluorescence: Furthermore, to investigate the interaction between HEWL and the surfactants, TNS was used as an external fluorophoric probe. The fluorescence quantum yield of TNS increases when it interacts with hydrophobic surfaces, compared to polar surroundings.[124] This property was used to probe the exposure of the hydrophobic residues of proteins upon their interaction with denaturants.[126],[127] In general, the fluorescence emission of the dye varies with varying the concentration of surfactants.[124] Therefore, the emission

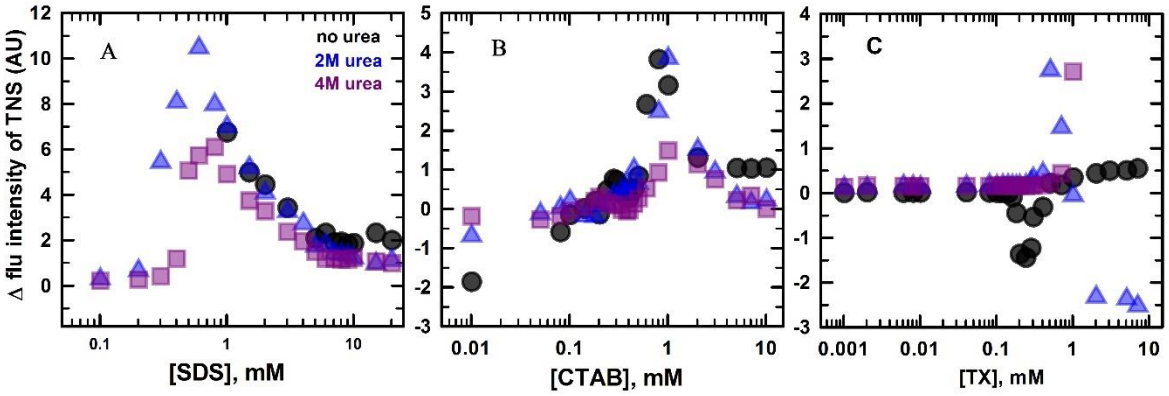

Figure 3.13. Differences in the fluorescence intensity of TNS before and after addition of protein in varying concentrations of (A) SDS and (B) CTAB (C) Tx and in presence of 0M (black circles), 2M urea (blue triangles) and 4M urea (pink squares).

intensity of TNS was measured in the presence and in the absence of the protein at different concentrations of the surfactants. In order to understand the change in TNS fluorescence due to the protein–surfactant interactions, the change in fluorescence intensity of TNS after the addition of HEWL into the surfactant solutions was calculated (Fig. 3.13). Since the protein was insoluble at lower concentrations of SDS in the absence of urea, data could be obtained for the SDS concentrations above 1 mM only. The TNS fluorescence increased when HEWL was added into 1 mM of SDS. However, the intensity came down upon increasing the SDS concentration, and no change in dye intensity was observed above 6.5 mM of SDS. In the presence of 2M and 4M urea, TNS fluorescence increases at the concentrations of SDS above 0.2 mM and 0.3 mM, respectively. In both cases, the addition of SDS above 0.6 mM reduced the florescence intensity, up to 6 mM, and no difference in fluorescence was observed at concentrations of SDS above 6 mM. TNS fluorescence at the lower concentrations of CTAB decreased upon the addition of HEWL in the absence of urea, but increased as the concentration of CTAB was increased above 0.1 mM. At concentrations above 0.8 mM of CTAB, TNS fluorescence decreased, and above 3 mM of CTAB, there was little fluorescence change. In the presence of 2 M and 4 M urea, TNS fluorescence was not altered up to 0.2 mM and 0.4 mM of CTAB concentrations, respectively, by the addition of HEWL. Above these concentrations, TNS fluorescence increased with increasing the CTAB concentration, which again decreased above 1 mM and 2 mM of CTAB upon the addition of the protein in the presence of 2 M and 4 M urea, respectively. At concentrations above 4 mM of CTAB, no change in the TNS fluorescence was observed in both the cases. In the case of Tx, the difference in the TNS fluorescence before and after the addition of protein was insignificant, both in the presence and in the absence of urea.

3.3.5. Secondary structure analysis: To analyze the changes induced by the surfactants on the secondary structure of lysozyme, changes in the ellipticity of the protein was measured at the far-UV region in varying concentrations of the surfactants. The changes in the ellipticity at 220 nm are shown in Fig 3.14. SDS, in the presence and in the absence of urea, increased the ellipticity of the protein up to 1.5 mM; however, the protein lost this increased ellipticity upon further addition of SDS. It was also observed that in 4M urea, the extent of the increase in the secondary structure of lysozyme is less compared to the samples in 2M urea and in the absence of urea. Contrary to the SDS case, CTAB showed no significant change in the secondary structure of the protein in the absence and in the presence of 2M urea. In the presence of 4M

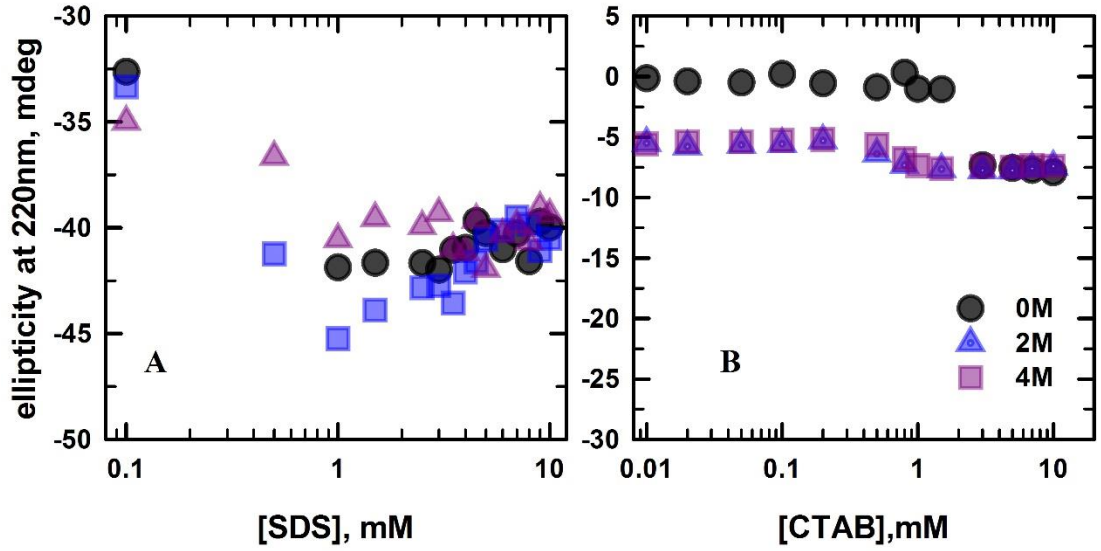

Figure 3.14. Changes in the ellipticity of HEWL followed at 220 nm with (A) increasing concentrations of SDS in 0M urea (black circles), 2M urea (blue triangles) and 4M urea (dark pink squares). (B) increasing concentrations of CTAB in 0M (black), 2M (blue) and 4M urea (pink).

urea, and up to 3 mM of CTAB, the ellipticity of lysozyme slightly increased. However, further additions of CTAB destabilized these secondary structures, and thus decreased the ellipticity.

3.3.6. Thermal denaturation: Though the addition of urea did not show any considerable

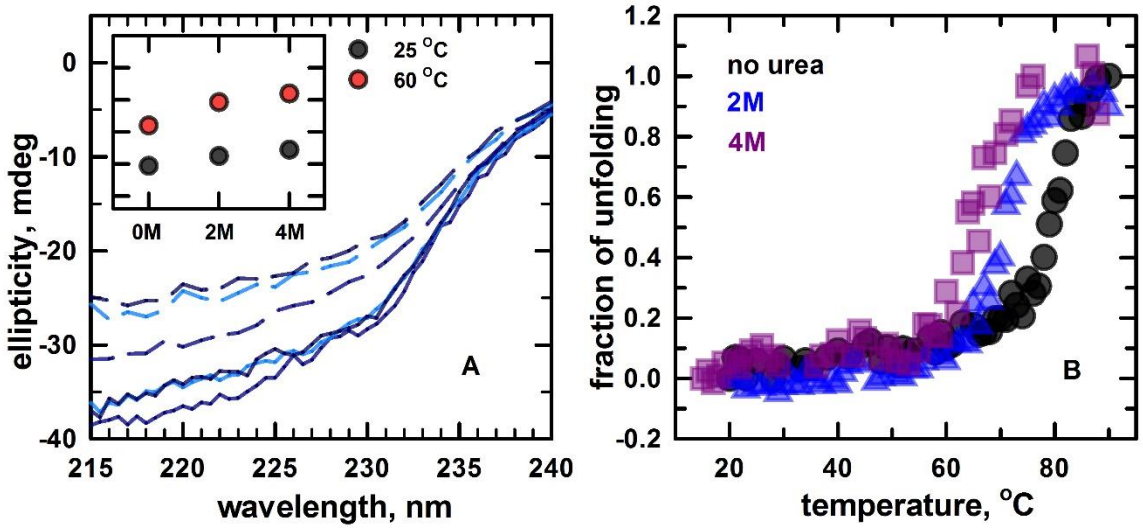

Figure 3.15. (A) Far-UV CD spectra of HEWL followed both at room temperature (solid lines) and at 60 ºC (dashed lines). Inset shows changes plotted at 220nm. (B) Changes in the HEWL structure by thermal denaturation followed at 220 nm in the absence (black circles) and in presence of 2M (blue triangles) and 4M urea (pink squares).

change in the overall structure of the protein, it altered the fibril-forming propensity of HEWL. In order to evaluate the stability changes implied by urea, changes in the ellipticity of the protein in the far-UV region at higher temperature were compared with the spectra obtained at room temperature. The results suggested that at room temperature lysozyme did not show any considerable changes, but at higher temperatures the protein displayed a relatively higher loss of the secondary structure in the presence of urea (Fig. 3.15A). For further evaluation, the thermal denaturation of lysozyme was followed using ellipticity changes at 220nm in the presence and in the absence of urea (Fig. 3.15B). As the concentration of urea increased, the thermal denaturation midpoint (T_m) decreased to 70 ^oC and 64 ^oC in 2M and 4M urea, respectively compared to the Tm value of 74 ^oC for lysozyme in the absence of urea at pH 7.

3.4. Discussion

3.4.1. Lysozyme fibril formation at pH 7:

Though the fibril formation of lysozyme has been extensively characterized at non-neutral pH conditions, the studies at neutral pH are very limited.[105,128] Since our study aimed to probe the effect of surfactants on the fibril formation and to determine the role of the charge interactions, it was considered advantageous to monitor the changes at neutral pH. The change in pH alters the surface charges on the protein and the micelle-forming concentrations of the surfactants. However, lysozyme does not form fibrils at neutral pH under normal conditions. Our earlier studies showed that the addition of 2–4 M urea to lysozyme at higher temperature induced fibril formation. These conditions were used for analysing the effects of the surfactants on the fibrillation. In 2M urea, lysozyme shows an initial lag phase, followed by a fibril elongation phase, suggesting a nucleation-dependent fibrillation pathway. However, in 4M urea, the protein loses slightly more secondary structural contents at higher temperature, but does not show any lag phase and follows a nucleation-independent fibril formation. The nucleation-independent pathway is observed in HEWL at pH 2 and in high salt concentration conditions,[74] as well as in a few other proteins, such as bovine serum albumin.[129] This pathway might occur through a classical coagulation or via a downhill aggregation mechanism[130]. Analysing the effects of the surfactants under both these conditions could provide valuable information on the role of the surfactants at different stages of fibril formation.

3.4.2. Lysozyme–surfactants interaction:

Conformational changes followed by the intrinsic fluorescence of lysozyme show that SDS has no considerable effect up to 0.4 mM. However, as the concentration of SDS increases, the protein fluorescence displays a cooperative increase in intensity (Fig. 3.12), which might arise from the tertiary structural changes of the protein. Further insights on the structural changes with an external fluorophoric probe, TNS, (Fig. 3.13) suggest that at the lower concentrations of SDS the hydrophobic residues of the protein are partially exposed, which are then occupied by TNS molecules, thus enhancing the fluorescence. As the SDS concentration is further increased (above ~0.6 mM), the SDS molecules interact with the protein through hydrophobic interactions and replace the bound TNS. The TNS molecules released from the protein surface to the solvent reduces its fluorescence intensity. Above 6.0 (±0.5) mM of SDS, the protein's surface could be completely occupied with SDS micelles, and thus any further increases in the surfactant concentration will not provide any conformational change of the protein. Under these concentrations, free micelles of SDS (i.e., not interacting with the protein) could also be found in the free solvent. TNS might bind to these free micelles, and thus its fluorescence would not be altered compared to its fluorescence in the absence of HEWL.

The far-UV CD spectra (Fig. 3.14A) demonstrate that for up to ~1.5 mM of SDS, the secondary structure content of the protein is increased. This could be due to the property of SDS to induce helicity of lysozyme at lower concentrations.[131] Increases in the SDS concentrations above 1.5 mM destabilize these additional secondary structures. Further increases in the concentration of SDS (>6.5 mM in 0M urea; >6 mM in 2M urea; >5 mM in 4M urea) does not affect the secondary or tertiary structure of the protein. By comparing these results with the earlier studies [118,120,132.133,119,134] on lysozyme–SDS interactions, it could be inferred that lysozyme interacts with SDS through ionic interactions at concentrations below 0.5 (±0.1) mM, and that it initiates the protein-associated early micelle formation of SDS (critical aggregation concentration - CAC[128,135]). Above this concentration of SDS, hydrophobic interactions predominate between lysozyme and SDS molecules, which affect the tertiary structure of the protein. These tertiary structural changes are accompanied by a change in helicity of the protein. Such protein–SDS complexes, including for lysozyme, have been well characterized by various techniques.[119,126,136,137] Though the presence of urea decreases the concentration needed for complete protein–micelles complex formation, it has an insignificant effect on the critical aggregation concentration. Moreover, the slopes of the denaturation curves are similar in the presence and in the absence of urea (Fig. 3.15B), suggesting that urea at the studied concentrations has less interference on the SDS interactions with the protein.

Protein-induced early aggregation is also observed in CTAB (Fig. 3.12B). In the case of CTAB, the slope of the denaturation curve is similar for all the urea concentrations, but the CAC is notably higher at higher urea concentrations. In 2M and 4M urea, the CAC values are 0.2 and 0.4 mM, respectively, compared to 0.1 mM in the absence of urea. Urea also increases the concentration of CTAB required to form the complete micelles around the protein. This is evident from the saturation of lysozyme fluorescence, which occurs at 1.0 and 1.5 mM of CTAB in 2M and 4M urea, respectively, whereas in the absence of urea it is observed at 0.8 mM of CTAB. These results are further verified by the change in TNS fluorescence in CTAB upon the addition of HEWL (Fig. 3.13B). In the absence of urea at above 0.1 mM of CTAB, the TNS fluorescence increases with increasing the CTAB concentration upon the addition of HEWL, suggesting a partial exposure of the hydrophobic residues of the protein. The CTAB concentration at which the TNS fluorescence starts increasing is also shifted to higher surfactant concentrations in the presence of urea (0.2 and 0.4 mM in 2 and 4M urea, respectively). This might be due to the simultaneous ionic and hydrophobic interactions of CTAB on the protein surface at lower surfactant concentrations, which could be affected by urea. Studies [133,134] on the interaction of lysozyme with CTAB and dodecyl trimethyl ammonium bromide (DTAB – a cationic surfactant similar to CTAB) using calorimetric methods propose that the initial interaction between HEWL and cationic surfactants at lower concentrations is due to the simultaneous electrostatic and hydrophobic interactions, whereas at higher concentrations, hydrophobic interactions predominate. These interactions expose some of the hydrophobic sites of the protein, which leads to conformational changes. This could be correlated with the spectroscopic changes observed for HEWL in the presence of CTAB. In the absence of urea at above 0.8 mM of CTAB, the TNS fluorescence decreases. This might be due to the occupation of the exposed hydrophobic sites of HEWL by CTAB through hydrophobic interactions by replacing the bound TNS. A similar effect is observed in the presence of 2M and 4M urea, as well at the concentrations of CTAB above 1.0 and 2.0 mM, respectively. Furthermore, CTAB does not show any significant secondary structural changes in the protein, except in the presence of 4M urea. In 4M urea, it is noted that CTAB slightly increases the secondary structure content of the protein, which is then destabilized with further increases in the surfactant concentration. These results suggest that the lysozyme–CTAB interaction mostly affects the tertiary interactions only.

Tx, a non-ionic surfactant, also showed a cooperative transition, which could correspond to the tertiary structural changes of the protein. Interestingly, urea has no notable effect on the CAC of Tx in lysozyme, which is 0.2 mM in all the cases, nor does it affect the

concentration of the complete micelle formation by Tx around the protein (at 2 mM). In other words, the presence of urea has little or no effect on the protein–non-ionic surfactant interaction. Moreover, the change in the TNS fluorescence intensity in Tx upon the addition of HEWL is minimal, both in the presence and in the absence of urea. This suggests that the extent of the protein denaturation is minimal in the presence of Tx. In the presence of all the studied surfactants, the fluorescence emission maximum was observed at around 350 nm. The absence of any wavelength shift during the titrations against surfactants suggests that the extent of the unfolding is less, and that the exposure of the hydrophobic tryptophan residues to the solvent is minimal. This corroborates with the less or no changes observed in the secondary structure content of the protein with the surfactants.

3.4.3. Effect of surfactants on fibril formation:

Changes in the fibrillation of lysozyme in the presence of surfactants can be broadly categorized into ionic and non-ionic surfactant effects. In the presence of ionic surfactants, i.e., SDS and CTAB, the fibrillation propensity (formation or inhibition) of lysozyme is similar, although the rates of fibril formation are different. In 2M urea solution, lysozyme forms fibrils with a nucleation phase of ~2.1 h^{-1} and an elongation rate of ~1.6 h^{-1}. In the case of the addition of SDS at lower concentrations, where the ionic interaction predominates (i.e., <0.4 mM SDS), the nucleation period is marginally increased. However, at higher concentrations, where the charge neutralization is complete and the tertiary structures are also slightly altered, the nucleation time is gradually reduced. The addition of CTAB at lower concentrations, where there are no tertiary structural changes and at <0.2 mM CTAB, the lag phase is also extended, but the change in the fibrillation rate is minimal. In 2 mM SDS, the protein exceptionally had a shorter lag phase and slower fibrillation rate. At near the CMC of CTAB and above the CMC of Tx, the lag phase was reduced, compared at lower concentrations, but was still longer than the time observed in the absence of surfactants. The fibrillation rate shows insignificant changes under these conditions.

Overall, the initial binding of the surfactant molecules on the protein's surface residues increases the nucleation period. The binding of more surfactant molecules alters the tertiary structures by hydrophobic interactions and reduces this lag phase. By comparing the effect of different surfactants, it was clear that the surfactant with an opposite charge (i.e., SDS) to the protein surface charge shows a relatively lower nucleation time. These results suggest that surface charge neutralization of the protein by SDS might reduce the initial lag phase, whereas similarly charged and uncharged surfactants mostly interact with the hydrophobic surfaces and

thus extend the nucleation time. At the complete micelle forming concentrations both SDS and CTAB inhibit fibril formation. The addition of non-ionic surfactants does not inhibit the fibrillation of the protein, but it does increase the lag phase. In the case of ionic surfactants, the surfactants are known to form micellar-like aggregates [136,137,138] around protein by interacting with the protein through their hydrophobic tails and by exposing their charged head groups to the solvent. These charged surfaces of the protein–ionic surfactant complexes can reduce the interaction between the individual protein chains, thus inhibiting fibril formation. However, non-ionic surfactants cannot produce such charged surfaces, which could lead to the fibril forming aggregates.

Earlier studies have shown that SDS could induce the amyloid fibril formation of lysozyme at lower concentrations, and that above the CMC it inhibits fibrillation.[128,116] Also, SDS is found to evade the lag phase of lysozyme fibrillation at pH 2.0 [128] and of apolipoprotein C-II at pH 7,[114] and to facilitate the direct elongation phase. Furthermore, increases in the ionic strength of the solution have also been shown to alter the mechanism of lysozyme fibrillation.[74] Though our results do not show a complete abstinence of the nucleation phase at near the CMC, SDS shows a shorter nucleation time. This might be due to the varying surface charge distribution of the protein at different pHs, which could alter its interaction with SDS. SDS has also been shown to induce the fibrillation of other proteins as well at lower concentrations, namely by converting α-helical structures of the proteins into β-sheets.[139,140,141] Recently, Khan *et al.*[117] has shown that 0.5 mM SDS induces the aggregation of 25 different proteins, including lysozyme at the pH of two units less than their pI. Also, molecular simulation studies on amyloid-β peptides suggest that changes in the ionization states of charged amino acid residues due to changes in the solution pH could alter the electrostatic interactions within and between the peptides chains, thus influencing the fibrillation propensities of the peptides.[142,143] Comparing these observations with our results reiterates the fact that the surface charge neutralization by ionic surfactants could reduce the nucleation time, whereas the occupation of hydrophobic sites by the hydrophobic tail of a similarly charged surfactant or non-ionic surfactant would show an inverse effect. Thus, it could be concluded that the nucleation phase of lysozyme fibrillation is mostly influenced by the charge interactions and by micellation of the surfactant around the protein.

In 4 M urea conditions where no lag phase is observed, the initial binding of SDS to the protein slowed down the fibrillation rate, but accelerated it by the further addition of SDS. Higher concentrations of CTAB and Tx are shown to reduce the rate of fibrillation. Though the exact reasons for these variations could not be deduced due to the limitations of our

experiments, the effects observed in these cases suggest that the fibril elongation phase might be controlled by the additional factors,[19,114] such as exposure of the protein's hydrophobic residues, changes in the surfactant binding sites, and by their structural features. Moreover, studies on the effect of amphiphiles and other small molecules on protein fibrillation [114,115] suggest that these molecules could have distinct effects on different stages of protein fibrillation and aggregation. Therefore, it could be concluded that the different stages of lysozyme fibrillation, nucleation, and elongation, are differently influenced by the surfactants. Comparing the kinetics profiles obtained in 2M and 4M urea conditions indicates that the surfactants do not switch the fibrillation mechanism from nucleation-dependent into nucleation-independent or the other way around, even though the formation of protein–ionic micelle complexes inhibit fibril formation under all the conditions. Non-ionic micelles do not inhibit the fibrillation, but can affect the fibrillation process at each phase. Interestingly, the fibrillation rate is five-fold slower in the presence of 4M urea compared to the fibril elongation rate in 2M urea. In the case of the 2M urea samples, where also the shortest nucleation time was observed (in 0.2 mM of SDS), the elongation rate is reduced. This suggests that the initial nucleus formation before fibril elongation may accelerate the fibrillation rate. However, considering the distinct effects of the surfactants on the different phases of fibrillation and the urea induced change in the fibrillation mechanism, this assumption needs to be verified by further experiments on the lysozyme fibril formation under similar conditions and with other fibril forming proteins as well.

3.5. Summary

The effect that ionic and non-ionic surfactants had on each step of the fibril formation was investigated. All of the surfactants showed increase in the nucleation time of the protein, but the extent of the increase was less near the CMC of the ionic surfactants and above the CMC of the non-ionic surfactants. This predicts that the lag phase is mainly controlled by the ionic interactions and the micellation property of the surfactants. The fibril elongation rate is not generally affected under the 2M urea conditions and has differential effects in 4M urea. This indicates that the elongation phase is influenced by multiple factors. Moreover, ionic surfactants inhibit fibril formation above their CMC, while non-ionic surfactants could only extend the time for nucleation and the elongation.

Chapter 4

Navigating the Conformational Changes Induced by Surfactants: Relevance to the Fibrillation of α-Lactalbumin, an Acidic Protein

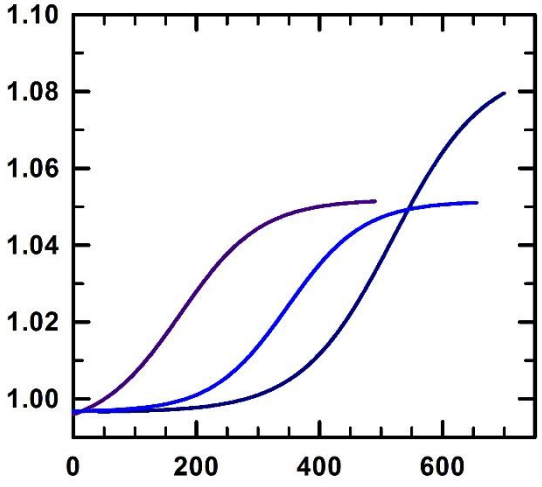

Abstract

Studies focussed on protein-surfactant interactions can help in navigating the associated changes on structure, aggregation and fibrillation propensities of the protein. The fibrillation pathway and kinetics are mainly determined by the surface charge on the protein and the added co-solvents. To get insights into the interplay between these phenomena, the effects of anionic, cationic and non-ionic surfactants on α-lactalbumin (α-LA, an acidic protein) fibrillation were studied. Our earlier studies on the effects of sodium dodecyl sulfate (SDS), cetyltrimethyl-ammonium bromide (CTAB), and triton X-100 (Tx) on lysozyme (a basic protein) fibrillation indicated that there are differential effects of ionic and non-ionic surfactants. In case of α-LA as well, above the critical micelle concentrations (CMC) of anionic surfactant SDS, protein could not form fibrils. However, cationic CTAB and non-ionic Tx does not inhibit fibril formation at all the concentrations. SDS at lower concentrations increased lag time by two-fold, but the elongation rate was not significantly altered whereas at the concentrations above 0.2 mM, a huge increase in lag time accompanied by 3-6fold increase in the elongation rate were observed. CTAB, bearing opposite charge to the protein accelerated the fibril formation at lower concentrations whereas near-CMC it showed a increase in lag time. Above the CMC, CTAB again shorten the lag time. The elongation rate decreased as the concentration of CTAB is increased. Tx also showed concentration-dependent changes. As the concentration of Tx is increased, there is concomitant increase in the lag time. However, elongation rate for final fibril assembly was larger in the presence of lower concentrations and micellar concentration of Tx compared to near-CMC concentrations. These results point out to the fact that the nucleation phase of α-LA fibrillation is primarily controlled by charge interactions and micellation of the surfactants, but multiple factors might influence the fibril elongation. Furthermore, the surfactants do not alter the fibrillation pathway from nucleation-dependent to nucleation-independent or *vice versa* in the studied conditions.

4.1. Introduction

Surfactants or surface active agents are small amphipilic molecules that reduce the interfacial tension between two phases by acting at interfaces. Lowering of the free energy of the phase boundary is the major driving force for surfactant adsorption.[144] Protein-surfactant interactions depend on the protein under consideration and the nature of surfactant (charge on the head group and length of tail). Denaturation in the presence of surfactants requires almost

1000 times less concentration compared to chemical denaturants and does so by increasing the affinity towards denatured state.[69,111,77] Monomeric and micellar forms of surfactants interact differently with proteins and their micellation is significantly affected in presence of proteins.[69] For instance, RNase A unfolding showed formation of 3 different types of intermediates in the presence of different concentrations of SDS ranging from monomeric forms to micelles.[127] On the contrary, SDS has been found to play two opposite roles in case of BSA as stabilizer at low concentrations and as destabilizer in the presence of micelles.[145] Sudies on S6 show that two different micellar formations can occur during the unfolding of protein in SDS at above the CMC. Spherical micelles results in unfolding of protein with saturation of unfolding rates (mode 1) while cylindrical micelles, prevalent at higher SDS concentrations, induced unfolding dependent on power-law (mode 2).[77] Also, SDS and LTAB[77] show strong pH-dependence suggesting the crucial role of head groups in modulating the unfolding of proteins. Further, experiments on cytochrome *c* suggest that "tertiary structure unfolding in the presence of sub-micellar concentrations and chain expansion in the micellar range of SDS concentrations" to a good approximation.[137] α-lactalbumin unfolding in the presence of ionic, non-ionic and zwitterionic surfactants has been extensively characterized, because of the protein's versatility in comparing different denaturation mechanisms making it an excellent model.[146,147] The results propose that unfolding occurs at much faster rate in the presence of anionic and cationic surfactants and monomers and micelles operate mutually exclusive. In the presence of non-ionic and zwitterionic surfactants, both monomers and micelles were found to cooperate in the denaturation phenomenon[146].

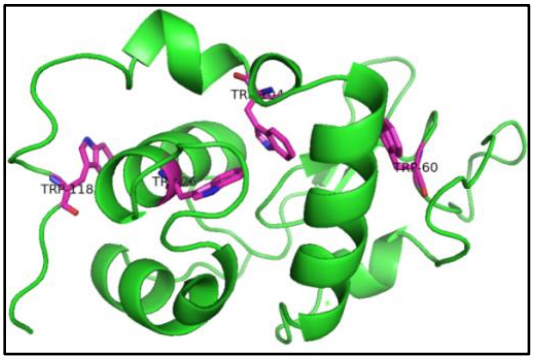

Figure 4.1 Ribbon diagram of α-LA showing alpha helices and beta sheets with the four tryptophan residues presented as stick models.

It has been shown that the aggregation propensity of many proteins such as amyloid beta peptides[112], alpha-synuclein, lysozyme[64] and lactoglobulin[113] is altered by surfactants, though a general mechanism cannot be attributed as to how different monomeric, near-CMC

and micellar forms of surfactants play a role in protein fibril assembly and the associated kinetic pathways.[114,115,116,117] A recent study has shown to first approximation that the effect of Na^+ detergents on β_2-microglobulin is a result of competition between the super-saturation limited fibrillation and the unlimited capacity to form mixed protein-micelle complexes in a concentration-dependent detergent effect. Also, there is a structural transition from β-sheet structures to α-helices as the detergent changes phase from monomers to micelles.[148] SDS-induced fibrillation of alpha-synuclein represents the versatility of protein association and by formation of shared micelles.[149] Ionic and non-ionic surfactants micelles were shown to inhibit fibrillation of HEWL[64] and β-lactoglobulin[150] by solubilizing and making unfolded monomers unavailable for protein association. However, studies on how these structural changes affect the fibrillation propensity of the proteins are limited, particularly on α-lactalbumin (α-LA). Our present study focuses on the conformational changes induced by differently charged surfactants on α-LA and its effects on the protein's fibrillogenicity.

α-LA is a two-domain protein consisting of 123 amino acids with α/β – fold class (Fig. 4.1) and widely used as a model to study folding intermediates and molten globule structures.[151,152] α-LA forms fibrils in its reduced form at neutral pH or in apo-form at lower pH and higher temperature (37 to 55 ℃).[153,154] These properties of α-LA is employed to understand fibril formation and inhibition mechanisms *in vitro*.[153–156] In this present work, we have studied the effect of surfactants, SDS, CTAB and Tx on the fibrillation mechanism of this acidic protein (pI ~4.5) and compared with earlier reported basic protein (lysozyme, pI ~9).[64] The results suggest that the effect of surfactants on the fibril forming ability of the proteins with different surface charges is different and also differ in their kinetics mechanism.

4.2. Materials and Methods

4.2.1. Materials: Chemicals and the necessary reagents were procured as mentioned in section 2.2.1.

4.2.2. Sample preparation: Samples were prepared and the fibrillation kinetics was followed as mentioned in section 3.2.2. In brief, desired protein concentration of 140 μM or 15 μM was achieved by adding α-LA directly to the aliquots of surfactants' solutions for fibril or unfolding studies, respectively. Fibrils were formed by incubating the protein in phosphate buffer at pH 7 at 60 ℃ for 12-14 hrs. TNS fluorescence changes in the presence of the protein were also measured following the method described in section 3.2.2.

4.2.3. Spectroscopic measurements: ThT emission spectra were recorded as described in section 2.2.1. For the kinetics measurements, method described earlier in section 2.2.3 was followed. The protein's fluorescence changes and CD measurements were carried out following the method described in 3.2.3. Ellipticity changes at 220 nm for thermal denaturation studies were followed in the presence and absence of surfactants by increasing temperature by 1℃/min from 20 ℃ to 90 ℃.

4.2.4. Microscopic Imaging*:* TEM images were obtained following the protocol mentioned in section 2.1.2 to capture the images of fibrils.

4.3. Results

4.3.1. Surfactants effect on α-LA ***fibrillation:*** Protein's surface charge and micellation property of surfactants are altered with change in solution pH. Hence, in order to evaluate the effect of surfactants on an acidic protein, α-LA, the fibril forming conditions were optimized at near-neutral pH. Of the various conditions studied, apo-form of α-LA was found to form fibrils by heating the protein at 60 ℃ for 12-14 hrs. Once the fibril forming conditions were identified, the effect of surfactants SDS (anionic), CTAB (cationic), and Tx (non-ionic) on the fibrillation were analysed to determine how the surface charge on the protein was screened by the surfactants bearing different head groups

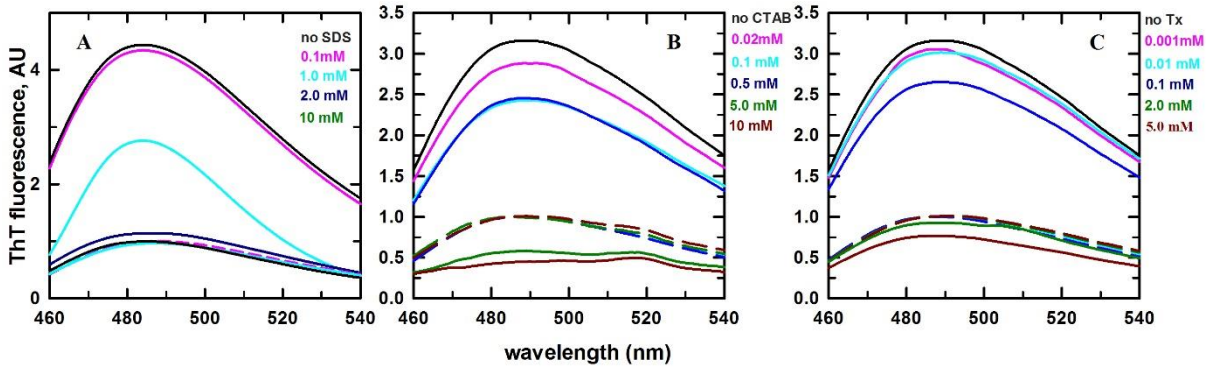

Figure 4.2 Effect of surfactants on α-LA fibrillation at pH 7. Dashed and solid lines represent ThT spectra measured before and after heating the protein samples at 60 ºC for 12-14 h. ThT fluorescence in presence of (A) 0 (black), 0.1 (pink), 1.0 (cyan), 10 (blue), and 20 mM (green) of SDS, (B) 0 (black), 0.01 (pink), 1.5 (cyan), 5 (blue), and 10 mM (green) of CTAB, and (C) 0 (black), 0.01 (pink), 0.2 (cyan), 2.0 (blue), and 5.0 mM (green) of Tx.

and concomitant changes in the kinetic parameters. Surfactants exist as monomers at lower concentrations and as micelles at higher concentrations (CMC). The equilibrium between these

two states of a surfactant is affected by the solvent condition adapted. From section 3.3.1, it was noted that under the buffer conditions employed, the three surfactants SDS, CTAB and Tx showed CMC values of 3.5 mM, 0.2 mM, and 0.3 mM, respectively.

In order to evaluate the effects of surfactants on α-LA fibrillation, different concentrations of surfactants ranging from monomeric to micellar forms were added to protein solution and heated at 60 °C for 12-14 hrs at pH 7. As reported in earlier chapters, ThT was used as probe to check for the formation of fibrils. Fluorescence intensity of ThT increases by 7-fold upon binding to fibrils.[157,121] The fluorescence intensities of ThT containing protein samples were measured before and after heating the samples at 60 °C. When lower concentrations of SDS, CTAB and Tx were added to the samples containing α-LA, the fluorescence intensity of ThT increased after incubating the samples at higher temperature (Fig.4.2).

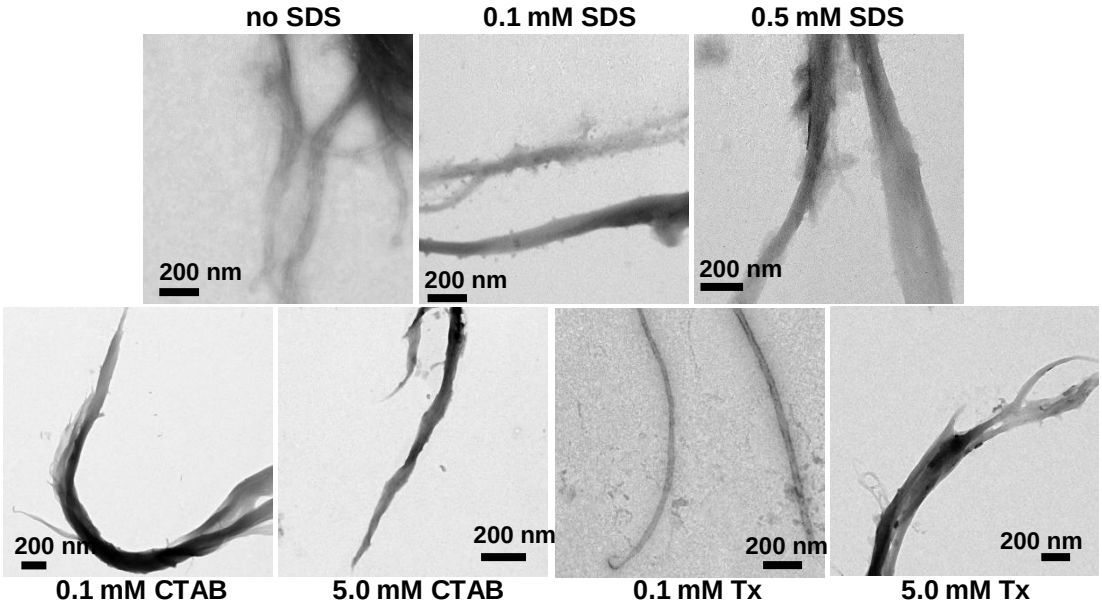

Figure 4.3 TEM images of α-LA fibrils in the presence and absence of different concentrations of surfactants (as mentioned in the labels of each panel).

There were no considerable changes in the intensity of dye when protein samples were heated in the presence of micellar concentrations of SDS. However, in the case of CTAB and Tx even the micellar concentrations could form fibrils. Though there was no considerable change in the intensity of ThT dye in the presence of micellar concentrations of CTAB and Tx, the fibrils could be clearly viewed under TEM (Fig. 4.3). TEM images showed that the protein formed long and twisted fibrils even in 5.0 mM (above CMC) of CTAB or Tx (Fig.4.3).

4.3.2. Kinetics of α-LA fibrillation: ThT fluorescence intensity was used to monitor the changes in the fibrillation kinetics of α-LA. The protein showed characteristic sigmoidal kinetics with lag, elongation and saturation phases. The kinetic traces were analyzed using eq. (2.1)[125] and the resultant parameters are presented in Table 4.1. In the absence of any surfactant, α-LA showed a lag phase of ~20 min and the conversion of entire monomers to fibrils was completed in ~10 h. Addition of anionic SDS resulted in a biphasic effect. The concentrations

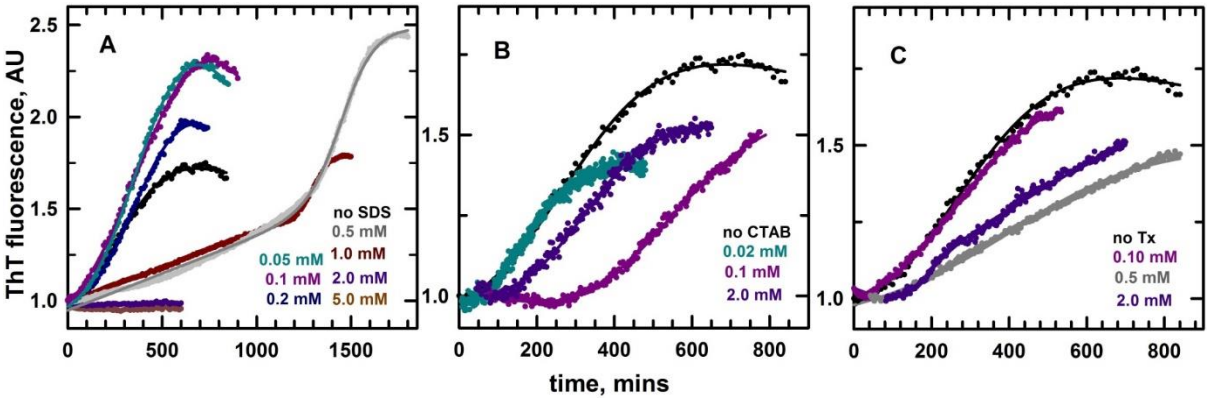

Figure 4.4 The kinetic curves of α-LA in the presence of different surfactants (A) SDS, (B) CTAB, and (C) Tx as monitored by ThT fluorescence change. The different color codes in each panel correspond to the concentration of surfactants used and the concentrations are presented in the respective panels. There is no increase in the fluorescence intensity of ThT in the presence of 2 and 5 mM of SDS in panel A.

below 1 mM were able to induce fibrillation and the addition of SDS above 2 mM resulted in the formation of amorphous aggregates. The fluorescence intensity of samples containing less than 2 mM of SDS showed an increase with characteristic three phases. The lag phase was increased by two to 4-fold and the elongation rates were comparable at the lower concentrations of SDS. However, at the concentrations near-CMC, the lag period was extended to nearly 20 h whereas the elongation rate was accelerated. ThT fluorescence did not show any considerable changes when the SDS concentrations were above CMC. Kinetic traces in the presence of CTAB and Tx resulted in a monophasic effect and ThT fluorescence was found to increase in the presence of all the concentrations of the surfactants employed. The lag time was found to be increased whereas the elongation rate was accelerated in the presence of CTAB. Similar trend was observed in for α-LA in the presence of non-ionic surfactant, Tx. Microscopic images also confirmed the observations that α-LA formed fibrils in the presence of all the concentrations of CTAB and Tx employed (Fig. 4.3).

Table 4.1 Lag time and elongation rate of fibrils formed in the presence of different surfactants

Surfactant	Concentration (mM)	Lag time (min)	Elongation rate ($\times 10^{-3}$)
SDS	0	20.0	4.2
	0.05	83.4	5.2
	0.10	45.0	3.4
	0.20	44.5	5.6
	0.50	1283.5	11.3
	1.0	1237.0	27.0
	≥ 2.0	no fibrils	--
CTAB	0.02	54.34	65.33
	0.10	230.0	153.45
	2.0	90.0	110.0
Tx 100	0.1	40	110.0
	0.5	95.5	162
	2.0	143.7	82.85

4.3.3. Unfolding of α-LA by surfactants: Unfolding of α-LA in all the three surfactants was followed using the change in intrinsic fluorescence of the protein. As reported by earlier

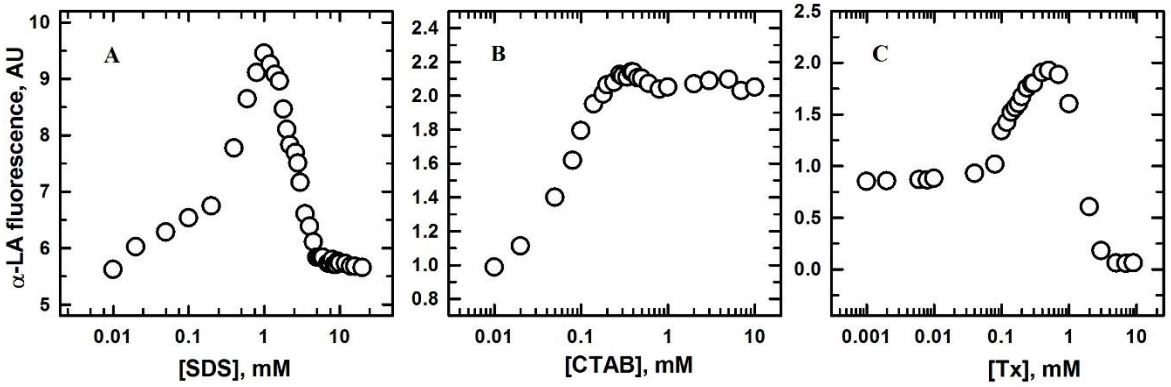

Figure 4.5 Changes in the intrinsic fluorescence of α-LA monitored at 350 nm with increasing concentrations of SDS (A), CTAB (B), and Tx (C).

studies, the unfolding of α-LA by anionic SDS involves three different phases (Fig. 4.5A). (i) SDS binds to the surface of protein without much conformational changes upto ~ 0.8 mM. (ii) SDS forms quasi-micellar structures with secondary structural changes from 0.8-3 mM. (iii)

The micelles of SDS completely surround the protein surface with significant conformational changes when used above 3 mM.[146] In the present study also following the changes of α-LA by intrinsic fluorescence showed three major transitions, though there is a shift in the SDS concentrations at which these steps occur probably because of the buffer conditions employed. Unfolding of α-LA in the presence of cationic surfactant CTAB showed two distinct transitions as reported in earlier literature.[147,134] There is an increase in the Trp emission maxima with concomitant increase in the concentration of CTAB which suggested the exposure of Trp residues to hydrophilic environment as a result of unfolding.[158,159] The fluorescence intensity approaches a saturation level in the presence of micellar concentrations of CTAB, i.e., above 0.2 mM (Fig 4.5B). Earlier reports based on stopped-flow experiments[146] suggest that the rate of unfolding shows a single relaxation phase with rapid unfolding at lower concentrations of cationic surfactant. However, the unfolding rate declines to a small but reproducible extent at higher concentrations of CTAB which can be attributed to the additional binding of micelles around the protein surface. This additional binding might not significantly alter the conformation of the protein.

Non-ionic surfactant, Tx did not show any significant changes in the fluorescence of α-LA up to concentrations below CMC. The initiation of protein denaturation was noted only in the presence of near- or above-CMC concentrations of Tx as shown in Fig 4.5C. The increase in fluorescence of α-LA, when the concentration of Tx was increased above 0.05 mM, could be due to exposure of Trp residues up on denaturation. However, when the concentration of Tx was increased above 0.1 mM, the protein's fluorescence came down probably due to the formation of Tx micelles around the hydrophobic surfaces of the protein including Trp residues which could reduce the solvent accessibility of Trp residues. Further increase in the concentration of surfactant only might assist the micellation, hence, not altering the protein conformation. Earlier studies showed that the final plateau value depends on the length of non-ionic surfactant and a linear dependence was found indicating monomers contributions on the efficiency of unfolding.[146]

For further insights into these effects, micellation of surfactants and unfolding of protein were followed using an external fluorophore TNS. The dye binds to the hydrophobic patches such as those found in micelles or denatured protein upon which its fluorescence increases. Initially TNS fluorescence was measured in SDS and CTAB alone. There was no considerable change in the dye emission in the presence of lower concentrations of both the surfactants as shown in Fig 4.6. The intensity of TNS increased steeply from 3.5 mM in case of SDS and 0.2 mM in the presence of CTAB and indicated that the CMC of SDS and CTAB

in the studied buffer conditions to be 3.5 mM and 0.2 mM. Addition of protein altered these transitions and the intensity of TNS started to increase when 0.1 mM of SDS was added that decreased after1mM. The intensity of TNS fluorescence again increased from at above 4 mM

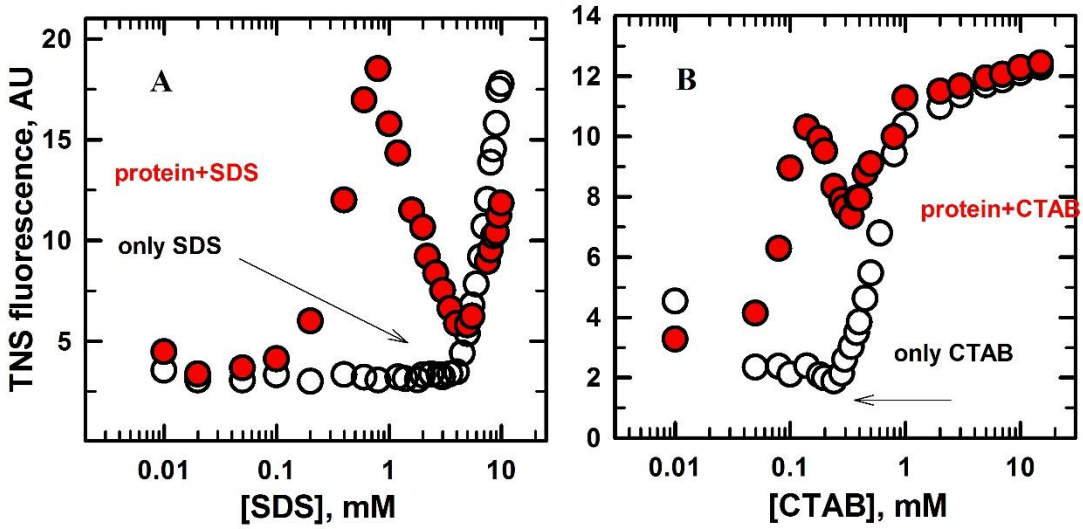

Figure 4.6 Changes in the TNS fluorescence (empty circles) and in the presence of α-LA (filled red circles) with (A) Increasing concentrations of SDS and CTAB (B) respectively.

of SDS in the presence of protein. In CTAB, TNS fluorescence showed no change till 0.05 mM, but started increasing from 0.05 mM to 0.15 mM in the presence of α-LA. Above this concentration, the TNS fluorescence decreased until the addition of 0.4 mM of CTAB which again increased when the surfactant concentration was above 0.4 mM in the presence protein. Above 1 mM of CTAB, the fluorescence intensity of TNS was slightly but monotonously increased. As observed in the case of lysozyme (Fig. 3.13), the difference in change in TNS fluorescence in the presence of Tx, before and after the addition of α-LA, was very less (data not shown).

Secondary structural changes upon addition of SDS and CTAB were followed at far-UV CD. The ellipticity changes observed in the presence of SDS suggested that the secondary structure of α-LA was only partially affected by SDS at the concentrations even up to 5 mM (Fig. 4.7A). Moreover, SDS was found to increase the helicity of the protein at the concentrations up to ~1 mM which came down at higher concentrations. At 60 °C, a similar trend was found, but extent of increase in helicity was less. A completely opposite trend was observed in the presence of CTAB (Fig. 4.7B). Lower concentrations led to increased loss of structure when compared to changes observed in the presence of higher concentrations of

CTAB. At higher temperature, there was a slight increase in the structure of protein up to 0.5 mM of CTAB, but further increase in the surfactant concentration caused destabilization of the structure. Tertiary structural changes observed in the presence of SDS showed that there was a cooperative loss in the structure of the protein with concomitant increase in SDS concentration (Fig 4.8A). There was no significant change in the tertiary interactions of the

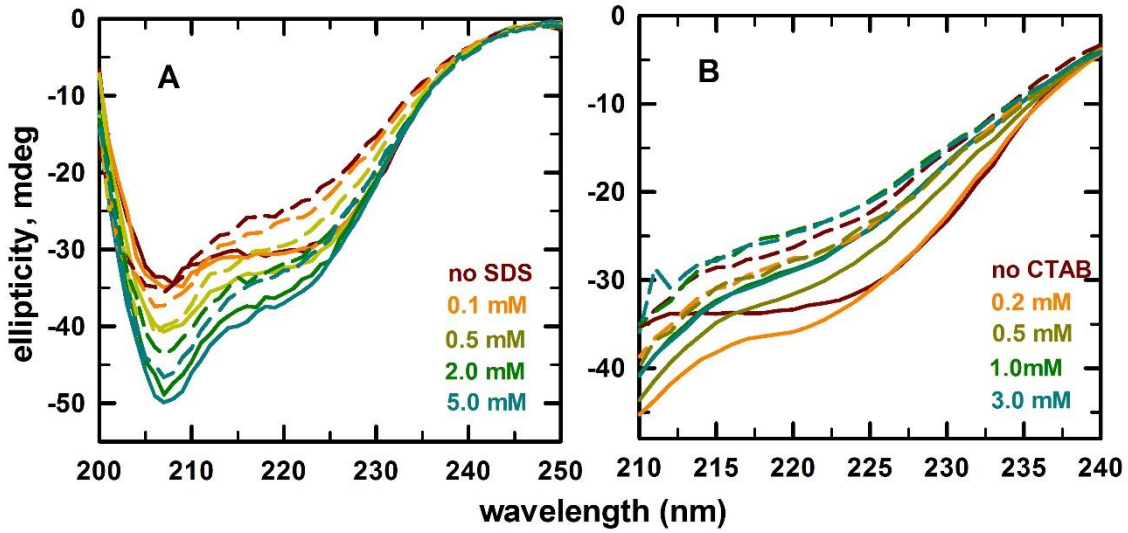

Figure 4.7 Far-UV CD spectra of α-LA followed both at room temperature (solid lines) and at 60 °C (dashed lines) in the presence of increasing concentrations of SDS (A) and CTAB (B).

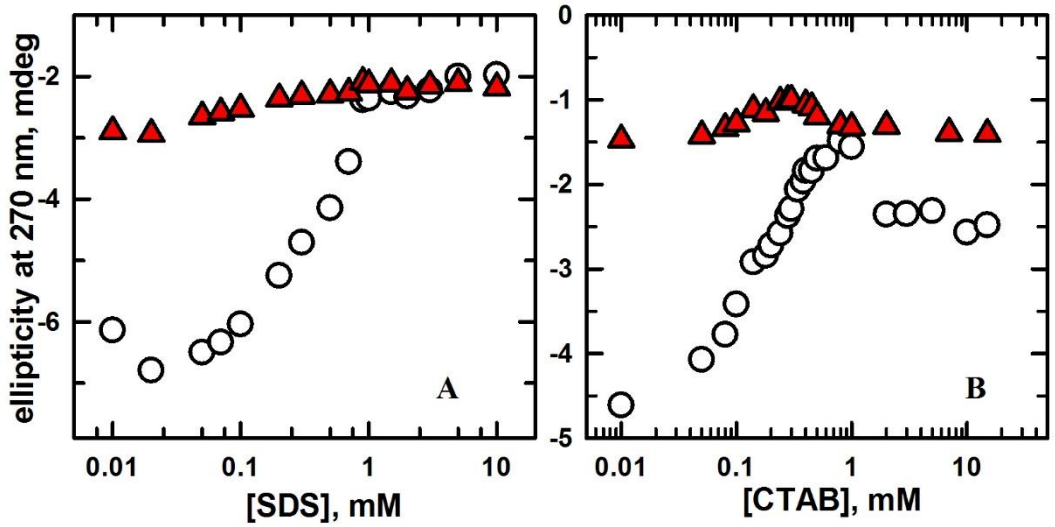

Figure 4.8 Ellipticity changes of α-LA at 270 nm followed both at room temperature (empty circles) and at 60 °C (filled red triangles) in the presence of varying concentrations of SDS (A) and CTAB (B).

protein up to the addition of 0.02 mM of SDS and complete loss in the structure occurred by 1.0 mM. Further addition of SDS did not induce much change in the structure of protein. There

is a greater degree of loss in the structure of protein at higher temperatures and the denaturation sets in at much lower concentration of SDS, though it follows a similar trend. In the presence of CTAB, gradual destabilization of structure sets in even at lower concentrations and the complete loss in tertiary structure occurred by 1 mM. Not much change was observed up on further addition of CTAB (Fig 4.8B). At higher temperature, a similar trend in the destabilization of the protein was followed and the transition in saturation also sets in at much lower concentrations.

Thermal denaturation studies were carried out in the presence of SDS by following the ellipticity changes at far-UV region. Lower concentrations of SDS induced cooperative loss in the structure of protein up to 2 mM and became non-cooperative when concentration

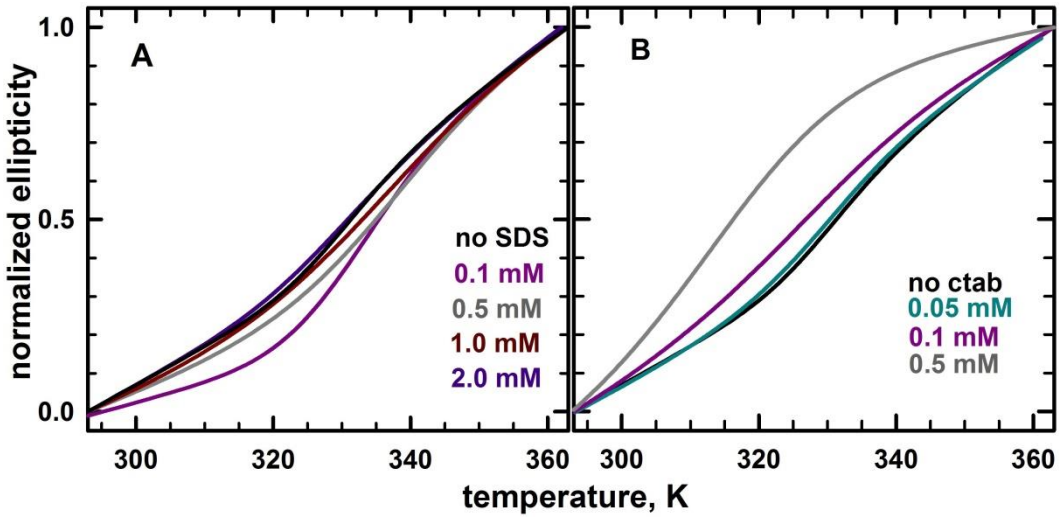

Figure 4.9 Thermal denaturation of α-LA followed at 222 nm in the presence of varying concentrations of SDS (A) and CTAB (B). The denaturation profiles were fitted into simple two-state transitions and only the fit-lines are presented for clarity. The different color codes represent the varying concentrations of the surfactants as mentioned in the labels in the respective panels.

Table 4.2. Thermal denaturation midpoint (T_m) of α-LA in the presence of SDS and CTAB†

[SDS], mM	T_m, K	[CTAB], mM	T_m, K
0.1	335.5	0.05	330.3
0.5	336.0	0.1	326.8
1.0	335.0	0.5	316.4
2.0	331.5	...	...

† - in the absence of any surfactant T_m value of α-LA is 332.2 K.

was increased above 2 mM. Also, SDS stabilized the protein against denaturation by temperature up to 1 mM but destabilized at higher concentrations. There was no complete unfolding of the protein in all the solution conditions studied, even at 90 °C. In the presence of CTAB, there is a cooperative loss in the structure of protein and complete denaturation was observed in the studied temperature range. Increasing concentrations of CTAB led to increased loss in the structure as evident from the left shift in the thermal curves indicating that the denaturation sets earlier in the presence of the cationic surfactant. At above 1.0 mM of CTAB, non-cooperative transitions were observed.

4.4. Discussion

The conformational changes on α-LA in the presence of surfactants have been characterized in some of the earlier studies[146,147], but their influence on the fibrillation propensity has not been studied in detail. The fibrillation condition for α-LA at pH 7 was optimized by following changes in ThT fluorescence (Fig 4.2) and the fibril formation was confirmed by microscopic images (Fig 4.3). The effect of surfactants on α-LA in the presence of varying concentrations of SDS, CTAB and Tx was followed to get insights into the role of charge interactions in producing different denatured states and their influence on fibril formation. In the presence of SDS, there is a biphasic effect with lower concentrations promoting or inducing fibrillation whereas >2 mM concentration induces formation of amorphous aggregates. At lower concentrations, the lag time is extended slightly, but insignificant changes in the elongation rates are observed. In the presence of 0.05 mM SDS, the increase in lag time can be attributed to charge neutralization of proteins surface residues and without much exposure of the buried hydrophobic residues. 0.5 mM to 2.0 mM SDS is found to significantly extend the lag time and elongation rate shows three to 6-fold increase in magnitude.

In CTAB and Tx, fibrillation is induced in the presence of all the concentrations employed i.e. both monomeric and micellar forms had the ability to drive the orderly formation of fibrils. In the presence of lower concentrations of CTAB, the lag time is slightly increased probably due to opposite charge interactions between α-LA and CTAB (Fig 4.4B). However, at near-CMC concentration the lag time is prolonged by ten-fold compared to the lag time in the absence of surfactants. Above the CMC of CTAB, the lag time is comparable to that of the time observed at lower concentrations. In all the cases, the elongation rate is increased; particularly the fastest elongation is noted near-CMC of CTAB. These changes are similar to

that observed in lysozyme in the presence of SDS (Table 3.3) suggesting that the surface charge on the protein and the surfactant head group plays an essential role on the fibrillation kinetics of these proteins. Tx shows almost a linear increase in the lag time with increasing surfactant concentration which might be due to its non-ionic nature. Though the elongation rates are higher in the presence of Tx compared to water, there is a slight retardation noted above the CMC of the surfactant. In overall changes, it is interesting to note that the prolonged lag time, in general, accelerated the elongation phase. The extent of increase is not linear, probably due to different charge-charge interaction factors.

Conformational changes followed in the presence of SDS at far-UV CD shows loss of helical content at higher temperatures (Fig 4.7A). The tertiary structural changes are also substantially lost at these concentrations, assisting in the exposure of hydrophobic residues corroborated by the red-shift in the emission maxima.[147] The TNS fluorescence suggests an initial charge interaction between protein and monomeric form of SDS, above 0.2 mM quasi-micellar aggregates are formed around the protein resulting in greater exposure of hydrophobic surface. SDS-micellar aggregates formed might delay the association of protein chains representative of nucleation, thus increasing the lag time. In the presence of CTAB also similar charge interactions prevail resulting in only trivial changes in TNS fluorescence (Fig 4.6B) till 0.01 mM correlating with little conformational change in α-LA structure which is also evident from the Trp fluorescence. TNS fluorescence starts to rise in the intensity till 0.15 mM, and then declines till 0.3 mM, though the proteins fluorescence increases linearly. These effects propose that CTAB and TNS initially bind to the hydrpphobic patches of the protein. As the CTAB concentration is increased above 0.15 mM, TNS binding sites are replaced by CTAB and TNS molecules are released back to the solvent from the protein surface. During this event, the continuous binding of CTAB unfolds the protein. Above 0.3 mM, the protein's hydrophobic surface is completely occupied by CTAB where further increase in CTAB could not change the protein's conformation. At these concentrations, CTAB could form free micelles which can act as hydrophobic surfaces for TNS, thus, increasing the fluorescence of TNS molecules. These events suggest that though SDS and CTAB have different charges they might act up on the protein surfaces via a common mechanism in denaturation.

The ellipticity changes followed at near-UV region (Fig 4.8) suggests gain in secondary structure at higher temperatures in the presence of monomeric forms of CTAB where most of the tertiary contacts are lost. However, further increase in CTAB concentration resulted in loss of structure. These results suggest that both monomeric and micellar forms of CTAB induce different conformational states in α-LA. Nevertheless, both could drive the protein to fibril

formation with different rates. In case of lysozyme, the conformational state induced by micellar concentration of CTAB could not direct the protein towards fibrillation pathway. This suggests that though these two proteins can have common mechanism on surfactant induce unfolding, they can exert differential behaviour on their fibrillation propensity. Non-ionic surfactant shows similar effect on both the proteins as expected.

4.5. Summary

The present study shows that the effect of surfactant on protein depends on the charge of surfactants' head group and the surface charge on the protein. All of the surfactants are found to increase the lag time in both α-LA and lysozyme. SDS shows an increase in the lag time by many fold in α-LA compared to lysozyme. Elongation rate is also increased more in α-LA while the changes observed in lysozyme are insignificant. However, fibrillation is inhibited in case of both the proteins in the presence of micelles of SDS. The unfolding behaviour also is similar in case of both α-LA and lysozyme. Near-CMC concentrations of CTAB show huge increase in the lag time in case of α-LA. In contrast, CTAB resulted in opposite changes in lysozyme with near-CMC concentrations have shorter lag phase than the monomers. Interestingly, the micelles of CTAB could not inhibit the fibril formation by α-LA whereas they could do so in lysozyme. This evidences that the inhibition effect is protein conformation dependent as well. Increase in the Tx concentration shows a linear increase in the lag time in α-LA, in contrast to the completely different trend observed in lysozyme where micelles induce shorter lag time. Overall, the results suggest that surface charge on the protein and the type of surfactant dictate the kinetics of microscopic steps and the associated macroscopic formation of fibril assemblies.

Chapter 5

How do Polyols and a Molecular Crowder Influence Protein Fibrillation? - A Case Study on α-Lactalbumin

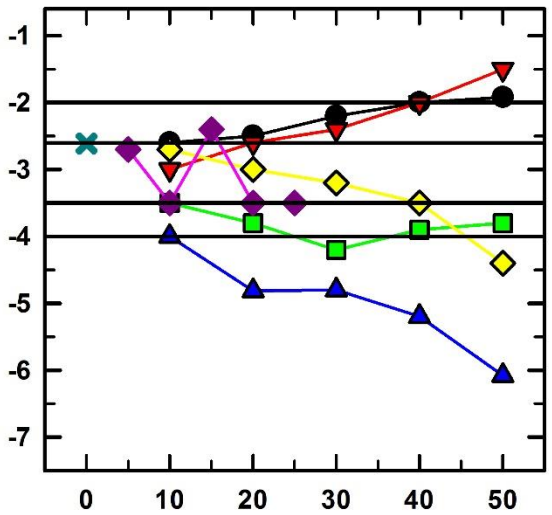

Abstract

Molecular crowding refers to the effect of high solute concentrations on chemical reactions. Model compounds used to mimic the cellular environment generally alter the thermodynamic stability of the proteins by excluded volume effect and also impart viscosity to the solution which is generally ignored in most of the *in vitro* studies. The present study attempts to follow the effect of crowding and viscosity on the fibrillation propensity of α-lactalbumin (α-LA) using polyols as co-solvents. The free energies of unfolding of the protein in the presence of varying concentrations of different polyols were calculated and four isostable solution conditions were identified based on their unfolding free energies i.e., 2.0 *kcal/mol.*, 2.6 *kcal/mol.*, 3.5 *kcal/mol.*, 4.0 *kcal/mol*. The fibrillation kinetics of α-LA were followed using thioflavin T (ThT) fluorescence. The results showed that the kinetic parameters vary in different polyol solutions, though they were initiated from similar isostable conformations. The effects imparted by polyols mainly fell into 3 categories: Category1- polyols showed inhibition of fibrillation. For instance, glycol at the concentrations above 20%. In Category2- elongation rate decreases with an increase in viscosity. In Category3- elongation rate increases with increase in viscosity. These results suggest that polyols exert their own individual effects irrespective of initial conformation of the protein and solution viscosity. Increase in the concentration of PEG400, a crowding agent which promotes effective interactions between the protein molecules, resulted in shorter lag time and slower elongation.

5.1 Introduction

Cells contain a variety of solutes occupying as much as 40% of their internal volume[160], a fact that is often ignored by in-vitro experiments.[161] Such media are referred to generically as 'crowded' rather than 'concentrated', as no individual macromolecular species is present at high concentration.[162] There is no direct interaction between these cellular solutes and proteins, they are preferential excluded from the protein surface. Net result is the change in macromolecular thermodynamic stability due to rise in the protein's free energy in proportion to the preferentially excluding exposed surface area.[163] Proteins lower this free energy penalty by reducing interfacial area *via* folding and assuming more compact conformations. This ''chemical chaperone'' effect mechanism may be sufficient to drive proteins to fold, bind, or shift towards aggregation.[162,164-165] The only requirement is the exclusion of co-solutes from the protein-water interface because of unfavourable interactions termed as solvophobic effect.[76,166] Many theories published discuss the effect of crowding on solution equilibria based on

the assumptions of models such as available volume theory (AVT), scaled particle theory (SPT) and statistical-mechanical models.[163,167,168] A complicated enthalpy-entropy compensation has been found to be the responsible for polyol-induced stabilization of proteins and closely related to solvent ordering around the solute molecules.[169,170] Recent simulation experiments have suggested that apart from routine entropic crowding mechanism, folding of proteins and peptides by osmolyte action can be enthalpic in nature.[171–174] The peptides first hydration shell is affected by perturbation of solution hydrogen bonding network. As a result, lesser hydrogen bonds are disrupted between peptides 1st hydration shell and water, internal hydrogen bonds are strengthened and the internal peptide-water bonds are favoured resulting in stabilization of proteins that can even protect the proteins against denaturation by agents as urea and GdmCl.[175–180] Also, the leakiness in the chaperonin-mediated protein folding is evaded (or differentially assisted in comparison to chaperones)[181,180] in the presence of crowders that prevail in cells cytosol[182,183] and can prevent abnormalities arising due to folding.[176,184–187] The extent of stabilization can in fact promote unfolded proteins to fold as seen in case of many proteins[188–190] and as far related as MET16 peptide,[191] altered forms of RNase T1 and SNase. [192] The enzymatic activity of ligases, polymerases, recA under crowding was also found to be enabled otherwise in a variety of inhibitory conditions suggesting possible role in homeostasis. [163] Crowding can also result in altered substrate specificity and altered reaction products by enzymes proving their efficacy. Polyols have been shown to stabilize the molten globule of proteins by preventing electrostatic repulsion between charged residues and enhancing the hydrophobic interactions.[158,159,193–195]

Assembly of a variety of native proteins such as in case of deoxyhemoglobin, microtubule formation, actin fibers, blood clotting phenomenon occurs under normal physiological conditions and a thermodynamic equilibrium is established between monomers in solution and condensed phase.[162] Excluded volume phenomenon predicts that condensation reactions in crowded environment are transition-state limited rather diffusion-limited and an increase in association rate constant is attributed to shift in equilibrium towards aggregated state.[162,196] There is decreased water activity that will favour decreased protein solubility and self-association; also increased viscosity will lead to decreased diffusion rates and hence decreased kinetics of diffusion-controlled reactions, as in aggregation.[162,197–201] The amorphous aggregates are insoluble forms of protein that lack long-range order (but contain secondary structure) in contrast to ordered fibril deposits and are mostly seen in aqueous protein formulations.[202,203] Many proteins have been studied in detail to compare the effect of crowders such as synuclein[165], *S*-carboxymethyl-α-lactalbumin, human insulin, bovine core histones.[204]

HIV capsid protein association has been inhibited by polyols and sugars whereas n-methyl amines increased it suggesting role of folding state of capsid and higher-order stuctures.[205]

In the present study, we have chosen smaller polyols with increasing –OH groups ethylene glycol, triethylene glycol (TEG), glycerol, sorbitol, sucrose (grouped under osmolytes), and larger macromolecular crowder PEG 400 to dissect the role of chemical identity of polyol, viscosity and excluded volume phenomenon on the aggregation of α-LA. *α*-Lactalbumin (*α*-LA) is a 123-residue mixed *α* + *β* protein with 4 disulfide bonds and the native state binds Ca^{2+} (dissociation constant of 10^{-6}–10^{-9} M). A member of lysozyme family and found majorly in milk, where it acts as a regulatory subunit of the dimeric enzyme lactose synthase. It catalyses the formation of lactose from glucose and galactose, forming the regulatory subunit of lactose synthase along with β-1,4- galactosyl transferase. *α*-LA has been studied for decades as a model for protein stability and folding due to its conformational versatility. [151,206–210] It remains folded between pH 4.2 and 9.5; in the pH-range 4.2–3 and above pH 9.5 it forms the so-called A-state, which is prone to aggregation that results in interaction as well as fusion with the phospholipids vesicles.[211,212] Owing to its simpler structure and sufficient data on its stability and conformations, *α*-LA serves as a good model for crowding and fibrillation studies.

5.2 Materials and Methods

5.2.1 Materials: The materials and chemicals required were procured as mentioned in section 2.2.1.

5.2.2 Sample preparation: Chemical denaturation of α-LA were performed in presence of various polyols (with increasing –OH groups), using guanidium hydrochloride (GdmCl). Native and unfolding buffers were prepared separately ranging from 10% to 50% (w/v) of polyol solutions, concentration of GdmCl was adjusted by measuring refractive index of both the buffers. [213] All the experiments were carried out at 25 °C.

5.2.3 Spectroscopic measurements: The protein conformational changes were followed by fluorescence emission at 350 nm after exciting the samples at 280 nm. The resultant unfolding transitions were fitted into two-state equation to obtain unfolding free energies (Δ*G*) and transition midpoint (C_m).[213]

$$f = \frac{(C_f + (m_f x) + ((C_u + (m_u x)) * exp\left(\frac{(-\Delta G + (m_g x))}{(0.00198 * 303)}/RT\right)}{1 + exp\left(\frac{(-\Delta G + (m_g x))}{(0.00198 * 303)}/RT\right)} \quad 5.1$$

In the equation c_f and c_u are the intercepts, m_f and m_u the slopes of the pre- and post-transition base lines, ΔG is an estimate of conformational stability and m_g is a measure of dependence of ΔG on denaturant concentration (in this study GdmCl). Fibril formation kinetics was followed using change in ThT fluorescence (refer section 2.1.3).

5.2.4 Microscopic Imaging: TEM imaging was performed following the same protocol as mentioned in section 2.1.2 to obtain the images of fibrils.

5.3 Results

5.3.1 Unfolding curves in the presence of Ethylene Glycol: The stability of α-LA in varying concentration of glycol was measured using the free energy of unfolding against GdmHCl. Figure 5.1A shows the transition curves of GdmCl induced denaturation of α-LA in the presence of different concentrations of ethylene glycol. The data were fitted with the assumption of two-state unfolding using the equation 5.1. The resultant concentration mid-point (C_m) and unfolding free energy (ΔG) values are also presented (Fig 5.1B & 1C). The left shift in the unfolding curves towards lower GdmCl concentration with increasing concentration of glycol up to 50% suggests that the protein structure is less protected against denaturation but the co-operativity of the transition was not affected in its presence. It is evident from both the ΔG and *C*m plots that as the concentration of glycol is increased, the

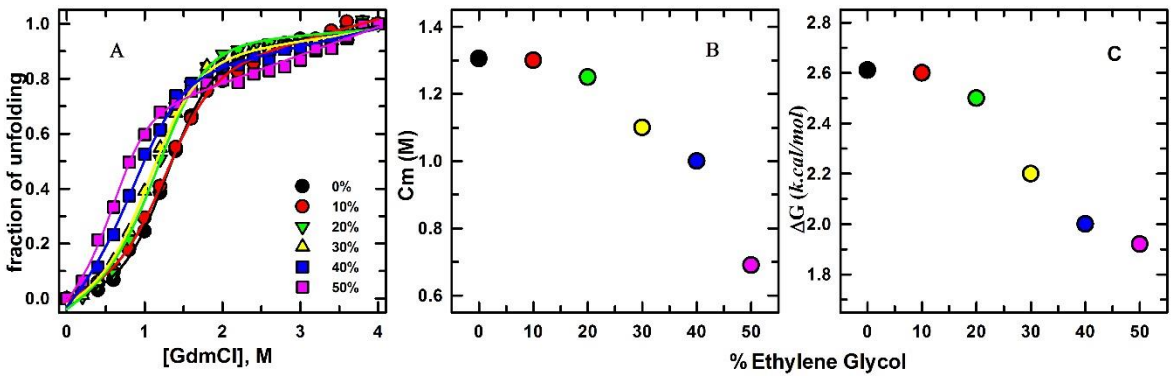

Figure 5.1 (A) The unfolding transitions of α-LA measured from the protein's intrinsic fluorescence in the presence of different concentrations of ethylene glycol. (B) C_m values and (C) the unfolding free energies of α-LA in different concentrations of glycol.

values tend to decrease and can be attributed to the destabilization of protein. The change in free energy between the folded and unfolded protein or the associated energy barrier is decreased in a cooperative manner from 2.6 *kcal/mol.* to *1.9 kcal/mol.* with the concomitant increase in the glycol concentration indicative of more access to glycol.

5.3.2 Unfolding curves in the presence of Trigol

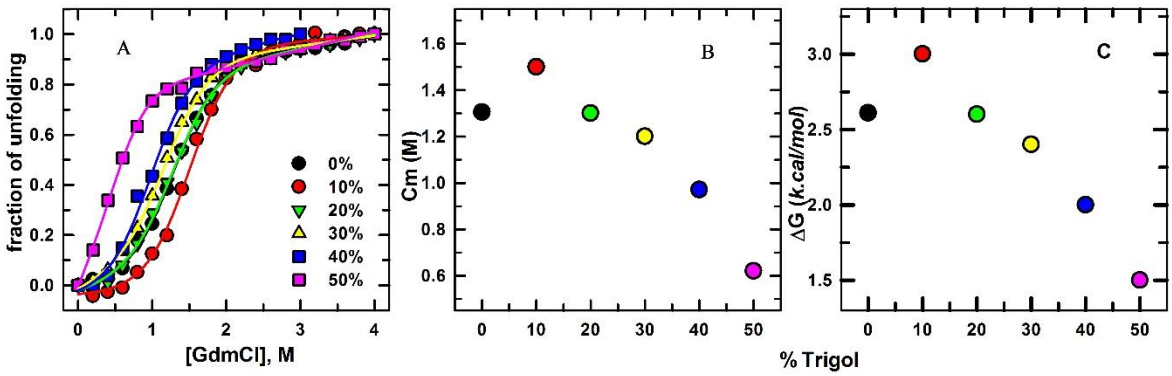

Figure 5.2 (A) The unfolding transitions of α-LA measured from the protein's intrinsic fluorescence in the presence of different concentrations of trigol. (B) C_m values and (C) the unfolding free energies of α-LA in different concentrations of trigol

.

Triethylene glycol (TEG) showed a similar kind of effect as ethylene glycol and causes destabilization of α-LA structure. In 10% TEG, the protein showed a slight increase in both the free energy as well as the effective concentration of Gdmcl required to unfold it (Fig 5.2B & C). The values of *Cm* and free energy difference between the folded and unfolded state complement each other and show a decreasing trend as the concentration of TEG was further increased from 10%. Protein in 50% TEG showed a free energy value of 1.5 *kcal/mol.,* least among all the polyols studied and implies a greater access to the denaturant. The changes induced by TEG were more pronounced compared to glycol and established the fact that TEG is least effective as a co-solvent in protecting the protein structure. Though the unfolding curves showed shift towards left, the cooperativity was not lost and all the transitions were two-state in the presence of TEG.

5.3.3 Unfolding curves in the presence of Glycerol: In contrast to glycols, glycerol protected the native-like conformation of α-LA as is evident from the right shift of unfolding curves shown in Fig 5.3A. The effective concentration of denaturant required to unfold the protein that represents co-operative loss of structure complements with the change in free energy (Fig 5.3B & C) as the concentration of glycerol is increased. The magnitude of changes observed in the free energy in absence of glycerol (*2.6 kcal/mol.*) and in the presence of 50% glycerol (*3.8 kcal/mol.*) suggested greater stabilization of protein. However, comparison of the effects induced by glycerol at the concentrations above 20% showed that they did not cause pronounced changes in the free energy difference (*3.5 kcal/mol to 3.8 kcal/mol*). The results

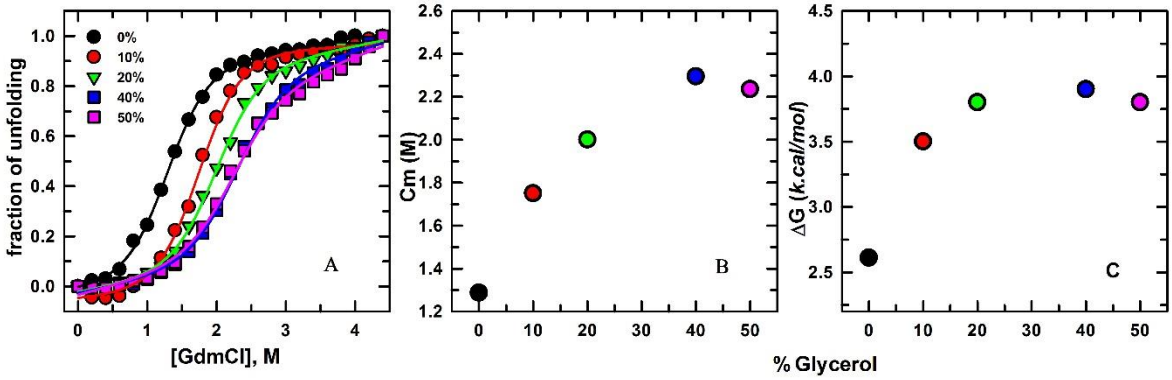

Figure 5.3 (A) The unfolding transitions of α-LA measured from the protein's intrinsic fluorescence in the presence of different concentrations of glycerol. (B) C_m values and (C) the unfolding free energies of α-LA in different concentrations of glycerol.

are in marked contrast to the effects of glycol and trigol and protect the protein structure against denaturation as evident from the increase in C_m values. Certain polyols have been known to decrease the partial specific volume and adiabatic compressibility of several native proteins, suggesting that they become more compact in their presence .[214,215] Also, the polyols including glycerol have been reported to lower the surface tension of water and act via the solvophobic effect in stabilizing the proteins.[216]

5.3.4 Unfolding curves in the presence of Sorbitol: The transition curves in the presence of sorbitol showed shift towards higher GdmCl concentration and provided protection to the protein structure against chemical denaturation. It was evident from the C_m plot that the effective GdmCl concentration required to unfold the protein was also increased from 1.3 M in its absence to 2.3 M in the presence of 50% of sorbitol. Sorbitol also raised the free energy difference between the folded and unfolded states of the protein from *2.6 kcal/mol* in the

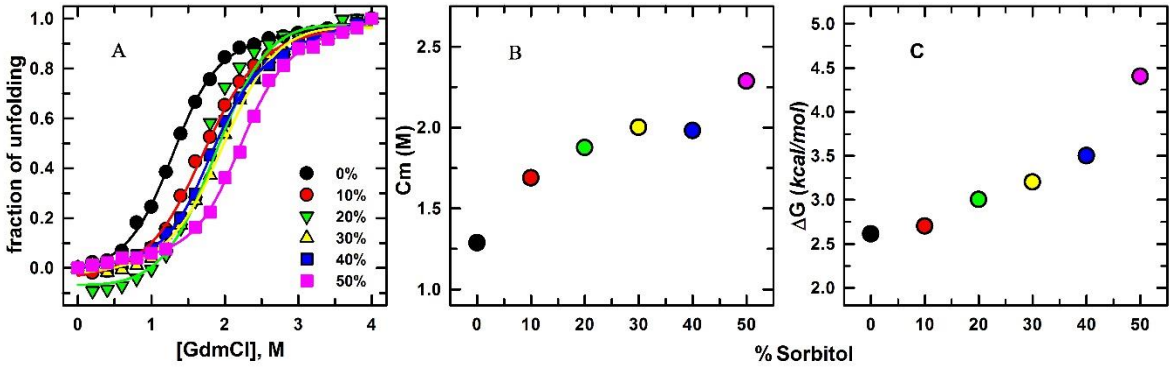

Figure 5.4 (A) The unfolding transitions of α-LA measured from the protein's intrinsic fluorescence in the presence of different concentrations of sorbitol. (B) C_m values and (C) the unfolding free energies of α-LA in different concentrations of sorbitol.

absence of any polyol to *5.0 kcal/mol* in the presence of 50% sorbitol, indicative of stabilization. Earlier rigorous thermodynamic analyses of the effect of sugars such as sucrose[217], glucose[70] & trehalose[218] showed that increase in surface tension acts as the main driving force behind stabilization of proteins and their preferential hydration.

4.3.5 Unfolding curves in the presence of Sucrose: Among all the polyols studied, sucrose showed the maximum shift in the unfolding curves towards higher denaturant concentration. The C_m value increased from 1.3 M to 2.6 M indicated the stabilization of α-LA in the presence of these polyols. Similar to the sugar sorbitol, sucrose also raised the free energy of unfolding from *2.6 kcal/mol* in the absence of polyol to *6.1 kcal/mol* in 50% of sucrose. Earlier studies carried out on amino acid solubility, preferential solvent interactions of proteins, and their thermal stabilities in aqueous polyol solutions have demonstrated that the main driving force for protein stabilization by polyols could be strengthening of the hydrophobic interactions and that water structure and activity also plays a significant role in the stabilization effects of polyols. The results are shown in Fig 5.5.

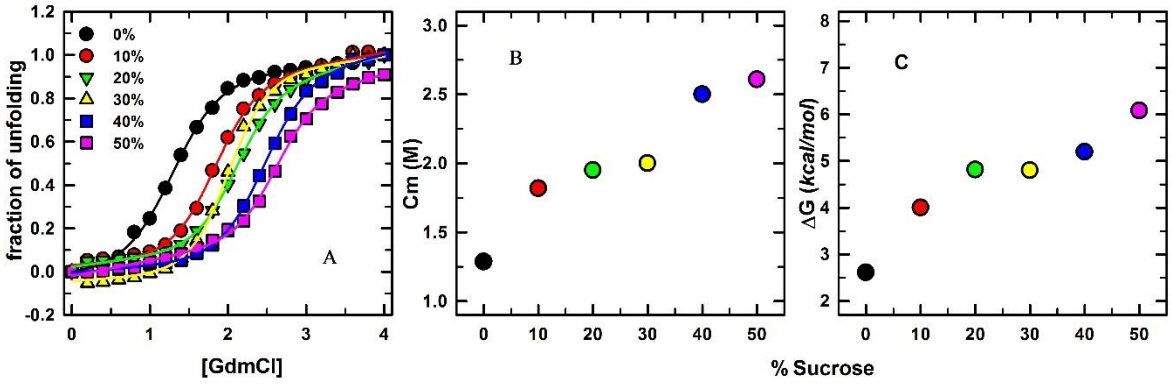

Figure 5.5 (A) The unfolding transitions of α-LA measured from the protein's intrinsic fluorescence in the presence of different concentrations of sucrose. (B) C_m values and (C) the unfolding free energies of α-LA in different concentrations of sucrose.

5.3.6 Unfolding curves in the presence of PEG 400: Large polymeric crowders such as PEG though not naturally occurring, are used to mimic the crowded cellular environment. At lower concentrations, they follow entropy stabilization that often mitigates enthalpic loss while at higher concentrations they penetrate into enthalpically stabilized zone.[216] In the case of α-LA, the stabilization by PEG solutions was small compared to other cosolutes as is evident from the Fig 5.6. Free energy change between folded and unfolded states of α-LA in 50% of PEG

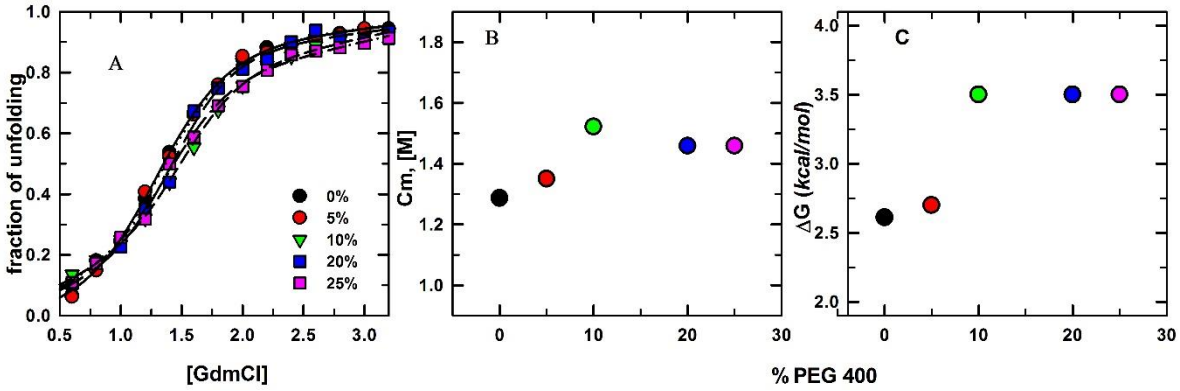

Figure 5.6 (A) The unfolding transitions of α-LA measured from the protein's intrinsic fluorescence in the presence of different concentrations of PEG 400. (B) C_m values and (C) the unfolding free energies of α-LA in different concentrations of PEG 400.

showed an increase only by 1 *kcal/mol* and the effective concentration of GdmCl required to unfold also showed only a slight increase from 1.3 M to 1.5 M.

5.3.7 Free energy change in different polyols: To identify the solution conditions where the initial folded monomer populations are equally stabilised (an isostable state), the $\Delta\Delta G$ values (difference between the free energy of unfolding in presence of polyols and the free energy of unfolding in water) were calculated for all the condition employed. Four isostable conditions were identified with similar unfolding free energies.

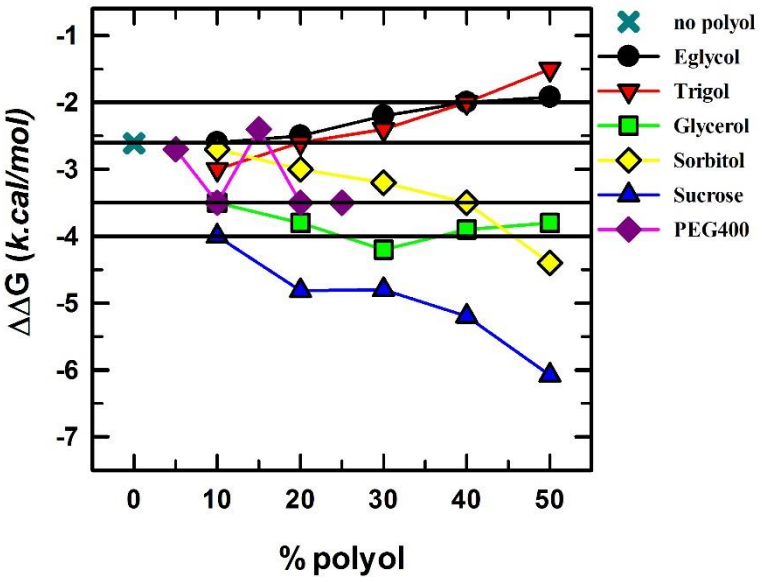

Figure 5.7 Unfolding free energy of α-LA obtained in presence of different polyols plotted against % of polyols. The straight lines represent the isostable conditions of α-LA corresponding to the unfolding free energies of 2.0, 2.6, 3.5, and 4.0 kcal/mol identified in the presence of different polyols.

(i) The solution conditions with free energy of unfolding equal to 2.0 *kcal/mol* which represented a destabilized conformation of the protein compared to its native structure. (ii) The cosolutes that did not alter the stability of the protein, thus, resulted with the unfolding free energy equal to that of the protein in water, i.e., 2.6 *kcal/mol.* (iii) The protein-cosolute system with unfolding free energies of 3.5 *kcal/mol* which showed stabilization of protein in polyols. (iv) Still higher stabilizing conditions of the protein which had unfolding free energy of 4.0 *kcal/mol.* It was presumed that at an isostable condition, the most probable conformation of the protein might be similar. With this assumption, the role of chemical identity and viscosity of polyols on the aggregation kinetics was investigated at four of these isostable conditions.

5.3.8 Kinetics of Lactalbumin at Unfolding free energy of 2.0 kcal/mol.: The effect of co-solutes on α-LA fibrillation was followed by measuring changes in the ThT fluorescence. The fibril forming conditions for the protein at neutral pH were adapted from chapter 4. However, the concentration of protein was increased from 2.0 mg/mL to 2.5 mg/mL in the present study. All the kinetic profiles obtained were fitted to the logistic equation 1.8, and the parameters are presented in Table 5.1.

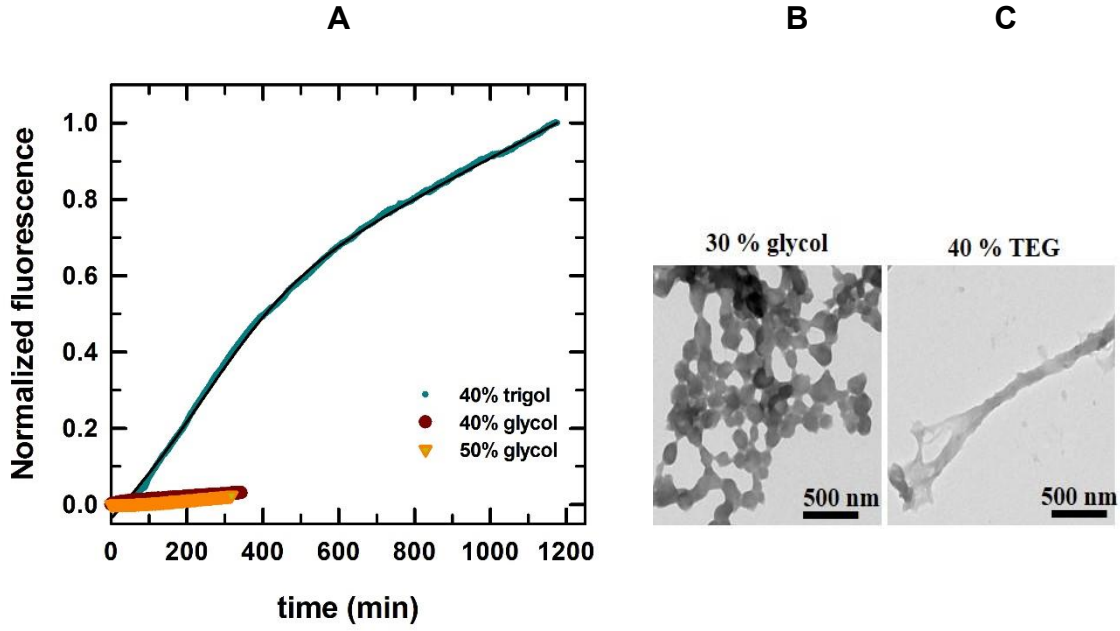

Figure 5.8 Fibrillation kinetics of α-LA followed by the change in ThT fluorescence the presence of 40% TEG, 40 % glycol and 50% glycol. (B) TEM images of the α-LA amorphous aggregates and fibrils in the presence of different concentrations of co-solvents (parentheses).

Figure 5.8A shows fibrillation of α-LA followed using change in the ThT fluorescence in the presence of 40% TEG, 40% and 50% glycol. Only TEG could induce fibril formation by α-LA with a shorter lag phase (Fig 5.8A) whereas glycol could not drive the protein towards orderly formation of fibrils which was evident from the changes observed from ThT fluorescence. Figure 5.8B shows the TEM images of the aggregates as well as the fibrils formed in the presence of glycol and trigol respectively. α-LA in the absence of any cosolute forms fibrils with a longer lag time (discussed below) that is significantly reduced by TEG. However, the rate of fibril elongation was reduced in TEG which finally took almost the same extend of time (~20 h) for complete fibrillation as in water.

5.3.9 Kinetics of Lactalbumin at Unfolding free energy of 2.6 kcal/mol. and 3.5 kcal/mol.: The fibril formation by protein in the presence of polyols that doesn't affect the unfolding free energy occurs at much faster rate compared to kinetics followed in their absence. α-LA without

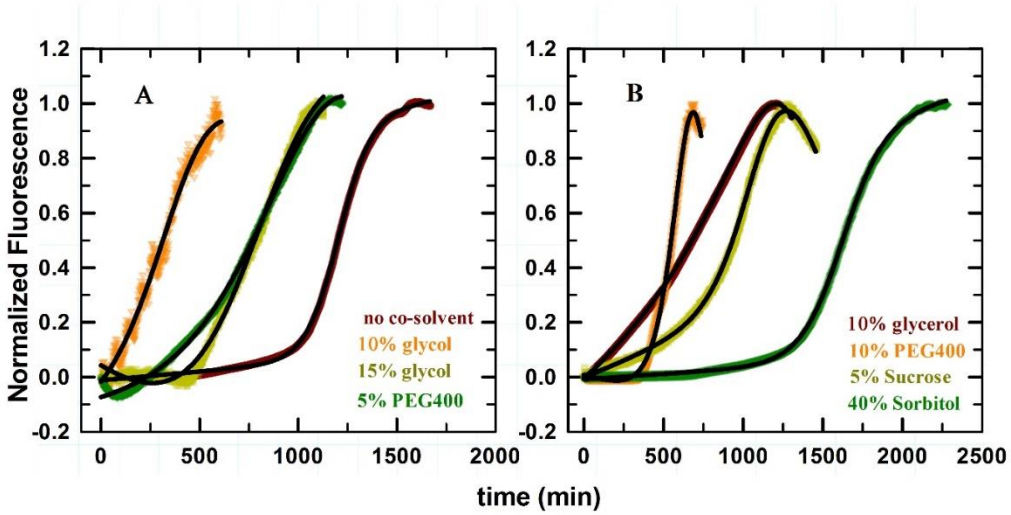

Figure 5.9 Fibrillation kinetics of α-LA followed by change in ThT fluorescence. The solution conditions with the unfolding free energy of α-LA (A) *2.6 kcal/mol.* and (B) *3.5 kcal/mol*. The solid lines represent the fit into empirical logistic equation 2.1. The type and concentrations of polyols employed are shown in the color corresponding to their kinetic curves.

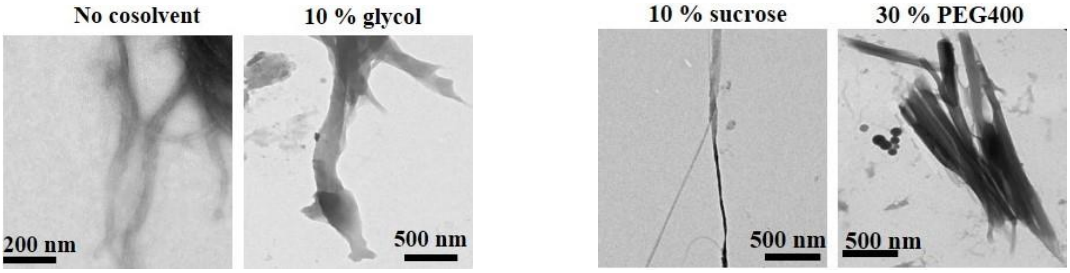

Figure 5.10 TEM images of the α-LA fibrils in the presence and absence of different concentrations of co-solvents representing different isostable free energies (parentheses).

any co-solute shows a lag phase of ~15 h and saturation in fibril formation occurs by ~24 h. In 10% glycol, there is a huge reduction in the lag phase than any other polyols used in this study. In 15% glycol, the lag time was increased compared to 10% of glycol, however, it was still shorter than the lag phase observed in water. PEG at the concentration of 5% also induced a shorter lag phase with increased elongation rate. Figure 4.11 shows the kinetic curves followed at unfolding free energies of *2.6 kcal/mol., and 3.5 kcal/mol.* The kinetics in the presence of stabilizing polyols showed different kinetic profiles. In sorbitol, the protein showed a longer lag phase of ~20 h and faster elongation rate compared to the fibril formation in water. Kinetics in the presence of 10% PEG showed the shortest lag phase compared to other polyols used in this isostable condition. The kinetic data is further strengthened by the TEM images obtained in the presence of different polyols in that fall in to both the unfolding free energies (Fig 5.10).

5.3.10 Kinetics of Lactalbumin at Unfolding free energy of 4.0 kcal/mol.: The solution conditions providing the unfolding free energy of *4.0 kcal/mol* showed varying kinetic profiles in different polyols used. Fig 4.12 presents the fibril formation kinetics followed by ThT fluoresence. In sorbitol, α-LA showed the longest lag time compared to sucrose and glycerol. The lag phase in the presence of sucrose was shorter than sorbitol, but longer than glycerol as it was observed in the solution conditions representing the unfolding free energy of *3.5 kcal/mol.* In glycerol, the lag time was reduced compared to other polyols particularly at the

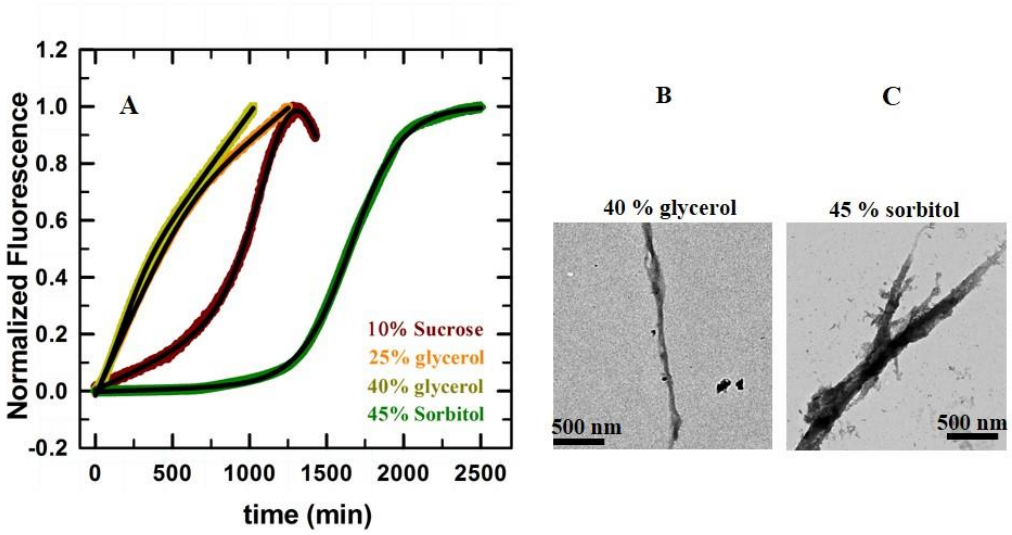

Figure 5.11 Fibrillation kinetics of α-LA followed by change in ThT fluorescence. The solution conditions with the unfolding free energy of α-LA of *4.0 kcal/mol*. The solid lines represent the fit into empirical logistic equation 2.1. (B) & (C) Representative TEM images of the α-LA fibrils at the above mentioned free energy.

higher concentration, i.e., 40%. However, the elongation rate was reduced in the presence of 40% glycerol.

Table 5.1 Lag time and elongation rate of α-LA in different unfolding conditions

% of Polyol	Lag time (min)	Elongation rate (min^{-1})
Unfolding free energy at 2.0 *kcal/mol*		
40% trigol	48	127
40% glycol	*No fibrils*	*No fibrils*
40% glycol	*No fibrils*	*No fibrils*
Unfolding free energy at 2.6 *kcal/mol*		
No polyol	***1037***	***83***
10% glycol	100	150
15% glycol	400	200
5% PEG400	632	239
Unfolding free energy at 3.5 *kcal/mol*		
10% glycerol	700	350
10% PEG400	502	73
5% Sucrose	873	125
40% Sorbitol	1354	132
Unfolding free energy at 4.0 *kcal/mol.*		
10% Sucrose	936	133
25% glycerol	58	221
40% glycerol	20	96
45% Sorbitol	1327	165

5.3.11 Comparison of fibrillation parameters

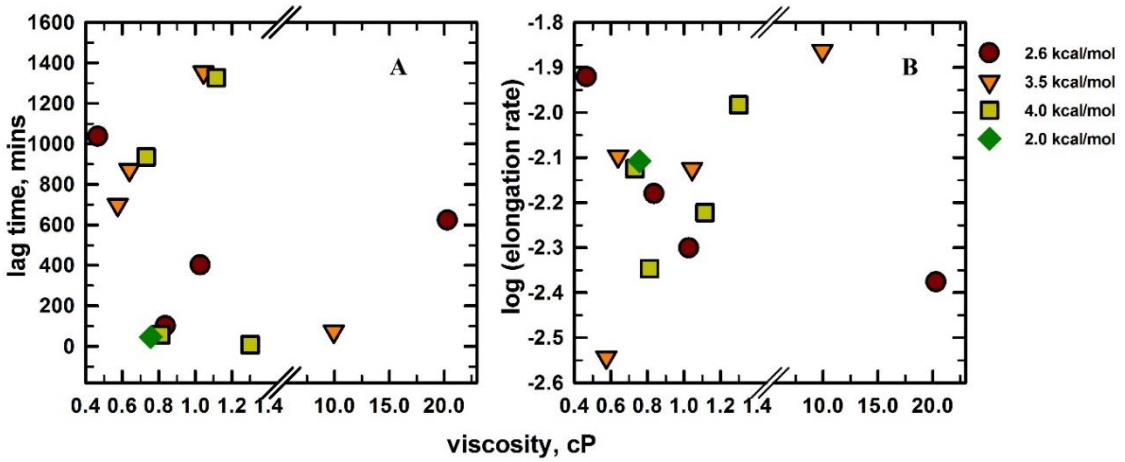

Figure 5.12 (A) Lag time and (B) Elongation rate of α-LA fibrillation followed by ThT fluorescence and calculated using Eqn. 1.1. at different unfolding free energies. The brown circles represent *2.6 kcal/mol.*, orange triangles are points taken at 3.5 *kcal/mol.*, light green squares are of *4.0 kcal/mol.* and dark green diamonds are of *2.0 kcal/mol.* unfolding free energies.

The lag times and elongation rates evaluated at different conditions are plotted against the solution viscosity imparted by the polyols at the fibrillation temperature and presented in Fig 5.12A. imparted the unfolding free energy equivalent to the native state of α-LA (*2.6 kcal/mol*) showed increase in elongation rate as the solution viscosity increased whereas no specific correlation could be drawn between solution viscosity and lag time. The elongation rate for the protein with the isostable unfolding free energy of 3.5 and 4.0 kcal/mol was found to be decreasing with increasing viscosity of the cosolvent. In these cases also no significant correlation between viscosity and lag time was observed.

The effects imparted by polyols mainly fell into 3 categories: Category 1- where

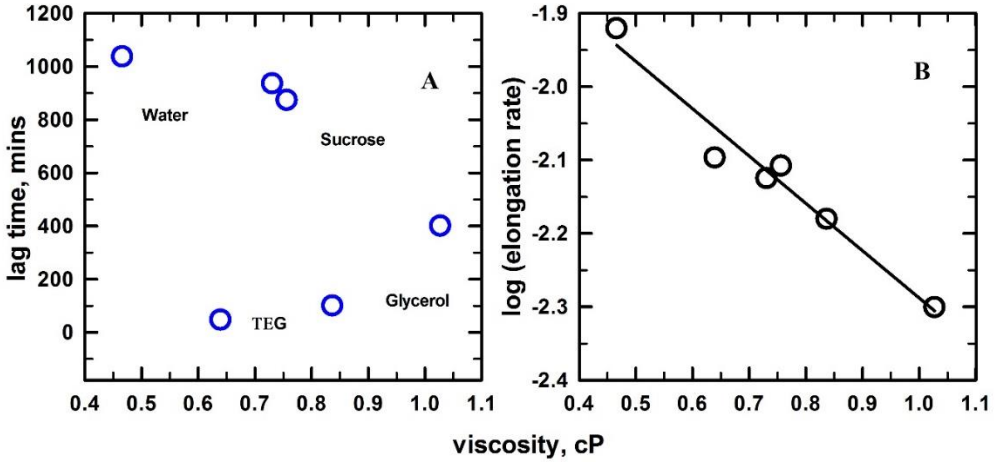

Figure 5.13 Effect imparted by polyols with respect to solution viscosity plotted for the selected solution conditions representing category 2. (A) Increase in the elongation rate with increasing viscosity (B) Non-specific changes in the lag time vs viscosity.

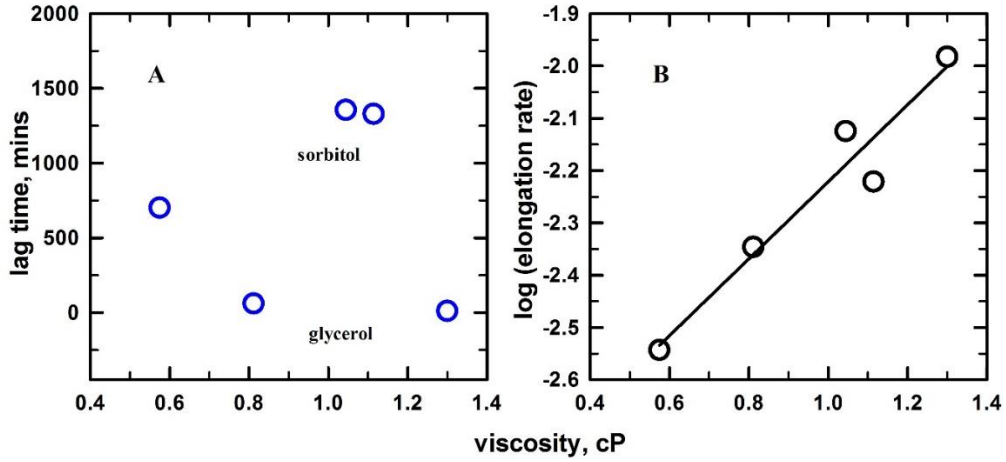

Figure 5.14 Effect imparted by polyols with respect to solution viscosity plotted for the selected solution conditions representing category3. (A) Decrease in the elongation rate with increasing viscosity (B) Non-specific changes in the lag time vs viscosity.

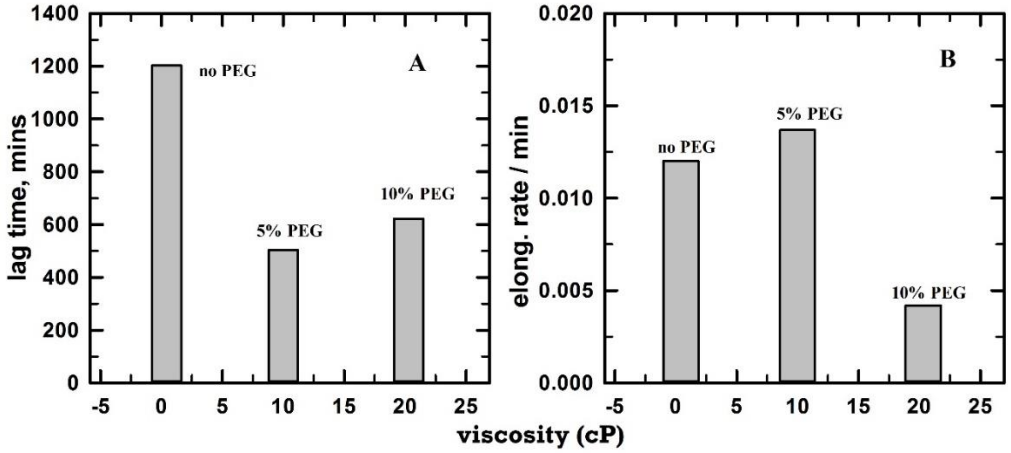

Figure 5.15 PEG induced effects with respect to solution viscosity. (A) Increase in the lag time with viscosity. (B) Decrease in the elongation rate with viscosity.

polyols inhibited protein fibrillation. For instance, glycol at the concentrations above 20% (Fig. 5.8). Category 2- elongation rate decreased with an increase in viscosity and shown in Fig 5.13B. However, sucrose and sorbitol showed longer lag times despite of their low viscosity, and TEG and lower concentrations of glycol decreased the lag time (Fig 5.13A). Category 3- the elongation rate increased with viscosity whereas lag time showed distinct effects for different polyols (Fig 5.14). The results suggest that polyols exert their own individual effects irrespective of initial conformation of the protein and solution viscosity. Increase in the concentration of PEG400, a crowding agent which promotes effective interactions, resulted in shorter lag time and reduced elongation rates as shown in Fig 5.15.

5.4 Discussion

5.4.1 *Effect of polyols on α-LA structure probed by chemical denaturation.*

The conformational changes associated with the addition of polyols with increasing -OH groups were followed using GdmCl as a denaturant. In our present study ethylene glycol, triethylene glycol (TEG), glycerol, sorbitol, sucrose and PEG400 were employed to follow the effect of poyols. The protein's stability in ethylene glycol with varying concentrations ranging from 10% to 50% were measured and it was found to induce destabilization of the protein as is evident from the left shift in the transition curves (Fig 5.1B). This could be due to the fact that the amino acid side chains buried inside in the native state of the protein which are exposed to the solvent upon denaturation by GdmCl are well dissolved in ethylene glycol in a concentration-dependent manner.[219] The slope of the transition curves follow a similar trend in all the percentages of glycol employed and a cooperative decrease in free energy values support the above observations (Fig 5.1C). Ethylene glycol has been previously shown to be less effective than urea in unfolding proteins' such as β-lactoglobulin, RNaseA, hexokinase[194], conalbumin.[219] and can populate different conformations from the native state of proteins. The present study also showed that glycol populates different conformations of α-LA that can either drive the fibril formation or can inhibit it.

Though chemically different from glycol, TEG was also seen to offer less protection to the protein structure against chemical denaturantion (Fig 5.2A). It has been asserted that the thermodynamic interaction between osmolyte and proteins' functional groups is the major driving force behind preferential exclusion.[76] In thermodynamic sense, the denatured ensembles formed in different percentages of TEG exhibit favourable interaction and causes it to expand. Timasheff *et al*[220] has shown that in a three-component system, the effects of additives on protein stability and solubility are determined by the preferential interaction between protein and solvent components. The observations reiterate the above fact and can be extended to four-component system as in our present study (protein-water-GdmCl-TEG). Recently *S.Sukenik et al* [191] have shown that TEG and sorbitol though of same size (with partial molar volume of 130 mL/mol. & 120 mL/mol. of TEG and sorbitol respectively) yet (de) stabilize peptide by different thermodynamic mechanisms. TEG follows entropy gain whereas sorbitol by enthalpy driven mechanism that overrides unfavourable entropy and highlights the importance of chemical identity of co-solute that goes beyond excluded volume.

Glycerol has been used by biochemists for many years to stabilize native structure of proteins' and the activity of enzymes.[221] Earlier reported studies have shown that proteins are

preferentially hydrated when added to mixed solvents and do so by raising the chemical potential of glycerol.[221] This thermodynamically unfavourable interaction minimises the surface contact between protein and glycerol and stabilises the native structure of globular proteins. In case of α-LA also, a similar effect of stabilisation of native structure is observed. The amount of denaturant required to unfold protein in the presence of glycerol is increased, in a way glycerol opposes the effect of GdmCl and provides protection to the protein. Polyols have been known to decrease the partial specific volume and adiabatic compressibility of several native proteins, suggesting that they become more compact in their presence.[216,214] Polyols including glycerol have been reported to lower the surface tension of water and act via the solvophobic effect.[169]

The effect of sugars on protein structure has been characterised well. Long back sucrose has been shown to prevent heat coagulation of ovalbumin.[222] Simpson and Kauzmann[223,224] observed that sucrose increased the amount of urea required to unfold ovalbumin. Increased thermal stabilities were found for lysozyme and ribonuclease in sorbitol solutions by Gerlsma[225] and gecko.[226] Stabilisation of peptide conformation in presence of sugar's is due to water mediated effects such as increase in surface tension, in contrast reduction in the chemical potential is the major driving force in glycerol solutions.[169] Increase in surface free energy of water plays vital role in preferential hydration of proteins as BSA[227] by decreasing hydrogen bonding rupturing capacity of medium. The major types of interactions that govern the protein stability in a multicomponent system include between polyol-water, polyol-protein, protein-water and protein-denaturant. Denatured RNaseA has been shown to exhibit greater extent of preferential hydration in presence of sorbitol compared to native state.[226] α-LA also showed similar kind of stabilisation in the presence of sorbitol and sucrose. Both the sugars raised the amount of the denaturant GdmCl required to cause unfolding or the denatured ensembles exhibited greater preferential hydration. Of the both, sucrose was found to stabilise the protein more than sorbitol.

The macromolecular crowder, PEG has been shown to stabilise the proteins by steric exclusion mechanism. It is proposed that this effect might mainly arises due to size differences between water and the additives, with PEG being larger than protein results in the preferential exclusion from protein surface.[71] Solvent interaction studies proposed another mechanism by which such additives increase the preferential hydration of proteins leading to their stabilisation. The situation in case of PEG is uncertain. Ingham reported that PEG also stabilises proteins.[228] Knoll and Hermans[229] and Atha and Ingham[230] showed that PEG has no effect on the melting temperature of RNaseA. In the present study PEG has been categorised

under co-solute type with neutral effect as it has no significant changes on the conformation of α-LA. The denaturant required to unfold the protein is similar to that of water even in the higher % of PEG's employed. Also, the change in unfolding free energy by the addition of PEG is ~ 1 *kcal/mol* only.

5.4.2 Effect of polyols on α-LA fibrillation

The kinetics of α-LA fibrillation initiated from different isostable conditions were followed by change in the ThT fluorescence with time. Results suggest that though the fibril formation is initiated from similar isostable conditions, polyols exert their own individual effects compatible with both solvophobic and excluded volume mechanisms. The samples that are included in the unfolding free energy condition of 2.0 *kcal/mol* represent destabilizers, 40% and 50% glycol, 40% TEG. In both the glycol percentages there is a decrease in the ThT fluorescence indicative of inhibition of fibrillation. Probably the non-native structures formed in the presence of higher percentages of glycol could not form the fibrils. Kinetics in presence of 40% TEG showed a lag phase of ~ 1.5 hour and the complete conversion of monomers to fibrils is completed within 20 hrs. The native protein without any co-solute showed a lag phase of ~ 15 hrs, and the saturation in the fibril kinetics is seen after ~ 24 hrs. Samples with similar free energy of stabilization as native protein between folded and unfolded states upon denaturation include 10% and 15% glycol, 5% PEG. Kinetics in the presence of lower percentages of glycol showed a nucleation-dependent polymerization. 10% glycol induced faster aggregation of monomers to fibrils with a very meagre lag phase, whereas in 15% glycol the lag phase was extended up to ~ 7 hrs. The time taken for complete fibril formation is also increased in presence of 15% glycol (~ 20 hrs) in comparison to 10% glycol which took ~ 8 hrs. Recent study showed that conalbumin was not able to form fibrils in all the % of glycol and does so by restoring the secondary structure content of protein.[222] The same phenomenon of restoration of secondary structure is also seen in case of reduced lysozyme and showed more enzymatic activity in presence of glycol than the reduced counter-part alone.[231] In the present case, α-LA showed concentration dependent changes in the fibril kinetics i.e. glycol when used below 20% could induce fibrillation whereas above 20% was shown to inhibit fibrillation. PEG showed faster aggregation kinetics when used at 5%, with a shorter lag phase of ~ 2 hrs, but the overall reaction is completed in the same time frame as 15% glycol (Fig 5.9).

The combination of co-solutes that fall under the unfolding free energy of 3.5 *kcal/mol* include 10% glycerol, 10% PEG, 5% sucrose and 40% sorbitol (Fig 5.10). Sorbitol showed longer lag time of ~ 20 hrs followed by sucrose. These two osmolytes are naturally found in

many life forms in protecting the native conformation of proteins from osmotic stress. Sorbitol acts by strengthening the internal peptide and water-associated hydrogen bonds through the perturbation of the solution hydrogen bonding network in first hydration shell around the proteins, consequently fewer water molecules are lost upon folding.[171] Consistent with the above observations, present study also replicates the above results and sorbitol protects the native conformation of α-LA as evident from the longer time taken for complete fibril formation. Sucrose also being a protective osmolyte also acts by same mechanism in protecting the protein structure. Glycerol mostly used as stabilizing agent for many proteins indeed showed faster aggregation kinetics with shorter lag phase. This may be attributed to the induction of aggregation prone non-native conformation by glycerol which might have more hydrophobic residues exposed to the solvent. Thus, the conversion of the monomers into nucleation occurs quickly. Fibril formation in 10% PEG occurred at a faster rate with lag phase slightly extended when compared with 5% PEG. The overall time taken for complete fibril formation is drastically reduced from ~ 20 hrs to ~ 10 hrs when concentration of PEG is increased. Kinetic curves in the presence of PEG exhibit sharp transitions, probably because it promotes fibril fragmentation. PEG was shown to accelerate fibrillation of diverse proteins as S-carboxy-methyl-lactalbumin (disordered form of the protein), human insulin (rigid α-helical protein), bovine core histones (natively unfolded), human recombinant α-synuclein (natively unfolded) and in a size and concentration-dependent manner.[204] These results are in agreement with the earlier reported studies that compare the chemical structure of osmolytes and PEG and their mechanism of action. Of the several differences, most of the polyols act both as acceptor and donor[232] of hydrogen bonds while forming multiple hydrogen bonds with the surrounding water molecules whereas PEG can act only as acceptor of hydrogen bonds leading to the differences in their action as "chemical chaperones". The results further affirm the fact theoretically established by applying Kirkwood-Buff theory of solutions to system containing co-solutes and an aggregating protein that states monomeric form of proteins are affected differently than the fibrils by various co-solutes.[168]

The unfolding free energy of 4.0 *kcal/mol* is the most stabilizing of all and the co-solutes included in this category are 25% and 40% glycerol, 10% sucrose and 45% sorbitol. Glycerol indeed accelerates fibrillation in a concentration-dependent manner with 40% showing faster aggregation or a very short lag phase of ~ 20 min followed by 25% that showed a lag phase of ~1 hr. Sorbitol and sucrose increased the time taken for complete fibrillation with longer lag times consistent with their protective role as osmolytes. Glycerol accelerates fibrillation by decreasing the lag time as the concentration was increased whereas PEG showed

the opposite effect by inducing quicker formation of fibrils by faster elongation rate. Sucrose and sorbitol increased the time taken for complete fibrillation as their concentration is increased with concomitant increase in the lag time. Based on the above observations, the effects imparted by polyols on the fibrillation of α-LA can be categorised into three types: Category-1 effect, fibrillation is inhibited in the presence of higher concentrations of glycol. In Category -2 (Fig 5.13), the elongation rate decreased with increase in viscosity whereas non-specific changes in lag time are noted. In Category-3, the elongation rate increased with increase in viscosity whereas non-specific changes in lag time are noted (Fig 5.14). The modification of folding states of the protein in the presence of co-solutes for fibrillation are determined by their attractive and repulsive interactions in the ternary system (water-protein-co-solute) are not resolved, makes it difficult for the association reactions to be predicted. Because the co-solutes are preferentially excluded from the proteins surface, it is reasonable to assume that the properties of bulk water surrounding the protein are responsible for the altered fibril formation kinetics. Also, it is observed that rather than viscosity the chemical identity of polyol plays a major role. This is consistent with the crowding models which state that increase in co-solutes translational entropy drives the folding of proteins with a decrease in preferential hydration.[162] Osmolytes while contributing in a similar entropic fashion to proteins stability also have been shown to cause net repulsive interactions with the peptide backbone compared with the bulk water and modify the folding free energy.[233,76,234] Studies on MET16 peptide showed that in addition to entropic crowding mechanism, polyols also showed an alternative favourable enthalpic contribution to the folding free energy.[235] Though the mechanism of this enthalpic contribution is unclear, it is assumed that water structuring around the protein interface may be the key factor. In other words, these interfacial water acts as poorer solvents for osmolytes causing their depletion around the immediate vicinity of protein and allows for polyol-water interactions that results in enthalpic contribution.[76,234]

5.5 Summary

The stability of α-lactalbumin in presence of polyols with increasing –OH groups was studied using chemical denaturation of the protein with GdmHCl. Of the osmolytes chosen, ethylene glycol and TEG were found to destabilize the protein as is evident from the decrease in the free energy and Cm values. Glycerol stabilizes the protein, in agreement with the earlier studies. Both sugars, sorbitol and sucrose were found to stabilize the protein. Above said molecules mimic the role of compatible osmolytes, PEG400 used as macromolecular crowder did not

show much effect neither in effective Gdmcl concentration required to unfold protein or in the free energy of unfolding. Four isostable conditions, based on unfolding free energy, were identified with different polyol conditions. The fibril kinetics followed at these conditions suggested that rather than viscosity imparted by polyols, the chemical identity of individual polyols determines the fibrillation reaction parameters. This could be due to the fact that different polyols act upon the protein through different mechanisms on the (de)stability of the protein. Further, PEG, a represented molecular crowder used here accelerates the initial nucleation whereas reduces elongation rate.

Concluding Remarks

The work carried out broadly looks at the effect of small molecules such as urea, surfactants and molecular crowders on different proteins that vary in their final 3D-conformations attained under normal physiological conditions. Urea when taken in different molar concentrations results in variation of the kinetic pathways adopted by lysozyme at neutral pH. In the presence of 2M urea the protein mainly follows nucleation-dependent mechanism. When the urea concentration in the solvent system is 4M, HEWL shifts to nucleation-independent mechanism without lag phase. Rise in protein concentration doesn't alter the mechanism in case of 2M urea but in 4M urea, the kinetic pathway shifts from nucleation-independent to nucleation-dependent mechanism suggesting latter as the dominant mechanism for the conversion to fibrils and that the pathway is kinetically controlled. The linear dependency of various kinetic parameters on protein concentration such as lag time, elongation rate and scaling factor suggests that the protein follows monomer-dependent primary nucleation mechanism without any significant secondary nucleation events.

Surfactants represent a class of potent denaturants (act in millimolar concentrations) than the routinely employed denaturants such as urea and Gdmcl that are otherwise used in molar concentrations. Anionic, cationic and non-ionic surfactants effect on the structure and fibrillation propensity of two proteins HEWL and α-LA, bearing different surface charge was studied. The fibril forming conditions for lysozyme represent the 2M and 4M urea-induced solvent systems, the conditions that represent nucleation-dependent and nucleation-independent mechanism respectively. These solvent systems are good model to study the effect of surfactants on fibrillation propensity and on the different phases that involve lag, elongation and saturation respectively. There were differential effects of ionic and non-ionic surfactants on HEWL fibrilltion, SDS and CTAB micelles were efficient in inhibiting the fibrillation by HEWL whereas non-ionic Tx100 micelles could not do so. Monomeric forms of both the ionic non-ionic surfactants induced fibril formation by lysozyme with an increase in the initial lag phase and near-CMC concentrations being effective in reducing the lag time. The time taken for complete fibril formation in the presence of varying concentrations of Tx100 is increased. Even the rate of fibril elongation varied in the presence of different surfactants suggesting multiple factors might influence the elongation process.

To get further insights into the effect of surfactants on proteins, α-LA an acidic protein was chosen as model and results obtained were compared with that of HEWL. SDS showed similar effects as seen in HEWL with monomeric forms of SDS only capable of converting the monomers to fibrils whereas micelles inhibited the fibrillation. The near-CMC concentrations showed huge increase in lag time (~60 fold) with non-significant changes in the elongation

compared to lower concentrations. The results suggest that the inhibition of fibrillation by SDS micelles might be a common mechanism irrespective of proteins surface charge. CTAB and Tx100 showed varying effects with both monomers and micelles able to induce the fibrillation of lactalbumin. Only near-CMC concentrations of CTAB increased the lag time whereas lower and micellar concentrations resulted in quicker conversion of proteins monomers to orderly aggregates of fibrils. The elongation rate decreased as the CTAB concentration is increased. Tx showed concentration-dependent effects with lower concentrations being efficient on the overall assembly process i.e. lower lag times and quicker formation of fibrils when compared to micelles. The results in comparison to basic protein HEWL suggest that initial nucleation phase, in the presence of surfactants on proteins bearing different surface charges is primarily controlled by charge interactions whereas multiple factors might influence fibril elongation.

Further studies carried out made use of model compounds that mimic cellular environment and vary the macromolecular thermodynamic stability by preferential exclusion from proteins surface. The question is how the stabilized non-native conformations in the presence of molecular crowders were able to form fibrils? To probe the role of chemical identity and viscosity on the fibrillation of α-LA, polyols with increasing -OH groups were taken that include ethylene glycol, trigol, glycerol, sorbitol, sucrose and PEG400. Using different % of polyols, free energies of unfolding were calculated and four different isostable conditions chosen for fibrillation studies. The results showed that the kinetic parameters varied though the fibril formation is initiated from similar isostable conformers. The effects imparted by polyols mainly fell into 3 categories with type1 being inhibition of fibrillation as seen in case of glycol above 20%. In type 2, elongation rate decreased with increase in viscosity. Sucrose and sorbitol despite of their low viscosity showed huge lag times, TEG and lower concentrations of glycol decreased lag time. In type 3 that includes glycerol and sorbitol showed increase in elongation rate with an increase in viscosity. The results indicate that polyols try to exert their own individual effects irrespective of the initial conformation of protein and viscosity of solution.

References:

1. Díaz-Villanueva, J., Díaz-Molina, R. & García-González, V. Protein folding and mechanisms of proteostasis. *Int. J. Mol. Sci.* **(2015)** *16*, 17193–17230.
2. Chiti, F. & Dobson, C. M. Protein misfolding, functional amyloid, and human disease. *Annu. Rev. Biochem.* **(2006)** *75*, 333–366.
3. Gregersen, N., Bross, P., Vang, S. & Christensen, J. H. Protein misfolding and human disease. *Annu. Rev. Genomics Hum. Genet.* **(2006)** *7*, 103–124.
4. Sipe, J.D. & Cohen, S. I. A. Review: history of the amyloid fibril. *J. Struct. Biol.* **(2000)** *130*, 88–98.
5. Sipe, J. D. Amyloidosis *Annu. Rev. Biochem.* **(1992)** *61*, 947–975.
6. Blancas-Mejia, L. M. & Ramirez-Alvarado, M. Systemic amyloidoses. *Annu. Rev. Biochem.* **(2013)** *82*, 745–774.
7. Stefani, M., Dobson, C. M. & Pro-, J. H. P. Protein aggregation and aggregate toxicity : new insights into protein folding , misfolding diseases and biological evolution. *J. Mol. Med.* **(2003)** *81*, 678–699.
8. Dovidchenko, N. V, Leonova, E. I. & Galzitskaya, O. V. Mechanisms of amyloid fibril formation. *Biochem. Biokhimiia* **(2014)** *79*, 1515–27.
9. Guijarro, J. I., Sunde, M., Jones, J. A, Campbell, I. D. & Dobson, C. M. Amyloid fibril formation by an SH3 domain. *Proc. Natl. Acad. Sci. U. S. A.* **(1998)** *95*, 4224–4228.
10. Chiti, F., Webster, P.,Taddei, N., Clark, A., Stefani, M., Ramponi, G., and Dobson, C M. Designing conditions for in vitro formation of amyloid protofilaments and fibrils. *Proc. Natl. Acad. Sci. U. S. A.* **(1999)** *96*, 3590–4.
11. Fandrich, M., Forge, V., Buder, K., Kittler, M., Dobson, C M., and Diekmann, S. Myoglobin forms amyloid fibrils by association of unfolded polypeptide segments. *Proc. Natl. Acad. Sci. U. S. A.* **(2003)** *100*, 15463–15468.
12. Pertinhez. T. A., Bouchard, M., Tomlinson, E. J., Wain, R., Ferguson, S. J., Dobson, C M., Smith, L. J. Amyloid fibril formation by a helical cytochrome. *FEBS Lett.* **(2001)** *495*, 184–186.
13. Ramakrishna, D., Prasad, M. D. & Bhuyan, A. K. Hydrophobic collapse overrides Coulombic repulsion in ferricytochrome c fibrillation under extremely alkaline condition. *Arch. Biochem. Biophys.* **(2012)** *528*, 67–71.
14. Konno, T., Murata, K. & Nagayama, K. Amyloid-like aggregates of a plant protein: A case of a sweet-tasting protein, monellin. *FEBS Lett.* **(1999)** *454*, 122–126.
15. Tang, C. H., Zhang, Y. H., Wen, Q. B. & Huang, Q. Formation of amyloid fibrils from kidney bean 7s globulin (phaseolin) at pH 2.0. *J. Agric. Food Chem.* **(2010)** *58*, 8061–8068.
16. Anfinsen, C. B. Studies on the principles that givern the folding of polypeptide chains. *Lecture, N.* **(1972)** *55-71*.
17. Dobson, C. & Karplus, M. The fundamentals of protein folding: briging together theory and experiment. *Curr. Opin Struct. Biol.* **(1999)** *9*, 92–101.
18. Rochet, J. C. & Lansbury, P. T. Amyloid fibrillogenesis: Themes and variations. *Curr. Opin. Struct. Biol.* **(2000)** *10*, 60–68.

19. Uversky, V. N. & Fink, A. L. Conformational constraints for amyloid fibrillation: The importance of being unfolded. *Biochim. Biophys. Acta-Proteins Proteomics* **(2004)** *1698,* 131–153.
20. Smith, L. J., Fiebig, K. M., Schwalbe, H. & Dobson, C. M. The concept of a random coil. Residual structure in peptides and denatured proteins. *Fold. Des.* **(1996)** *1,* R95–R106.
21. Thirumalai, D., O'Brien, E. P., Morrison, G. & Hyeon, C. Theoretical perspectives on protein folding. *Annu. Rev. Biophys.* **(2010)** *39,* 159–183.
22. Levinthal, C. Are there pathways for protein folding? *J. Chim. Phys. Physico-Chimie Biol.* **(1968)** *65,* 44–45.
23. Chan, H. S. & Dill, K. A. The Protein folding problem. *Phys. Today* **(1993)** *46,* 24–32.
24. Ohnishi, S. & Takano, K. Amyloid fibrils from the viewpoint of protein folding. *Cell. Mol. Life Sci.* **(2004)** *61,* 511–524.
25. Fowler, D. M., Koulov, A. V., Balch, W. E. & Kelly, J. W. Functional amyloid- from bacteria to humans. *Trends Biochem. Sci.* **(2007)** *32,* 217–224.
26. Maury, C. P. J. The emerging concept of functional amyloid. *J. Intern. Med.* **(2009)** *265,* 329–334.
27. Fowler, D. M., Koulov, A. V Christelle., Jost, A., Marks, M. S., Balch, W. E., Kelly, J. W. Functional amyloid formation within mammalian tissue. *PLoS Biol.* **(2006)** *4,* 0100–0107.
28. Mostaert, A. S., Higgins, M. J., Fukuma, T., Rindi, F. & Jarvis, S. P. Nanoscale mechanical characterisation of amyloid fibrils discovered in a natural adhesive. *J. Biol. Phys.* **(2006)** *32,* 393–401.
29. Selkoe, D. J. Alzheimer's Disease: Genes, proteins, and therapy. *Physio. Rev.* **(2001)** *81,* 741–766.
30. Dobson, C. M. Protein misfolding, evolution and disease. *Trends Biochem. Sci.* **(1999)** *24,* 329–332.
31. Chapman, M. R., Robinson, L. S., Pinkner, J. S., Roth, R., Heuser, J., Hammar, M., Normark, S., Hultgren, S. J. Role of Escherichia coli curli operons in directing amyloid fiber formation. *Science* **(2002)** *295,* 851–855.
32. Hervás, R. Li, L., Majumdar, A., Ramírez, M. C. F., Unruh, J. R., Slaughter, B. D., Galera-Prat, A., Santana, E., Suzuki, M., Nagai, Y., Bruix, M., Tintó, S. C., Menéndez, M., Laurents, D. V., Singh, K., Vázquez, M. C. Molecular basis of Orb2 amyloidogenesis and blockade of memory consolidation. *PLoS Biol.* **(2016)** *14,* 1–32.
33. Kelly, J. W. & Balch, W. E. Amyloid as a natural product. *J. Cell Biol.* **(2003)** *161,* 461–462.
34. Maji, S. K., Perrin, M. H., Sawaya, M. R., Jessberger,S., Vadodaria, K., Rissman, R. A., Singru, P. F., Nilsson, K. P. R., Simon, R., Schubert, D., Eisenberg, D., Rivier, J., Sawchenko, P., Vale, W., Riek, R. Functional amyloids as natural storage of peptide hormones in pituitary secretory granules. *Science* **(2009)** *325,* 328–32.
35. Knowles, T. P., Fitzpatrick, A. W., Meehan, S., Mott, H. R., Vendruscolo, M., Dobson, C. M., Welland, M. E. Role of intermolecular forces in defining material properties of protein nanofibrils. *Science* **(2007)** *318,* 1900–1903.
36. MacPhee, C. E. & Dobson, C. M. Formation of mixed fibrils demonstrates the generic

nature and potential utility of amyloid nanostructures. *J. Am. Chem. Soc.* **(2000)** *122,* 12707–12713.

37. Fratzl, P. & Weinkamer, R. Nature's hierarchical materials. *Prog. Mater. Sci.* **(2007)** *52,* 1263–1334.
38. Niu, L., Chen, X., Allen, S. & Tendler, S. J. B. Using the bending beam model to estimate the elasticity of diphenylalanine nanotubes. *Langmuir* **(2007)** *23,* 7443–7446.
39. Li, C. & Mezzenga, R. The interplay between carbon nanomaterials and amyloid fibrils in bio-nanotechnology. *Nanoscale* **(2013)** *5,* 6207–18.
40. Reches, M. & Gazit, E. Casting Metal Nanowires Within Discrete Self-Assembled Peptide Nanotubes. *Science* **(2003)** *300,* 625–627.
41. Carny, O., Shalev, D. E. & Gazit, E. Fabrication of coaxial metal nanocables using a self-assembled peptide nanotube scaffold. *Nano. Lett.* **(2006)** *6,* 1594–1597.
42. Scheibel, T., Parthasarathy, R., Sawicki, G., Lin, X. M., Jaeger, H., and Lindquist, S. L. Conducting nanowires built by controlled self-assembly of amyloid fibers and selective metal deposition. *Proc. Natl. Acad. Sci. U. S. A.* **(2003)** *100,* 4527–32.
43. Liang, Y., Guo, P., Pingali, S. V., Pabit, S., Thiyagarajan, P., Berland, K. M., and Lynn, D. G. Light harvesting antenna on an amyloid scaffold. *Chem. Comm.* **(2008)** 6522-6524.
44. Eisenberg, D. & Jucker, M. The amyloid state of proteins in human diseases. *Cell* **(2012)** *148,* 1188–1203.
45. Sunde, M., Serpell, L. S., Bartlam, M., Fraser, P. E., Pepys, M. B., Blake, C. C. F. Common core structure of amyloid fibrils by synchrotron X-ray diffraction. *J. Mol. Biol.* **(1997)** *273,* 729–739.
46. Nelson, R. & Eisenberg, D. Recent atomic models of amyloid fibril structure. *Curr. Opin. Struct. Biol.* **(2006)** *16***,** 260–265.
47. Toyama, B. H. & Weissman, J. S. Amyloid structure: conformational diversity and consequences. *Annu. Rev. Biochem.* **(2011)** *80,* 557–85.
48. Ferrone, F. A, Hofrichter, J., Sunshine, H. R. & Eaton, W. A. Kinetic studies on photolysis-induced gelation of sickle cell hemoglobin suggest a new mechanism. *Biophys. J.* **(1980)** *32,* 361–380.
49. Ferrone, F. A., Double, I. I. A., Mechanism, N., Hofrichter, J. & Eaton, W. A. Kinetics of Sickle Hemoglobin. *J. Mol. Biol.* **(1985)** *183,* 611–631.
50. Cohen, S. I. A, Vendruscolo, M., Dobson, C. M. & Knowles, T. P. J. From macroscopic measurements to microscopic mechanisms of protein aggregation. *J. Mol. Biol.* **(2012)** *421,* 160–171.
51. Bishop, M. F. & Ferrone, F. A. Kinetics of nucleation-controlled polymerization. A perturbation treatment for use with a secondary pathway. *Biophys. J.* **(1984)** *46,* 631–44.
52. Knowles, T. P. J.,Waudby C. A., Devlin G. L., Cohen, S. I. A., Aguzzi, A., Vendruscolo, M., Terentjev E. M., Welland, M. E., Dobson, C. M. An analytical solution to the kinetics of breakable filament assembly. *Science* **(2009)** *326,* 1533–1537.
53. Michaels, T. C. T. & Knowles, T. P. J. Kinetic theory of protein filament growth: Self-consistent methods and perturbative techniques. *Int. J. Mod. Phys. B* **(2015)** *29,* 1530002.

54. Harper, J. D. & Lansbury, P. T. Models of amyloid seeding in Alzheimer's disease and scrapie: Mechanistic truths and physiological consequences of the time-dependent solubility of amyloid proteins. *Annu. Rev. Biochem.* **(1997)** *66,* 385–407.
55. Nielsen, L., Khurana, R., Coats, A., Frokjaer, S., Brange, J., Vyas S., Uversky, V. N., and Fink, A. L. Effect of environmental factors on the kinetics of insulin fibril formation: Elucidation of the molecular mechanism. *Biochemistry* **(2001)** *40,* 6036–6046.
56. Zhu, M., Souillac, P. O., Ionescu-zanetti, C., Carter, S. A. & Fink, A. L. Surface-catalyzed amyloid fibril formation. *J. Biol. Chem.* **(2002)** *277,* 50914–50922.
57. Smith, M. I., Sharp, J. S. & Roberts, C. J. Nucleation and growth of insulin fibrils in bulk solution and at hydrophobic polystyrene surfaces. *Biophys. J.* **(2007)** i 2143–2151.
58. Kumar, E. K., Haque, N. & Prabhu, N. P. Kinetics of protein fibril formation: Methods and mechanisms. *Int. J. Biol. Macromol.* **(2016)** doi.org/10.1016/ j.ijbiomac. 2016. 06. 052.
59. Hurshman, A. R., White, J. T., Powers, E. T. & Kelly, J. W. Transthyretin aggregation under partially denaturing conditions is a downhill polymerization. *Biochemistry* **(2004)** *43,* 7365–7381.
60. Hasegawa, K., Ono, K., Yamada, M. & Naiki, H. Kinetic modeling and determination of reaction constants of alzheimer's-Amyloid fibril extension and dissociation using surface plasmon resonance. *Biochemistry* **(2002)** *43,* 13489–13498.
61. Oosawa, F., Kasai, M. Theory of linear and helical aggregations of macromolecules. *J. Mol. Bio.* **(1962)** *4,* 10-21.
62. Chen, S., Ferrone, F. A. & Wetzel, R. Huntington's disease age-of-onset linked to polyglutamine aggregation nucleation. *Proc. Natl. Acad. Sci.* **(2002)** *99,* 11884-11889.
63. Lee, C., Nayak, A., Sethuraman, A., Belfort, G. & Mcrae, G. J. A Three-Stage kinetic model of amyloid fibrillation. *Biophys. J.* **(2007)** *92,* 3448–3458.
64. Kumar, E. K. & Prabhu, N. P. Differential effects of ionic and non-ionic surfactants on lysozyme fibrillation. *Phys. Chem. Chem. Phys.* **(2014)** *16,* 24076–24088.
65. Borzova, V. A., Markossian, K. A. & Kurganov, B. I. Relationship between the initial rate of protein aggregation and the lag period for amorphous aggregation. *Int. J. Biol. Macromol.* **(2014)** *68,* 144–150.
66. Cohen, S. I. A, Linse, S., Luheshia, L. M., Hellstrand, E., White, D. A., Rajah, L., Otzen, D. E., Vendruscolo, M., Dobson, C. M., and Knowles, T. P. J. Proliferation of amyloid-42 aggregates occurs through a secondary nucleation mechanism. *Proc. Natl. Acad. Sci.* **(2013)** *110,* 9758–9763.
67. Meisl, G., Yang, X., Hellstrand, E., Frohm, B., Kirkegaard, J. B., Cohen, S. I. A., Dobson, C. M., Linse, S., and Knowles, T. P. J. Differences in nucleation behavior underlie the contrasting aggregation kinetics of the A β 40 and A β 42 peptides. *Proc. Natl. Acad. Sci.* **(2014)** *111,* 9384-9389.
68. Jeong, J. S., Ansaloni, A., Mezzenga, R., Lashuel, H. a. & Dietler, G. Novel mechanistic insight into the molecular basis of amyloid polymorphism and secondary nucleation during amyloid formation. *J. Mol. Biol.* **(2013)** *425,* 1765–1781.
69. Otzen, D. Protein–surfactant interactions: A tale of many states. *Biochim. Biophys. Acta - Proteins Proteomics* **(2011)** *1814,* 562–591.
70. Arakawa, T. & Timasheff, S. N. Stabilization of protein structure by sugars.

Biochemistry **(1982)** *21,* 6536–6544.
71. Arakawa, T. & Timasheff, S. N. Mechanism of poly(ethylene glycol) interaction with proteins. *Biochemistry* **(1985)** *24*, 6756–6762.
72. Kaushik, J. K. & Bhat, R. Thermal stability of proteins in aqueous polyol solutions: Role of the surface tension of water in the stabilizing effect of polyols. *J. Phys. Chem. B* **(1998)** *5647,* 7058–7066.
73. Castner, E. W., Margulis, C. J., Maroncelli, M. & Wishart, J. F. Ionic Liquids: Structure and photochemical reactions. *Annu. Rev. Phys. Chem.* **(2011)** *62*, 85–105.
74. Hill, S. E., Miti, T., Richmond, T. & Muschol, M. Spatial extent of charge repulsion regulates assembly pathways for lysozyme amyloid fibrils. *PLoS oNE* **(2011)** *6,* 4e1871.
75. Velicelebi, G. & Sturtevant, J. M. Thermodynamics of the denaturation of lysozyme in alcohol--water mixtures. *Biochemistry* **(1979)** *18,* 1180–1186.
76. Bolen, D. W. & Baskakov, I. V. The osmophobic effect: natural selection of a thermodynamic force in protein folding. *J. Mol. Biol.* **(2001)** *310,* 955–963.
77. Otzen, D. E. Protein unfolding in detergents: Effect of micelle structure, ionic strength, pH, and temperature. *Biophys. J.* **(2002)** *83,* 2219–2230.
78. Shpasser, D., Balazs, Y. S., Kapon, M., Sheynis, T., Jelienk, R., and Eisen, M. S. A paradigm for solvent and temperature induced conformational changes. *Chem. Eur. J* **(2011)** *17,* 8285–9.
79. Macchi, F., Eisenkolb, M., Kiefer, H. & Otzen, D. E. The effect of osmolytes on protein fibrillation. *Int. J. Mol. Sci.* **(2012)** *13,* 3801–3819.
80. Sukenik, S. & Harries, D. Insights into the disparate action of osmolytes and macromolecular crowders on amyloid formation. *Prion* **(2012)** *6,* 26–31.
81. Blancas-Mejia, L. M. & Ramirez-Alvarado, M. Systemic amyloidoses. *Annu. Rev. Biochem.* **(2013)** *82,* 745–774.
82. Tycko, R. & Wickner, R. B. Molecular structures of amyloid and prion fibrils: Consensus versus controversy. *Acc. Chem. Res.* **(2013)** *46,* 1487–1496.
83. Eisenberg, D., Nelson, R, Saway, M. R., Balbirnie, M., Sambhashivan, S., Ivanova, M, I., Madsen, A., Reikel, C. The structural biology of protein aggregation diseases: Fundamental questions and some answers. *Acc. Chem. Res.* **(2006)** *39,* 568–75.
84. Fink, A. L. The aggregation and fibrillation of α-Synuclein. *Acc. Chem. Res.* **(2006)** *39,* 628–634.
85. Thorn, D. C., Meehan, S., Sunde, M., Rekas, A., Gras, S. L., Macphee, C. E., Dobson, C. M., Wilson, M. R., Carver, J. A. Amyloid fibril formation by bovine milk κ -casein and its inhibition by the molecular chaperones R S-and Casein. *Biochemistry* **(2006)** *44,* 17027–17036.
86. Pedersen, J. S., Christensen, G. & Otzen, D. E. Modulation of S6 fibrillation by unfolding rates and gatekeeper residues. *J. Mol. Biol.* **(2004)** *341,* 575–588.
87. Hartl, F. U. & Hayer-hartl, M. Converging concepts of protein folding in vitro and in vivo. *Nat. structl. Mol. Biol.* **(2009)** *16,* 574–581.
88. Stefani, M. Protein folding and misfolding on surfaces. *Int. J. Mol. Sci.* **(2008)** *9*, 2515–2542.
89. Jahn, T. R. & Radford, S. E. Folding versus aggregation: Polypeptide conformations on competing pathways. *Arch. Biochem. Biophys.* **(2008)** *469,* 100–117.

90. Arosio, P., Knowles, T. P. J. & Linse, S. On the lag phase in amyloid fibril formation. *Phys. Chem. Chem. Phys.* **(2015)** *17*, 7606–7618.
91. Calamai, M., Chiti, F. & Dobson, C. M. Amyloid fibril formation can proceed from different conformations of a partially unfolded protein. *Biophys. J.* **(2005)** *89*, 4201–4210.
92. Meisl, G., Yang, X., Dobson, C. M., Linse, S. & Knowles, T. P. J. A general reaction network unifies the aggregation behaviour of the A β 42 peptide and its variants. *Cornell. Univ. Libr. arXiv:1604.00828. [q-bio.MN]* **(2016)** 1-24.
93. Fändrich, M. Oligomeric intermediates in amyloid formation: Structure determination and mechanisms of toxicity. *J. Mol. Biol.* **(2012)** *421*, 427–440.
94. Lara, C., Adamcik, J., Jordens, S. & Mezzenga, R. General self-assembly mechanism converting hydrolyzed globular proteins into giant multistranded amyloid ribbons. *Biomacromolecules* **(2011)** *12*, 1868–1875.
95. Kayed, R., Head, E., Thompson, J. L., Mcintire, T. M., Milton, S. C., Cotman, C. W., Glabe, C. G. Amyloid oligomers implies common mechanism of pathogenesis. *Science* **(2003)** *300*, 486–489.
96. Nilsson, M. Techniques to study amyloid fibril formation in vitro. *Methods* **(2004)** *34*, 151–160.
97. Walsh, D. M., Hartley, D. M., Kusumoto, Y., Fezoui, Y., Condron, M. M., Lomakin, A., Benedek, G. B., Selkoe, D. J., Teplow, D. B., Biol, D. B. J. Amyloid β-protein fibrillogenesis: structure and biological activiy of protofibrillar intermediates. *J. Biol. Chem.* **(1999)** *274*, 25945–25952.
98. Morris, A. M., Watzky, M. A. & Finke, R. G. Protein aggregation kinetics, mechanism, and curve-fitting: A review of the literature. *Biochim. Biophys. Acta-Proteins Proteomics* **(2009)** *1794*, 375–397.
99. Buell, A. K., Galvagnion, C., Gaspar, R., Sparr, E., Vendruscolo, M., Knowles, T. P. J., Linse, S., and Dobson, C. M. Solution conditions determine the relative importance of nucleation and growth processes in α-synuclein aggregation. *Proc. Natl. Acad. Sci.* **(2014)** *111*, 7671–7676.
100. Cohen, S. I. A, Linse, S., Luheshia, L. M., Hellstrand, E., White, D. A., Rajah, L., Otzen, D. E., Vendruscolo, M., Dobson, C. M., and Knowles, T. P. J. Proliferation of amyloid-42 aggregates occurs through a secondary nucleation mechanism. *Proc. Natl. Acad. Sci.* **(2013)** *110*, 9758–9763.
101. Uversky, V. N., Li, J. & Fink, A. L. Evidence for a Partially Folded Intermediate in α-Synuclein Fibril Formation. *J. Biol. Chem.* **(2001)** *276*, 10737–10744.
102. Pepys, M. B., Hawkins, P. N., Booth, D. R., Vigushin, D. M., Tennent, G. A., Soutar, A. K., Totty, N., Nguyen, O., Blake, C. C. F., Terry, C. J., Feest, T. G., Zalin, A. M., Hsuan, J. J. Human lysozyme gene mutations cause hereditary systemic amyloidoses. *Lettr. Nature*. **(1993)** *362*, 553-557.
103. Morozova-roche, L. A., Zurdo, J., Spencer, A., Noppe, W., Receveur, V., Archer, D. B., Joniau, M., Dobson, C. M. Amyloid fibril formation and seeding by wild-type human lysozyme and its disease-related mutational variants. *J. Str. Biol*. **(2000)** *351*, 339–351.
104. Booth, D. R., Sunde, M., Bellotti, V., Robinsom, D. B., Hutchinson, W. L., Fraser, P. E., Hawkins, P. N., Dobson, C. M., Radford, S. E., Blake, C. C. F., Pepys, M. B.

Instability, unfolding and aggregation of human lysozyme variants underlying amyloid fibrillogenesis. *Nature* **(1997)** *385*, 787-93.

105. Vernaglia, B. A, Huang, J. & Clark, E. D. Guanidine hydrochloride can induce amyloid fibril formation from hen egg-white lysozyme. *Biomacromolecules* **(2004)** *5*, 1362–1370.
106. Wang, S. S. S., Hung, Y. T., Wang, P. & Wu, J. W. The formation of amyloid fibril-like hen egg-white lysozyme species induced by temperature and urea concentration-dependent denaturation. *Korean. J. Chem. Eng.* **(2007)** *24*, 787–795.
107. Khan, J. M., Chaturvedi, S. K., Rahman, S. K., Ishtikhar, M., Qadeer, A., Ahmad, E., Khan, R. H. Protonation favors aggregation of lysozyme with SDS. *Soft Matter* **(2014)** *10*, 2591–9.
108. Hawe, A., Sutter, M. & Jiskoot, W. Extrinsic fluorescent dyes as tools for protein characterization. *Pharm. Res.* **(2008)** *25*, 1487–1499.
109. Jain, N., Bhattacharya, M. & Mukhopadhyay, S. Kinetics of surfactant-induced aggregation of lysozyme studied by fluorescence spectroscopy. *J. Fluoresc.* **(2011)** *21*, 615–625.
110. Meisl, G., Yang, X., Frohm, B., Knowles, T. P. J. & Linse, S. Quantitative analysis of intrinsic and extrinsic factors in the aggregation mechanism of Alzheimer-associated A β -peptide. *Scientif. Reports **(2016)** 6:18278*, 1–12.
111. Nielsen, M. M., Andersen, K. K., Westh, P. & Otzen, D. E. Unfolding of β-Sheet Proteins in SDS. *Biophys. J.* **(2007)** *92*, 3674–3685.
112. Rangachari, V., Moore, B D., Reed, D. K., Sonoda, L K., Bridges, A. W., Conboy, E., Hartigan, D., and Rosenberry, T. L. Amyloid-β (1-42) rapidly forms protofibrils and oligomers by distinct pathways in low concentrations of sodium dodecylsulfate. *Biochemistry* **(2007)** *46*, 12451–12462.
113. Hansted, J. G., Wejse, P. L., Bertelsen, H. & Otzen, D. E. Effect of protein-surfactant interactions on aggregation of β-lactoglobulin. *Biochim. Biophys. Acta - Proteins Proteomics* **(2011)** *1814*, 713–723.
114. Ryan, T. M., Griffin, M. D. W., Teoh, C. L., Ooi, J. & Howlett, G. J. High-affinity amphipathic modulators of amyloid fibril nucleation and elongation. *J. Mol. Biol.* **(2011)** *406*, 416–429.
115. Necula, M., Kayed, R., Milton, S. & Glabe, C. G. Small molecule inhibitors of aggregation indicate that amyloid β oligomerization and fibrillization pathways are independent and distinct. *J. Biol. Chem.* **(2007)** *282*, 10311–10324.
116. Kumar, S., Ravi, V. K. & Swaminathan, R. How do surfactants and DTT affect the size, dynamics, activity and growth of soluble lysozyme aggregates? *Biochem. J.* **(2008)** *415*, 275–288.
117. Khan, J.M., Qadeer, A., Chaturvedi, S. K., Ahmad, E., Abdul Rehman, S. A., Gourinath, S., and Khan, R. H., Khan, J. M. SDS can be utilized as an amyloid inducer: A case study on diverse proteins. *PLoS One* **(2012)** *7*, e29694**,**.
118. Moren, A. K. & Khan, A. Phase equilibria of an anionic surfactant (Sodium Dodecyl Sulfate) and an oppositely charged protein (Lysozyme) in water. *Langmuir* **(1995)** *11*, 3636–3643.
119. Stenstam, A., Montalvo, G., Grillo, I. & Gradzielski, M. Small angle neutron scattering

sudy of Lysozyme−Sodium Dodecyl Sulfate aggregates. *J. Phys. Chem. B* **(2003)** *107*, 12331–12338.

120. Lad, M. D., Ledger, V. M., Briggs, B., Green, R. J. & Frazier, R. A. Analysis of the SDS-Lysozyme binding isotherm. *Langmuir* **(2003)** *19*, 5098–5103.
121. Kumar, S., Singh, A. K., Krishnamoorthy, G. & Swaminathan, R. Thioflavin T displays enhanced fluorescence selectively inside anionic micelles and mammalian cells. *J. Fluoresc.* **(2008)** *18*, 1199–1205.
122. Kelly, S. M., Jess, T. J. & Price, N. C. How to study proteins by circular dichroism. *Biochim. Biophys. Acta - Proteins Proteomics* **(2005)** *1751*, 119–139. 123.
123. Sarkar, N. & Bhattacharyya, K. Effect of urea on micelles: fluorescence of p-toluidino naphthalene sulphonate. *Chem. Phys. Lettr.* **(1991)** *180*, 283–286.
124. Das Gupta, P. K. & Moulik, S. P. Effects of urea and a nonionic surfactant on the micellization and counterion binding properties of cetyltrimethyl ammonium bromide and sodium dodecyl sulfate. *Colloid & Polymer Science* **(1989)** *267*, 246–254.
125. Uversky, V. N., Li, J. & Fink, A. L. Evidence for a partially folded intermediate in α-Synuclein fibril formation. *J. Biol. Chem.* **(2001)** *276*, 10737–10744.
126. Turro, N. J. & Lei, X. Spectroscopic probe analysis of protein-surfactant interactions: The BSA/SDS system. *Langmuir* **(1995)** *5*, 2525–2533.
127. Naidu, K. T. & Prabhu, N. P. Protein-Surfactant Interaction: Sodium Dodecyl Sulfate-Induced Unfolding of Ribonuclease A. *J. Phys. Chem. B* **(2011)** *115*, 14760–14767.
128. Hung, Y.-T., Lin, M.-S., Chen, W.-Y., and Wang, S. S.-S., Investigating the effects of sodium dodecyl sulfate on the aggregative behavior of hen egg-white lysozyme at acidic pH. *Korean. J. Chem. Eng.*, **(2007)** *24*, 787–795.
129. Holm, N.K., Jespersen, S.K., Thomassen, L.V., Wolff, T.Y., Sehgal, P., Thomsen, L.A., Christiansen, G., Andersen, C.B., Knudsen, A.D., and Otzen, D.E., Aggregation and fibrillation of bovine serum albumin. *Biochim. Biophys. Acta-Proteins Proteomics* **(2007)** *1774*, 1128–1138.
130. Ferrone, F. Analysis of protein aggregation kinetics. *Methods Enzymol.* **(1999)** *309*, 256–274.
131. Moriyama, Y., Kondo, N. & Takeda, K. Secondary structural changes of homologous proteins, lysozyme and α-lactalbumin, in thermal denaturation up to 130 °c and sodium dodecyl sulfate (SDS) effects on these changes: Comparison of thermal stabilities of sds-induced helical structures in these p. *Langmuir* **(2012)** *28*, 16268–16273.
132. Stenstam, A., Khan, A. & Wennerstro, H. The Lysozyme - Dodecyl Sulfate system . An example of protein-surfactant aggregation. *Langmuir* **(2001)** *7*, 7513–7520.
133. Behbehani, G. R., Saboury, A. A. & Taleshi, E. Determination of partial unfolding enthalpy for lysozyme upon interaction with dodecyltrimethylammonium bromide using an extended solvation model. *J. Mol. Recognit.* **(2008)** *21*, 132–135.
134. Chatterjee, A., Moulik, S. P., Majhi, P. R. & Sanyal, S. K. Studies on surfactant-biopolymer interaction. I. Microcalorimetric investigation on the interaction of cetyltrimethylammonium bromide (CTAB) and sodium dodecylsulfate (SDS) with gelatin (Gn), lysozyme (Lz) and deoxyribonucleic acid (DNA). *Biophys. Chem.* **(2002)** *98*, 313–327.
135. Tofani, L., Feis, A., Snoke, R, E., Berti, D., Baglioni, P., and Smulevich, G.

Spectroscopic and interfacial properties of myoglobin/surfactant complexes. *Biophys. J.* **(2004)** *87,* 1186–95.

136. Chen. A, Wu. D and Johnson.Jr C.S. Determination of the binding isotherm and size of the bovine serum albumin sodium dodecyl sulfate complex by diffusion-ordered 2D NMR . *J. Phys. Chem.B,* **(1995)** *99,* 828–834.
137. Andersen, K. K., Oliveira, C. L., Larsen, K. L., Poulsen, F. M., Callisen, T. H., Westh, P., Pedersen, J. S. and Otzen, D. The role of decorated SDS micelles in sub-CMC protein denaturation and association. *J. Mol. Biol.* **(2009)** *391,* 207–226.
138. Bhuyan, A. K. On the mechanism of SDS-induced protein denaturation. *Biopolymers* **(2010)** *93,* 186–199.
139. Pertinhez, T. A., Bouchard, M., Smith, R. A. G., Dobson, C. M. & Smith, L. J. Stimulation and inhibition of fibril formation by a peptide in the presence of different concentrations of SDS. *FEBS Lett.* **(2002)** *529,* 193–197.
140. Yamamoto, S., Hasegawa, K., Yamaguchi, I., Tsutsumi, S., Kardos, J., Goto, Y., Gejyo, F., and Naiki, H. Low concentrations of Sodium Dodecyl Sulfate induce the extension of β2-Microglobulin-related amyloid fibrils at a neutral pH. *Biochemistry* **(2004)** *43,* 14068-14072.
141. Ahmad, M. F., Ramakrishna, T., Raman, B. & Rao, C. M. Fibrillogenic and non-fibrillogenic ensembles of SDS-bound human α-Synuclein. *J. Mol. Biol.* **(2006)** *364,* 1061–1072.
142. Olubiyi, O. O. & Strodel, B. Structures of the amyloid β -Peptides Aβ 1−40 and Aβ 1−42 as influenced by pH and a D-Peptide. *J. Phys. Chem. B* **(2012)** *116,* 3280-3291.
143. Zidar, J. & Merzel, F. Probing amyloid-beta fibril stability by increasing ionic strengths. *J. Phys. Chem. B* **(2011)** *115,* 2075–2081.
144. Tadros, T. F. Applied surfactants: Principles and applications. *Wiley-VCH,* **(2005)**, 1-634.
145. Singh, R. B., Mahanta, S. & Guchhait, N. Destructive and protective action of sodium dodecyl sulphate micelles on the native conformation of Bovine Serum Albumin : A study by extrinsic fluorescence probe 1-hydroxy-2-naphthaldehyde. *Chem. Phys. Lett.* **(2008)** *463,* 183–188.
146. Otzen, D. E., Sehgal, P. & Westh, P. α-Lactalbumin is unfolded by all classes of surfactants but by different mechanisms. *J.Colloid.Interface.Sci.* **(2009)** *329,* 273–283.
147. Misra, P. P. & Kishore, N. Biophysical analysis of partially folded state of α-lactalbumin in the presence of cationic and anionic surfactants. *J. Colloid Interface Sci.* **(2011)** *354,* 234–247.
148. So, M.. Ishii, A., Hata, Y., Yagi, H., Naiki, H., and Goto, Y. Supersaturation-limited and unlimited phase spaces compete to produce maximal amyloid fibrillation near the critical micelle concentration of sodium dodecyl sulfate. *Langmuir* **(2015)** *31,* 9973-9982.
149. Giehm, L., Oliveira, C. L. P., Christiansen, G., Pedersen, J. S. & Otzen, D. E. SDS-induced fibrillation of α-Synuclein: An alternative fibrillation pathway. *J. Mol. Biol.* **(2010)** *401,* 115–133.
150. Hansted, J. G., Wejse, P. L., Bertelsen, H. & Otzen, D. E. Effect of protein-surfactant interactions on aggregation of β-lactoglobulin. *Biochim. Biophys. Acta - Proteins Proteomics* **(2011)** *1814,* 713–723.

151. Permyakov, E. A., & Berliner, L. J. α-Lactalbumin: structure and function. *FEBS Lett.* **(2000)** *473*, 269–274.
152. Greene, L. H., Grobler, J. A., Malinovskii, V. A., Tian, J., Acharya, K R., Brew K. Stability, activity and flexibility in α-lactalbumin. *Protein. Eng.* **(1999)** *12*, 581–587.
153. Goers, J., Permyakov, S. E., Permyakov, E. A., Uversky, V. N. & Fink, A. L. Conformational prerequisites for α-lactalbumin fibrillation. *Biochemistry* **(2002)** *41*, 12546–12551.
154. Ebrahim-Habibi, M. B., Amininasab, M., Ebrahim-Habibi, A., Sabbaghian, M. & Nemat-Gorgani, M. Fibrillation of α-lactalbumin: Effect of crocin and safranal, two natural small molecules from Crocus sativus. *Biopolymers* **(2010)** *93*, 854–865.
155. Borzova, V. A., Markossian, K. A. & Kurganov, B. I. Relationship between the initial rate of protein aggregation and the lag period for amorphous aggregation. *Int. J. Biol. Macromol.* **(2014)** *68*, 144–150.
156. Wang, S. S. S., Liu, K. N., Wen, W. S. & Wang, P. Fibril formation of bovine α-lactalbumin is inhibited by glutathione. *Food Biophys.* **(2011)** *6*, 138–151.
157. Levine, H. Thioflavine T interaction with synthetic Alzheimer's disease β-amyloid peptides: Detection of amyloid aggregation in solution. *Protein Sci.* **(1993)** *2*, 404–410.
158. Gupta, P., Khan, R. H. & Saleemuddin, M. Trifluoroethanol-induced 'molten globule' state in stem bromelain. *Arch. Biochem. Biophys.* **(2003)** *413*, 199–206.
159. Naeem, A., Khan, K. A. & Khan, R. H. Characterization of a partially folded intermediate of papain induced by fluorinated alcohols at low pH. *Arch. Biochem. Biophys.* **(2004)** *432*, 79–87.
160. Yancey, P.H., Clark, M.E., Hand S.C., Bowlus R.D. & Somero G.N. Living with water stress: evolution of osmolyte systems. *Science* **(1982)** *217*, 1214-1222.
161. Ellis, R.J. Macromolecular crowding: an important but neglected aspect of the intracellular environment. *Curr. Opin. Struct. Biol.* **(2001)** *11*, 114-119.
162. Minton, A.P. Implications of macromolecular crowding for protein assembly. *Curr. Opin. Struct. Biol* **(2000)** *10*, 34–39.
163. Zimmerman, S.B & Minton, A.P. Macromolecular Crowding - Biochemical, Biophysical and Physiological Consequences. *Annu. Rev. Biophys- Biomol. Struct* **(1993)** *22*, 27–65.
164. Zimmerman, S.B. & Trach, S.O. Effects of macromolecular crowding on the association of E.coli ribosomal particles. *Nucleic. Acids. Res* **(1988)** *16*, 6309–6326.
165. Munishkina, L.A., Ahmad, A., Fink, A.L. & Uversky, V.N. Guiding Protein Aggregation with Macromolecular Crowding. *Biochemistry* **(2008)** *47*, 8993–9006.
166. Politou, A. & Temussi, P. A. Revisiting a dogma: the effect of volume exclusion in molecular crowding. *Curr. Opin. Struct. Biol.* **(2015)** *30*, 1–6.
167. Gee, M. B., Smith, P. E., Gee, M. B. & Smith, P. E. Kirkwood – Buff theory of molecular and protein association , aggregation and cellular crowding. *J. Chem. Phys.* **(2009)** *131*, 165101, 1-10.
168. Shimizu, S. & Boon, C. L. The Kirkwood – Buff theory and the effect of cosolvents on biochemical reactions. *J. Chem. Phys.* **(2009)** *121*, 9147-9155.
169. Gekko, K. Enthalpy and entropy of transfer of amino acids and diglycine from water to

aqueous polyol solutions. *J. Biochem.* **(1981)** *90,* 1643–52.
170. Kim, Y. C. & Mittal, J. Crowding induced entropy-enthalpy compensation in protein association equilibria. *Phys. Rev. Lettr.* **(2013)** *208102*, 1–5.
171. Gilman-Politi, R. & Harries, D. Unraveling the molecular mechanism of enthalpy driven peptide folding by polyol osmolytes. *J. Chem. Theory. Comput.* **(2011)** *7,* 3816–3828.
172. Politi, R., Sapir, L. & Harries, D. The impact of polyols on water structure in solution: A computational study. *J. Phys. Chem. A* **(2009)** *113,* 7548–7555.
173. Zhou, H. Polymer crowders and protein crowders act similarly on protein folding stability. *FEBS Lett.* **(2013)** *587,* 394–397.
174. Mukherjee, S. K., Gautam, S., Biswas, S., Kundu, J. & Chowdhury, P. K. Do macromolecular crowding agents exert only an excluded volume effect? A protein solvation study. *J. Phy. Chem. B* **(2015)** *119,* 14145-14156.
175. Mason, P. E., Neilson, G. W., Dempsey, C. E., Barnes, A. C. & Cruickshank, J. M. The hydration structure of guanidinium and thiocyanate ions: Implications for protein stability in aqueous solution. *Proc. Natl. Acad. Sci. U.S.A* **(2003)** *100,* 4557-4561 .
176. Usha, R. & Ramasami, T. Stability of collagen with polyols against guanidine denaturation. *Colloids & surfaces B:Biointerfaces* **(2008)** *61,* 39–42.
177. Ota, C. Energy transfer at heterogeneous protein-protein interfaces to investigate the molecular behaviour in the crowding environment. *Spectrochim. Acta Part A Mol. Biomol. Spectrosc.* **(2017)** *175,* 145–154.
178. Hong, J. & Gierasch, L. M. Macromolecular crowding remodels the energy landscape of a protein by favoring a more compact unfolded state. *J. Am. Chem. Soc.* **(2010)** *132,* 10445–10452.
179. Harada, R., Sugita, Y. & Feig, M. Protein crowding affects hydration structure and dynamics. *J. Am. Chem. Soc.* **(2012)** *134,* 4842-4849.
180. Stepanenko, O. V, Stepanenko, O. V, Kuznetsova, I. M., Uversky, V. N. & Turoverov, K. K. Peculiarities of the super-folder GFP folding in a crowded milieu. *Int. J. Mol. Sci.* **(2016)** *11,* 1805, 1-14.
181. Mishra, R., Seckler, R. & Bhat, R. Efficient refolding of aggregation-prone citrate synthase by polyol osmolytes. *J. Biol. Chem.* **(2005)** *280,* 15553–15560.
182. Martin, J. & Hartl, U-F. The effect of macromolecular crowding on chaperonin-mediated protein folding. *Proc. Natl. Acad. Sci. U.S.A* **(2003)** *94,* 1107-1112
183. Danielsson, J., Mu, X, Lang, L., Wang, H., Binolfi, A., Theillet, F-X., Bekei, B., Logan, D.T., Selenko, P., Wennerström, H. and Oliveberg, M. Thermodynamics of protein destabilization in live cells. *Proc. Natl. Acad. Sci. U.S.A* **(2015)** *112,* 12402-12407.
184. Kuznetsova, N., Chi, S. L. & Leikin, S. Sugars and polyols inhibit fibrillogenesis of type I collagen by disrupting hydrogen-bonded water bridges between the helices. *Biochemistry* **(1998)** *37,* 11888–11895.
185. Vagenende, V., Yap, M. G. S. & Trout, B. L. Mechanisms of protein stabilization and prevention of protein aggregation by glycerol. *Biochemistry* **(2009)** *48,* 11084–11096.
186. Candotti, M. & Orozco, M. The differential response of proteins to macromolecular crowding. *PLoS Comp.Biol.* **(2016)** *12 (7)e,* 1–18.
187. Welch, W. J. & Brown, C. R. Influence of molecular and chemical chaperones on protein folding. *Cell stress & chaperones* **(1996)** *1,* 109–15.

188. Minton, A. P. Models for excluded volume interaction between an unfolded protein and rigid macromolecular cosolutes: Macromolecular crowding and protein stability revisited. *Biophys. J.* **(2005)** *88,* 971–985.
189. Uversky, V. N. Intrinsically disordered proteins and their environment: Effects of strong denaturants, temperature, pH, Counter ions, membranes, binding partners, osmolytes, and macromolecular crowding. *Protein J.* **(2009)** *28,* 305–325.
190. Kang, H., Pincus, P. A., Hyeon, C. & Thirumalai, D. Effects of macromolecular crowding on the collapse of biopolymers. *Phys. Rev. Lett.* **(2015)** *114,* 1–5.
191. Sukenik, S., Politi, R., Ziserman, L., Danino, D., Friedler, A. & Harries, D. Crowding alone cannot account for cosolute effect on amyloid aggregation. *PLoS One* **(2011)** *6,* e-15608.
192. Baskakov, I. & Bolen, D. W. Forcing thermodynamically unfolded proteins to fold. *J. Biol. Chem.* **(1998)** *273,* 4831–4834.
193. Kamiyama, T., Sadahide, Y., Nogusa, Y. & Gekko, K. Polyol-induced molten globule of cyrochrome c: an evidence for stabilization by hudrophobic interaction. *Biochim. Biophys. Acta* **(1999)** *1434,* 44–57.
194. Devaraneni, P. K., Mishra, N. & Bhat, R. Polyol osmolytes stabilize native-like cooperative intermediate state of yeast hexokinase A at low pH. *Biochimie* **(2012)** *94,* 947–952.
195. Khan, M. V., Ishtikhar, M., Rabbani, G., Zamana, M., Abdelhameed, A.S., Khan, R.H. Polyols (Glycerol and Ethylene glycol) mediated amorphous aggregate inhibition and secondary structure restoration of metalloproteinase-conalbumin (ovotransferrin). *Int. J. Biol. Macromol.* **(2017)** *94,* 290–300.
196. Hall, D. & Minton, A. P. Macromolecular crowding: Qualitative and semiquantitative successes, quantitative challenges. *Biochim. Biophys. Acta-Proteins Proteomics* **(2003)** *1649,* 127–139.
197. Annunziata, O., Asherie, N., Lomakin, A., Pande, J., Ogun, O. and Benedek, G.B. Effect of polyethylene glycol on the liquid-liquid phase transition in aqueous protein solutions. *Proc. Natl. Acad. Sci. U. S. A.* **(2002)** *99,* 14165–14170.
198. Roos, M., Ott, M., Hofmann, M., Link, S., Rössler, E., Balbach, J., Krushelnitsky, A. and Saalwächter, K. Coupling and decoupling of rotational and translational diffusion of proteins under crowding conditions. *J. Am. Chem. Soc.* **(2016)** *138,* 10365-10372.
199. Reese, L., Melbinger, A. & Frey, E. Crowding of molecular motors determines microtubule depolymerization. *Biophys. J* **(2011)** *101,* 2190–2200.
200. Breydo, L., Reddy, K.D., Piai, A., Felli, I.C., Pierattelli, R. & Uversky, V.N. The crowd you're in with: Effects of different types of crowding agents on protein aggregation. *BBA - Proteins Proteomics* **(2014)** *1844,* 346–357.
201. Co, N. T..Hu.., C-K. & Li, M.S. Dual effect of crowders on fibrillation kinetics of polypeptide chains revealed by lattice models Dual effect of crowders on fibrillation kinetics of polypeptide chains. *J. Chem. Phys.* **(2013)** *138,* 185101, 1-5.
202. Abbas, S. A., Sharma, V. K., Patapoff, T. W. & Kalonia, D. S. Opposite effects of polyols on antibody aggregation: Thermal versus mechanical stresses. *Pharm.Res.* **(2012)** *29,* 683–694.
203. Militello, V., Vetri, V. & Leone, M. Conformational changes involved in thermal

aggregation processes of bovine serum albumin. *Biophys. Chem.* **(2003)** *105,* 133–141.
204. Munishkina, L. A., Ahmad, A., Fink, A. L. & Uversky, V. N. Guiding protein aggregation with macromolecular crowding. *Biochemistry* **(2008)** *47,* 8993–9006.
205. Lampel, A., Bram, Y., Levy-sakin, M., Bacharach, E. & Gazit, E. The effect of chemical chaperones on the assembly and stability of HIV-1 capsid protein. *PLoS One* **(2013)** *8(4),* e60867 (25–29).
206. Kuwajima, K. A folding model of α-lactalbumin deduced from the three-state denaturation mechanism. *J. Mol. Biol.* **(1977)** *114,* 241–258.
207. Pfeil, W. Is thermally denatured protein unfolded? The example of a-lactalbumin. *Biochimi. Biophys. Acta* **(1987)** *911,* 114–116.
208. Ikeguchi, M., Kuwajima, K., Mitani, M. & Sugai, S. Evidence for identity between the equilibrium unfolding intermediate and a transient folding intermediate: a comparative study of the folding reactions of alpha-lactalbumin and lysozyme. *Biochemistry* **(1986)** *25,* 6965–72.
209. Peng, Z. Y. & Kim, P. S. A protein dissection study of a molten globule. *Biochemistry* **(1994)** *33,* 2136–2141.
210. Kuwajima, K. The molten globule state of alpha-lactalbumin. *FASEB J* **(1996)** *10,* 102–109.
211. Halskau, O., Underhaug, J., Froystein, N. A. & Martínez, A. Conformational flexibility of α-lactalbumin related to its membrane binding capacity. *J. Mol. Biol.* **(2005)** *349,* 1072–1086.
212. Hanssens, I., Houthuys, C., Herreman, W. & van Cauwelaert, F. H. Interaction of alpha-lactalbumin with dimyristoyl phosphatidylcholine vesicles. I. A microcalorimetric and fluorescence study. *Biochim. Biophys. Acta* **(1980)** *602,* 539–557.
213. Buchner, J. & Kiefhaber, T. *Protein Folding Handbook* **(2008)** *1-3*.
214. Sukenik, S., Sapir, L. & Harries, D. Balance of enthalpy and entropy in depletion forces. *Curr. Opin. Colloid Interface Sci.* **(2013)** *18,* 495–501.
215. Almagor, A., Priev, A., Barshtein, G., Gavish, B. & Yedgar, S. Reduction of protein volume and compressibility by macromolecular cosolvents: Dependence on the cosolvent molecular weight. *Biochim. Biophys. Acta - Protein Struct. Mol. Enzymol.* **(1998)** *1382*, 151–156.
216. Priev, A., Almagor, A., Yedgar, S. & Gavish, B. Glycerol decreases the volume and compressibility of protein interior. *Biochemistry* **(1996)** *35*, 2061–2066.
217. Lee, J.C. & Timasheff, S. N. the Stabilization of Proteins By Sugars. *J.Biol.Chem.* **(1981)** 256, 7193–7203.
218. Kita, Y.; Arakawa, T. Lin, T.-Y., Timasheff, S. N. Contribution of the surface free energy perturbation to protein-solvent interactions. *Biochemistry* **(1994)**, *33,* 15178-189.
219. Nozaki, Y. & Tanford, C. The solubility of amino acids and related compounds in aqueous urea solutions. *J. Biol. Chem.* **(1963)** *238,* 4074–4081.
220. Arakawa, T. & Timasheff, S. N. Protein stabilization and destabilization by guanidinium salts. *Biochemistry* **(1984)** *23,* 5924–5929.
221. Gekko, K. & Timasheff, S. N. Mechanism of protein stabilization by glycerol: preferential hydration in glycerol-water mixtures. *Biochemistry* **(1981)** *20,* 4667–4676.
222. Taneja, S. & Ahmad, F. Increased thermal stability of proteins in the presence of amino

acids. *Biochem. J.* **(1994)** *303*, 147–153.
223. Simpson, R.B. & Kauzmann, W. The kinetics of protein denaturation. I. The behavior of the optical rotation of ovalbumin in urea solution. *J. Am. Chem. Soc.* **(1953)** *75*, 5139–5152
224. Schellmann, J., Simpson, R.B. & Kauzmann, W. The kinetics of protein denaturation. 11. The optical rotation of ovalbumin in solutions of guanidinium salts. *J. Am. Chem. Soc.* **(1953)** *75*, 5152–5154.
225. Gerlsma, S. Y. & Stuur, E. R. The effect of polyhydric and monohydric alcohols on the heat-induced reversible denaturation of lysozyme and ribonuclease. *Int. J. Pept. Protein Res.* **(2009)** *4*, 377–383.
226. Gekko, K. & Ito, H. Competing solvent effects of polyols and guanidine hydrochloride on protein stability. *J. Biochem* **(1990)** *107*, 572–577.
227. Gekko, K., Science, F. & Culture, M. Preferential polyhydric hydration of bovine serum albumin in the presence of polyhydric alcohols (ethylene glycol , glycerol , xylitol , sorbitol , mannitol , and inositol) was investigated by a densimetric method with the application of multicom ponent theory. *J. Biochem* **(1981)** *90*, 39–50.
228. Ingham, K. C. Polyethylene glycol in aqueous solution: Solvent perturbation and gel filtration studies. *Arch. Biochem. Biophys.* **(1977)** *184*, 59–68.
229. Knoll, D. A. & Hermans, J. Effect of poly(ethylene glyol) on protein denaturation and model compound pKa's. *Biopolymers* **(1981)** *20*, 1747–1750.
230. Atha, D. H. & Ingham, K. C. Mechanism of precipitation of proteins by polyethylene glycols. Analysis in terms of excluded volume. *J. Biol. Chem.* **(1981)** *256*, 12108–12117.
231. Prabha, C. R. & Rao, C. M. Oxidative refolding of lysozyme in trifluoroethanol (TFE) and ethylene glycol: Interfering role of preexisting ??-helical structure and intermolecular hydrophobic interactions. *FEBS Lett.* **557,** 69–72 (2004).
232. Guo, F. & Friedman, J. M. Osmolyte-induced perturbations of hydrogen bonding between hydration layer waters: Correlation with protein conformational changes. *J. Phys. Chem. B* **(2009)** *113*, 16632–16642.
233. Siligardi, G. & Drake, A. F. The importance of extended conformations and, in particular, the PII conformation for the molecular recognition of peptides. *Biopolymers* **(1995)** *37*, 281–92.
234. Capp, M. W., Pegram, L.M., Saecker, R.M., Kratz, M., Riccardi, D., Wendorff, T., Cannon, J.G., and Record, M.T.,Jr. Interactions of the osmolyte glycine betaine with molecular surfaces in water: Thermodynamics, structural interpretation, and prediction of m-values. *Biochemistry* **(2009)** *48*, 10372–10379.
235. Politi, R. & Harries, D. Enthalpically driven peptide stabilization by protective osmolytes. *Chem. Commun.* **(2010)** *46*, 6449.